



universität  
wien

# DISSERTATION

Titel der Dissertation

## INTEGRATED BASIN ANALYSIS OF THE VIENNA BASIN, CENTRAL EUROPE

Verfasserin

EUN YOUNG LEE

angestrebter akademischer Grad

Doktorin der Naturwissenschaften (Dr. rer. nat.)

Wien, 2015

Studienkennzahl lt. Studienblatt: A 791 426

Dissertationsgebiet lt. Studienblatt: Erdwissenschaften

Betreuerin / Betreuer: Ao. Univ.-Prof. Dr. Michael Wagreich



## **ACKNOWLEDGEMENT**

In the first place, I would like to thank my supervisors, Michael Wagreich and Kurt Decker, for their insightful advice and guidance. In particular I am grateful to Michael for advising, helping and encouraging me around a few difficult corners this project went through, and for his efforts in reviewing the entirety of this thesis and publications. Through his advocacy I was able to seize many opportunities, from funding to IODP expedition participations. I thank Kurt not only for his support and discussion on issues related to the tectonics of the central Europe, but also for initially recruiting me to the University of Vienna. He also helped me to get back on track when I got lost in detail.

This work was initiated and supported partly by the 'Karpatic Tectonics Slovakia' project funded by OMV E&P. University of Vienna, KIOST and IAS provided financial support for several conference expenses. I would like to extend my thanks to the Dionyz Štur Institute, Slovakia for providing us with well data and geophysical data of the northern and central parts of the Vienna Basin. I also thank to Department of Earth and Planetary Sciences, UC Davis where I stayed as a visiting Doctoral student for 10 months and gained precious ideas for this thesis.

I also wish to thank some individuals who helped me at different stages of this project. My sincerest gratitude goes to my colleagues and friends, Andreas Beidinger and András Zámolyi for helping me to collect, arrange and analyze the data. Additionally, I would like to thank my fellow members in Department of Geodynamics and Sedimentology, Stephanie Neuhuber, Dana Tschegg Homolová, Esther Hintersberger, Clemens Porpacz for their friendship and advices on a broad range of geological and geophysical issues.

Thanks also to my brother Sang-Wook Lee for his help with checking data in details and to my family and friends in Korea who have been very supportive over the course of this long study experience. I would also like to thank professors and researchers at KIGAM, UST and other Korean institutes for their continued care, advice, and support. On a personal note, thanks to my friends and colleagues at KOSEAA, Koreanische Schule Wien and other Korean societies in Austria, for making my time here enjoyable.

Lastly, I want to thank my husband, Johannes Novotny. He is also a co-author of a scientific article based on Chapter 2 of this thesis. Although his working style caused me a lot of irritation, we realized that we are in considerably complementary relationship. With his excellent skills and knowledge in visualization and data modeling, acquired from his academic major, we were able to develop and release BasinVis 1.0. Many important images within this thesis have been created using the software. I appreciate his support and patience during last two years of my doctoral program, especially when he carefully read drafts of this thesis. I promise I will support him in the completion of his own doctoral study, based on my experiences.

*Thank you sincerely*

*Herzlichen Dank*

*진심으로 감사드립니다*

Dr.rer.nat. Eun Young Lee

## **ABSTRACT**

The Vienna Basin (central Europe) is a Neogene sedimentary basin situated on top of the Alpine fold-and-thrustbelt. It is located at the junction between the Eastern Alps, the Carpathians, and the Pannonian Basin system. Due to the special position of the basin, the Vienna Basin tectonic evolution has a complex history and has been influenced by the evolution of each of these geologic systems. The Vienna Basin is characterized mainly by four distinct tectonic phases; 1) Early Miocene piggy-back basin, 2) Middle - Late Miocene pull-apart basin, 3) Late Miocene - Pliocene compression and basin inversion and 4) Quaternary basin formation.

The northern and central parts (Czech and Slovakian parts) of the Vienna Basin are highly important to understand the overall stratigraphic and structural evolution of the basin. However, the studies focused mainly on the southern and central parts (Austrian part) of the basin for a variety of reasons. A comprehensive detailed study crossing the borders of Austria, Slovakia and Czech Republic is still missing. Therefore this thesis focused on the northern and central parts to investigate the basin evolution, and then the results are compared with previous studies arranged in the southern part to reach the goal of this thesis - the integrated basin analysis of the Vienna Basin, central Europe.

To analyze data acquired from the Vienna Basin, this study decided to develop a program for sedimentary basin analysis and visualization. Here the developed program, BasinVis 1.0, was designed to analyze and visualize stratigraphic setting and subsidence evolution of a sedimentary basin from wells or stratigraphic profile data. BasinVis 1.0 is mainly based on two numerical methods; interpolation and subsidence analysis. The numerical methods are computed in MATLAB® which is a multi-paradigm numerical computing environment used extensively in academic, research and industrial fields. The graphical user interface intuitively guides users through all process stages and provides tools to analyze and export the results. All 2D and 3D visualizations are created by using MATLAB plotting functions, which enables users to fine-tune the results using the full range of available plot options in MATLAB. BasinVis 1.0 performs the task of stratigraphic setting and subsidence evolution, and provides geologists with an easy-to-learn and user-friendly program for sedimentary basin analysis.

The well data reaching the pre-Neogene basement were analyzed for a detailed and quantitative subsidence history in the northern and central parts of the Vienna Basin. The results were compared with previous studies including the southern part of the basin, to understand the comprehensive basin evolution. After shallow subsidence of the piggy-back basins, the late Early Miocene data show abruptly increasing subsidence, which initiated the Vienna pull-apart basin system. From the Middle Miocene, the subsidence was decreasing overall, however the tectonic subsidence curves show regionally different patterns. This study suggests that a major tensional regime change, from transtension to E-W extension, can be related to the laterally varying tectonic subsidence across the Vienna Basin. From the late Middle to the Late Miocene, the tectonic subsidence occurred dominantly along the regional active normal faults, and corresponds to the E-W trending extension. This study arranged the tectonic subsidence history of the Vienna Basin to five phases; 1) E-W trending piggy-back subsidence (Early Miocene), 2) NE-SW transtensional subsidence (late Early Miocene), 3) NW-SE to E-W transitioning extensional subsidence (Middle Miocene), 4) E-W extensional subsidence (late Middle - Late Miocene) and 5) NE-SW transtensional subsidence (Quaternary).

BasinVis 1.0 was used to analyze and model well data for the depositional setting and the subsidence evolution of the northern and central Vienna Basin. The depositional setting for each stage was modeled to 3D sediments distribution models, 2D sediments isopach maps and cross-section profiles. Subsidence modeling resulted in 3D subsided depth surface models and 2D subsidence rate maps of the basement and tectonic subsidences of each stage. The models provided insights into the integrated and extensive basin evolution of the Vienna Basin, which is closely related with the regional stress change and the paleoenvironmental setting. After the shallow and E-W to NE-SW propagating synsedimentary thrust (piggy-back basin phase), the Vienna Basin changed to a pull-apart basin system with wider and deeper deposition and subsidence by sinistral strike-slip faults. The sediments deposited during the Early Miocene were supplied through the small deltaic system entering from the south. After shallow deposition and subsidence of the earliest Middle Miocene, the development of the Vienna Basin was controlled and accelerated mainly by NE-SW trending synsedimentary normal faults, especially the Steinberg fault. From the Middle to Late Miocene, enormous amount of sediments eroded from the Molasse area were supplied by a broad paleo-Danube delta complex on the western flank of the basin.

## **ZUSAMMENFASSUNG**

Das Wiener Becken (Mitteleuropa) ist ein neogenes Sedimentbecken im Alpinen Falten- und Überschiebungsgürtel. Es liegt im Grenzbereich zwischen den Ostalpen, den Karpaten und dem Pannonischen Beckensystem. Durch diese spezielle Position hat das Wiener Becken eine komplexe tektonische Entwicklungsgeschichte vorzuweisen, die von allen drei geologischen Systemen beeinflusst wurde. Das Wiener Becken ist durch vier eindeutige Phasen charakterisiert: 1) Fröhmiozänes Piggy-back Becken, 2) Mittel- bis Spätmiozänes Pull-apart Becken, 3) Spätmiozän bis Pliozäne Kompression und Beckeninversion und 4) Quartäre Beckenentstehung.

Die zentralen und nördlichen (in Tschechien bzw. der Slowakei gelegenen) Teile des Beckens sind von großer Bedeutung für das Verständnis der allgemeinen stratigraphischen und strukturellen Entwicklung des Beckens. Aus mehreren Gründen lag der Forschungsfokus allerdings hauptsächlich auf den südlichen und zentralen (in Österreich gelegenen) Bereichen des Beckens. Eine umfassende Studie über die Grenzen von Österreich hinaus ist bisher noch ausständig. Daher untersucht diese Dissertation vor Allem die Entwicklungsgeschichte in den zentralen und nördlichen Bereichen des Beckens und vergleicht die Resultate mit existierenden Studienergebnissen aus den südlichen Bereichen um das endgültige Forschungsziel dieser Arbeit zu erreichen – die vollständige Analyse des Wiener Beckens, Mitteleuropa.

Um die Daten aus dem Wiener Becken zu untersuchen, wurde im Zuge der Studie eine Software zur Analyse und Visualisierung von Sedimentationsbecken entwickelt. BasinVis 1.0, ist für die Analyse und Visualisierung des stratigraphischen Aufbau und der Subsidenzgeschichte von Sedimentationsbecken basierend auf Bohrkern- oder stratigraphischer Profildaten ausgelegt. BasinVis 1.0 benutzt dabei zwei grundlegende numerische Methoden, Interpolation und Subsidenzanalyse. Zur Berechnung dieser Methoden wird MATLAB®, eine im akademischen Bereich weit verbreitete Entwicklungsumgebung für numerische Berechnungen, verwendet. Die graphische Benutzeroberfläche führt Nutzer intuitiv durch alle Prozessphasen und stellt Funktionen zur Detailanalyse und zum Datenexport bereit. Alle 2D und 3D Visualisierungen werden mit MATLAB Plot Funktionen erstellt, dadurch haben Nutzer vollen Zugriff auf die von MATLAB gebotenen Plot Bearbeitungsoptionen.

Um eine detaillierte quantitative Subsidenzgeschichte in den zentralen und nördlichen Bereichen des Wiener Beckens zu erstellen wurden Bohrungsdatensätze die den pre-neogenen Beckengrund erreichen ausgewertet. Die Resultate wurden mit früheren Studien, verglichen zum Verständnis der beckenübergreifenden Entwicklungsgeschichte. Nach seichter Subsidenz der piggy-back Becken, ist im Späten Fröhmiozän ein abrupter Anstieg der Subsidenz zu verzeichnen der das Wiener Pull-apart Beckensystem eingeleitet hat. Basierend auf den Erkenntnissen dieser Studie könnten die lateralen Unterschiede in der tektonischen Subsidenz durch einen bedeutenden transtensionalen Regimewechsel von Transtension hin zu O-W Extension erklärt werden. Vom späten Mittelmiozän bis zum Spätmiozän trat tektonische Subsidenz hauptsächlich entlang der aktiven regionalen Verwerfungen auf, was auf eine O-W Extension schließen lässt. Diese Studie unterteilt die tektonische Entwicklungsgeschichte des Wiener Beckens in fünf Phasen: 1) O-W Piggy-back Subsidenz (Fröhmiozän), 2) NO-SW transtensionale Subsidenz (spätes Fröhmiozän), 3) NO-SW zu O-W Übergang extensionale Subsidenz (Mittelmiozän), 4) O-W extensionale Subsidenz (spätes Mittel - Spätmiozän) und 5) NO-SW transtensionale Subsidenz (Quartär).

BasinVis 1.0 wurde zur Analyse des Ablagerungsaufbaus und der Subsidenzentwicklung des zentralen und nördlichen Wiener Beckens eingesetzt. Zur Untersuchung des Ablagerungsaufbaus wurden für jede geologische Einheit ein 3D Sedimentverteilungsmodell, eine 2D Isopach Karte und diverse Querschnittsprofile erstellt. Gleichermaßen wurden für die Subsidenzanalyse für jede Einheit 3D Subsidenztiefenmodelle und 2D Subsidenzraten Karten für Basis- und tektonische Subsidenz erstellt. Diese Modelle gaben Aufschluss in die beckenübergreifende Entwicklung des Wiener Beckens, welche stark mit dem Paläogeography und regionalen Spannungswechseln zusammenhängt. Nach seichten Überschiebungen mit einem O-W Trend (piggy-back Beckenphase), fand im Wiener Becken ein Übergang zu einem pull-apart Beckensystem mit weiterer und tieferer Ablagerung und Subsidenz an sinistralen Strike-Slip Verwerfungen statt. Die Sedimente des Fröhmiozäns wurden von einem kleineren Deltasystem im Süden antransportiert. Nach den seichten Ablagerung und Subsidenzen des frühen Mittelmiozäns wurde die Entwicklung hauptsächlich durch synsedimentäre Verwerfungen mit NO-SW Trend, allen voran der Steinberg Verwerfung, beherrscht und beschleunigt. Vom Mittel- bis zum Spätmiozän wurden enorme Sedimentmengen, die durch Erosion in der Mollassezone entstanden sind, über einen breiten paleo-Donau Deltakomplex an die westliche Flanke des Beckens geschwemmt.

# CONTENTS

ACKNOWLEDGEMENT.....	i
ABSTRACT.....	iii
ZUSAMMENFASSUNG.....	v
CONTENTS.....	vii
<b>CHAPTER 1 INTRODUCTION.....</b>	<b>2</b>
1. 1 STUDY MOTIVATION AND OBJECTIVES	4
1. 2 GEOLOGIC OVERVIEW OF THE VIENNA BASIN	5
1. 2. 1 Early Miocene Piggy-back basin	7
1. 2. 2 Middle-Late Miocene Pull-apart basin	7
1. 2. 3 Late Miocene-Pliocene compression and basin inversion	9
1. 2. 4 Quaternary basins	9
1. 3 MAIN STRUCTURAL ELEMENTS OF THE VIENNA BASIN	10
1. 4 DATABASE	11
1. 5 DECOMPACTION AND BACKSTRIPPING	15
1. 5. 1 Decompaction	16
1. 5. 2 Backstripping	16
1. 5. 3 Dip-Slip Fault Backstripping	17
1. 6 POROSITY-DEPTH RELATION OF THE VIENNA BASIN	18
1. 7 THESIS OUTLINE	21
<b>CHAPTER 2 PROGRAM FOR BASIN ANALYSIS: BasinVis1.0.....</b>	<b>24</b>
ABSTRACT	25
2. 1 INTRODUCTION	26
2. 2 INTERPOLATION METHODS	28
2. 2. 1 Linear Interpolation	29
2. 2. 2 Natural Interpolation	29
2. 2. 3 Cubic Spline Interpolation	30

2. 2. 4	Thin-Plate Spline Interpolation	30
2. 3	EXAMPLE APPLICATION DATA BACKGROUND	32
2. 4	PROGRAM FRAMEWORK	34
2. 4. 1	Setup	35
2. 4. 2	Stratigraphic setting and Visualization	37
2. 4. 3	Subsidence analysis and Visualization	39
2. 4. 4	Cross-section	42
2. 4. 5	Dip-Slip Fault Backstripping	43
2. 5	DISCUSSION AND CONCLUSIONS	44
2. 5. 1	Evaluation of Example Application	44
2. 5. 2	Unsatisfactory parts	45
2. 5. 3	Further Study Plan	45
<b>CHAPTER 3</b>	<b>QUANTITATIVE SUBSIDENCE ANALYSIS.....</b>	<b>46</b>
	ABSTRACT	47
3. 1	INTRODUCTION	48
3. 2	DATA BACKGROUND	50
3. 3	SEDIMENTS DISTRIBUTION AND ISOPACH MAPPING	51
3. 4	SUBSIDENCE ANALYSIS	54
3. 4. 1	Subsidence trend of the Northern part	55
3. 4. 2	Subsidence trend of the Central part	56
3. 4. 3	Subsidence trend of the Basement highs	58
3. 5	TECTONIC SUBSIDENCE RATE MAPPING	59
3. 6	TECTONIC SUBSIDENCE OF THE SOUTHERN PART	61
3. 7	QUATERNARY BASIN SUBSIDENCE	63
3. 8	DISCUSSION	64
3. 8. 1	Different tectonic subsidence patterns	64
3. 8. 2	Badenian tectonic subsidence	65
3. 8. 3	Sarmatian – Pannonian tectonic subsidence	66
3. 8. 4	Uncertainty of Pannonian subsidence	67
3. 9	CONCLUSIONS	67

<b>CHAPTER 4</b>	<b>3D MODELING OF DEPOSITIONAL SETTING AND SUBSIDENCE...</b>	<b>70</b>
	ABSTRACT	71
4. 1	INTRODUCTION	72
4. 2	DATA AND METHODS	74
4. 3	3D MODELING OF DEPOSITIONAL SETTING	75
	4. 3. 1 Depositional setting of the Piggy-back basin system	76
	4. 3. 2 Depositional setting of the Pull-apart basin system	76
4. 4	3D MODELING OF SUBSIDENCE EVOLUTION	82
	4. 4. 1 Subsidence evolution of the Piggy-back basin system	82
	4. 4. 2 Subsidence evolution of the Pull-apart basin system	84
4. 5	DISCUSSION AND CONCLUSIONS	88
<b>CHAPTER 5</b>	<b>FINAL CONCLUSIONS.....</b>	<b>92</b>
<b>REFERENCES.....</b>		<b>97</b>
<b>APPENDIX.....</b>		<b>110</b>
	APPENDIX A    INPUT WELL DATA	112
	APPENDIX B    DIP-SLIP FAULT BACKSTRIPPING	120
<b>CURRILCULUM VITAE AND LIST OF PUBLICATIONS.....</b>		<b>122</b>



# **CHAPTER 1**

## **INTRODUCTION**



## 1.1 STUDY MOTIVATION AND OBJECTIVES

The Vienna Basin is situated on top of the Alpine fold-and-thrustbelt, located at the junction between the Eastern Alps, the Carpathians and the Pannonian Basin system (Fig. 1.1). The basin has been studied intensively starting with classical paleontological-stratigraphical papers and then continuing since the beginning of hydrocarbon exploration about 100 years ago.

The Vienna Basin is spreading over three countries in the central Europe; Austria, Slovakia and Czech Republic (Fig. 1.2). However, a number of studies focused mainly on the southern and central parts (Austrian part) of the basin for a variety of reasons. A comprehensive detailed study crossing the borders of the three countries is still missing. The northern and central parts (Czech and Slovakian parts) are highly important to understand the overall stratigraphic and structural evolution of the basin, because these parts contain up to 6 km of the Miocene sedimentary rocks, several complex structures, and the Steinberg Fault, one of the most prominent structure features of the basin.

This thesis tries to investigate the comprehensive basin setting and tectonostratigraphic subsidence evolution of the Vienna Basin. This project primarily targets the northern and central parts, and the results are compared with previous studies arranged in the southern and central parts (Austrian part). For this study, a number of well, seismic and geophysical data from the northern and central parts of the Vienna Basin were collected, arranged and analyzed by a variety of interdisciplinary techniques (e.g. decompaction, backstripping, interpolation, visualization, 3D modeling).

At the initial stage of this doctoral project, I found out that sediments distribution and subsidence patterns are quite different among the southern, central and northern parts in the Vienna Basin through the Miocene. The difference was more significant during the Middle Miocene time, and some results could not support the generally stated theory that the Vienna Basin is a classical thin-skinned pull-apart structure. To analyze regional depositional setting and subsidence history in integrated models, this thesis project started developing a MATLAB-based program to visualize extensively the stratigraphic/structural setting and subsidence evolution. The research results were intensively discussed in this doctoral thesis.

## 1.2 GEOLOGIC OVERVIEW OF THE VIENNA BASIN

The Vienna Basin tectonic evolution has a complex history due to the position of the basin which is bordered by the Eastern Alps in the West, the Western Carpathians in the North-East and the Pannonian Basin system in the Southeast (Fig. 1.1). The Eastern Alps and the Western Carpathians formed by collisional orogenies during the Mesozoic and the Cenozoic (Decker and Presson, 1996; Plašienka et al., 1997; Royden, 1988). The Pannonian Basin system is a result of Middle to Late Miocene lithospheric extension (Sclater et al., 1980; Royden et al., 1983a, 1983b). The Alpine-Carpathian-Pannonian system was deformed by the late Paleogene and Neogene lateral extrusion of the Eastern Alps towards the Pannonian area in the East (Ratschbacher et al., 1991a, 1991b). The extrusion caused complex and polyphase strike-slip faulting and back-arc-extension linked to the retreating subduction zone, and further resulted in development of Miocene pull-apart basins (e.g. Vienna Basin) and extensional rift basins (e.g. Pannonian basin) (Csontos et al., 1992; Decker and Peresson, 1996; Horváth, 1993; Huisman et al., 2001; Royden, 1985, 1988)

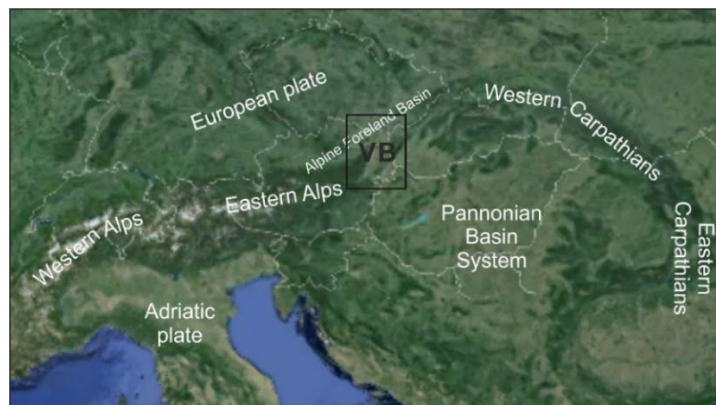


**Figure 1.1.** Location of the Vienna Basin (VB) in the region between the Eastern Alps, the West Carpathians and the Pannonian Basin System. Along the NW flank the Alpine Molasse Foreland Basin extends parallel to the Alpine-Carpathian units.

The Vienna Basin has been influenced by the evolution of each of these geologic systems. The basin is characterized by four distinct tectonic phases; 1) Early Miocene piggy-back basin, 2) Middle - Late Miocene pull-apart basin, 3) Late Miocene - Pliocene compression and basin inversion and 4) Quaternary basins formation (Beidinger and Decker, 2011; Decker et al., 2005; Peresson and Decker, 1997a, 1997b; Salcher et al., 2012; Seifert, 1992; Strauss et al., 2006).

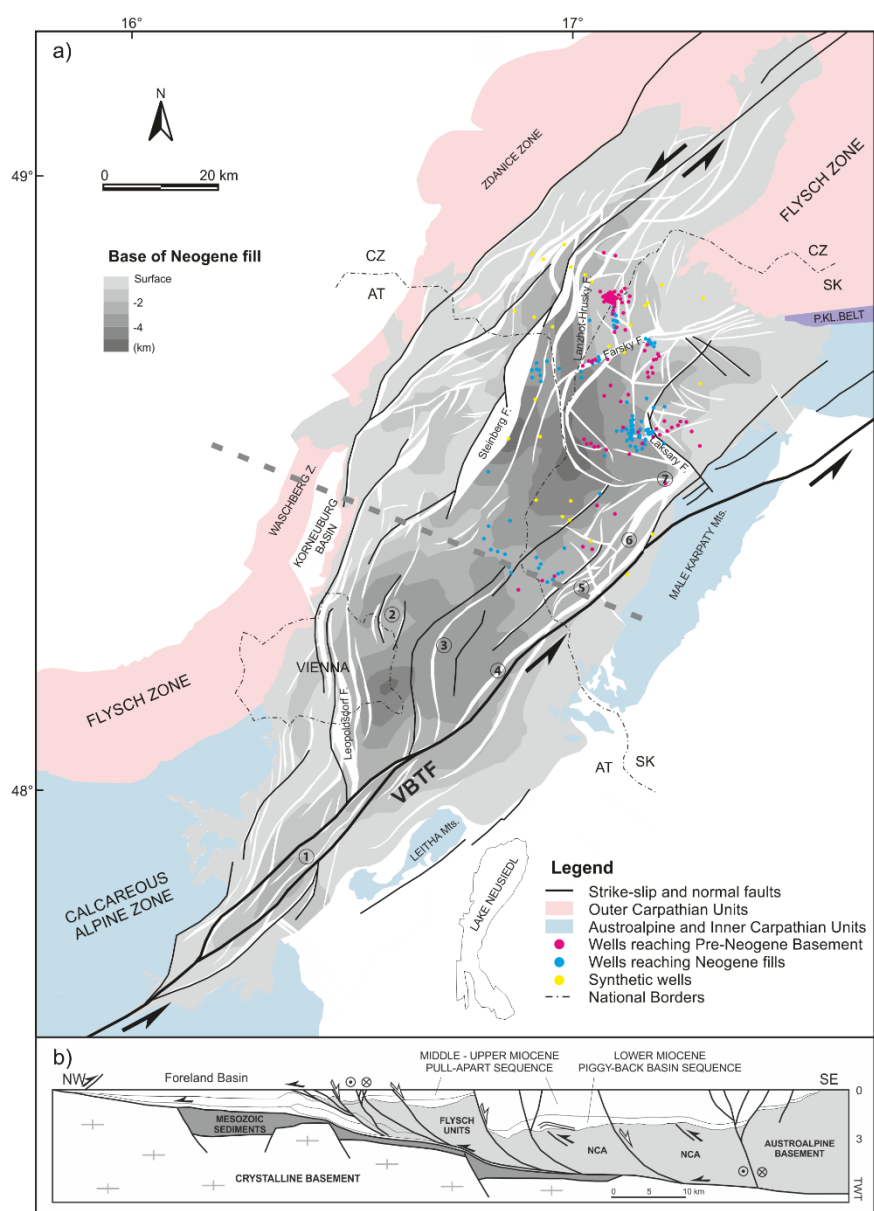


**Figure 1.2.** a) The tectonic and structural map of the Vienna Basin showing the faulted pre-Neogene basement surface and the base depth of the Neogene fill (revised from Arzmüller et al., 2006; Wessely et al., 1993). AT: Austria, SK: Slovakia, CZ: Czech Republic. Locations of wells and cross sections are shown in the study area. Quaternary basins are arranged along the Vienna Basin transfer fault system; ① Mitterndorf Basin, ② Aderklaa Basin, ③ Obersiebenbrunn Basin, ④ Lassee Basin, ⑤ Zohor Basin, ⑥ Pernek Basin and ⑦ Sološnica Basin (Beidinger and Decker, 2011). b) Geological cross section through the Vienna Basin and the adjacent Molasse foreland basin (revised from Beidinger, 2013).

### **1.2.1 Early Miocene Piggy-back basin**

In the Early Miocene (c. 20 – 17 Ma), several E-W trending small sub-basins subsided on the frontal parts of the N- to NW- propagating thrustbelt of the Eastern Alps. This basin stage was active from the Eggenburgian to the early Karpatian (Decker, 1996; Fodor, 1995; Jiříček and Seifert, 1990; Seifert, 1992, 1996). It is described as piggy-back basin system (wedge-top basin; Ori and Friend, 1984), formed on top of active thrust sheets. Although the Eggenburgian sediments were restricted to the northern part of the Vienna Basin, during the Ottnangian and the early Karpatian the sedimentation spread to the central part (Decker, 1996; Jiříček and Seifert, 1990; Strauss et al., 2006).

### **1.2.2 Middle – Late Miocene Pull-apart basin**

At the end of the Early Miocene (c. 17 – 16 Ma), the Vienna Basin became a pull-apart structure (Decker, 1996; Fodor, 1995). Structural styles within the pull-apart are dominated by NE-SW trending sinistral strike-slip duplexes and en-echelon listric normal faults with a left stepping geometry at the Vienna Basin transfer fault (Decker et al., 2005; Royden, 1985, 1988). The main tectonic elements are the Steinberg fault (5.6 km normal offset), the Leopoldsdorf fault (4.2 km normal offset), the Laksary fault, the Farsky fault and the Lanzhot–Hrusky fault (Čekan et al., 1990; Decker et al., 2005; Kröll et al., 1993) (Fig. 1.2 and 1.5). Growth strata along normal faults indicate that faulting occurred synsedimentary during the late Early and Middle Miocene (Decker, 1996). The geodynamic processes resulted in an intricate arrangement of prominent highs and partly deeper subsided depocenters (Hölzel et al., 2008b), where local variations in sedimentary evolution may exist (Arzmüller et al., 2006; Strauss et al., 2006). The pull-apart basin (c. 16 – 8 Ma) was filled by Badenian syn-tectonic deposition, which was blanketed by the deposition of the Sarmatian and Pannonian successions without major depositional breaks (Arzmüller et al., 2006). In the central Vienna Basin the Badenian sediments are divided into proximal deltaic clastics and a distal basinal facies, which continued throughout the Sarmatian in most parts of the Vienna Basin. During the Early and Middle Pannonian clay and sand was deposited in a lacustrine environment (Lake Pannon). During the Late Pannonian the Vienna Basin was filled with mainly with alluvial sediments (Harzhauser and Piller, 2004; Strauss et al., 2006).

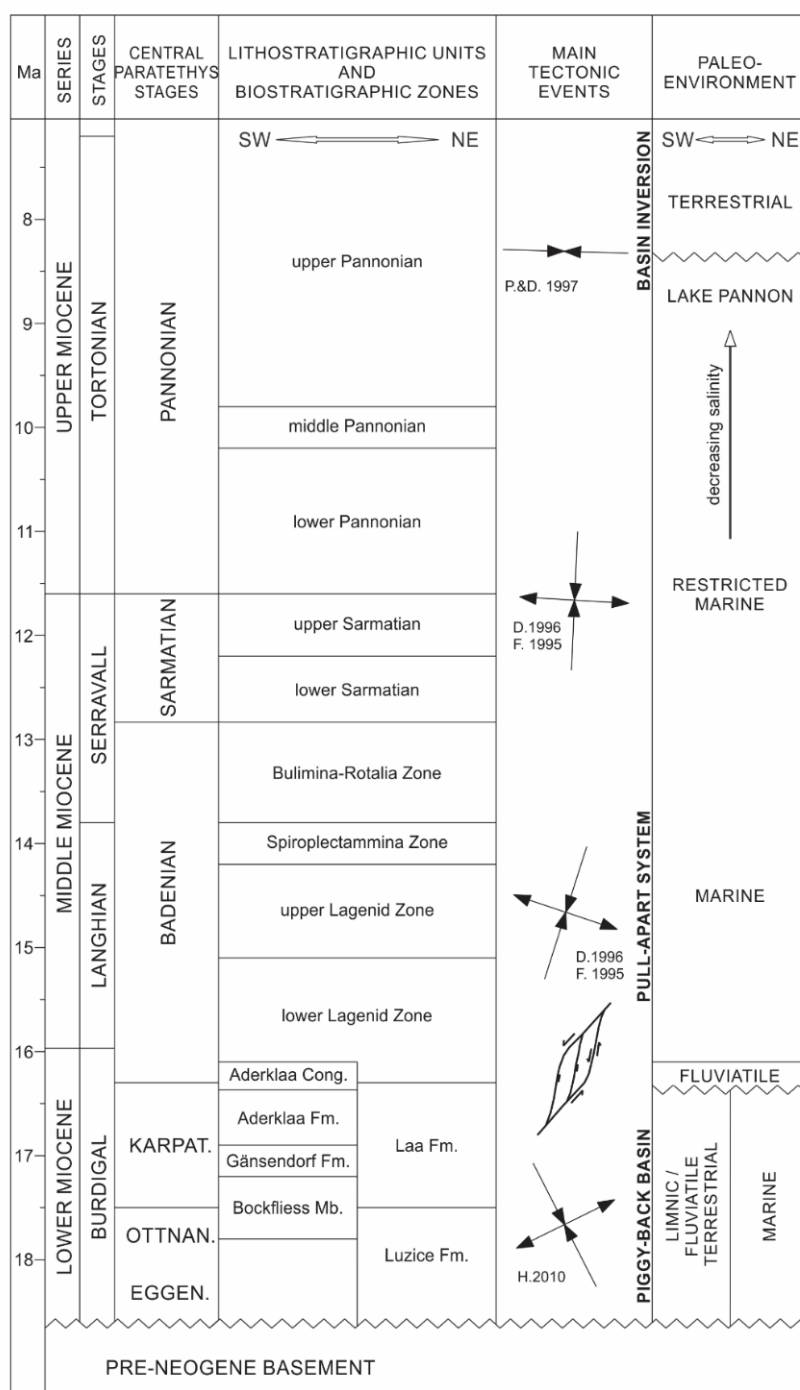


**Figure 1.3.** Stratigraphy and evolution of the Vienna Basin (Decker, 1996; Fodor, 1995; Fuchs and Hamilton, 2006; Hamilton et al., 2000; Hohenegger et al., 2014; Hölzel et al., 2010; Peresson and Decker, 1997a; Wagreich and Schmid, 2002).

### 1.2.3 Late Miocene – Pliocene compression and basin inversion

In the latest Pannonian, sinistral faulting and pull-apart subsidence halted during a major switch of the regional stress field from N(NW)-directed compression to E-W-directed compression for the central part of the Vienna Basin (Decker and Peresson, 1996; Peresson and Decker, 1997a, 1997b). This resulted in basin inversion with an uplift of more than 200 m, which also caused sediment deformation and erosion (Decker, 1996; Strauss et al., 2006).

### 1.2.4 Quaternary basins

The Quaternary and recent reactivation of the Vienna Basin is related to NE-SW extension of basins since c. 250 - 300 ka (Salcher, 2008) at a releasing bend along the slow moving sinistral strike-slip faults (1-2mm/y; Grenerczy et al., 2000; Decker et al., 2005). The Vienna Basin transfer system (VBTF) corresponds to a zone of moderate seismicity, proving the continued activity of the fault zone. These small Quaternary basins include the Mitterndorf, Aderklaa, Obersiebenbrunn, Lasseer, Zohor, Pernek and Sološnica basins (Fig. 1.2). They are filled mainly by fluvial sediments up to 150 m which are unconformably overlying Miocene sediments (Beidinger et al., 2011; Beidinger and Decker, 2011; Decker et al., 2005; Hinsch et al., 2005b; Kullman, 1966; Salcher et al., 2012).

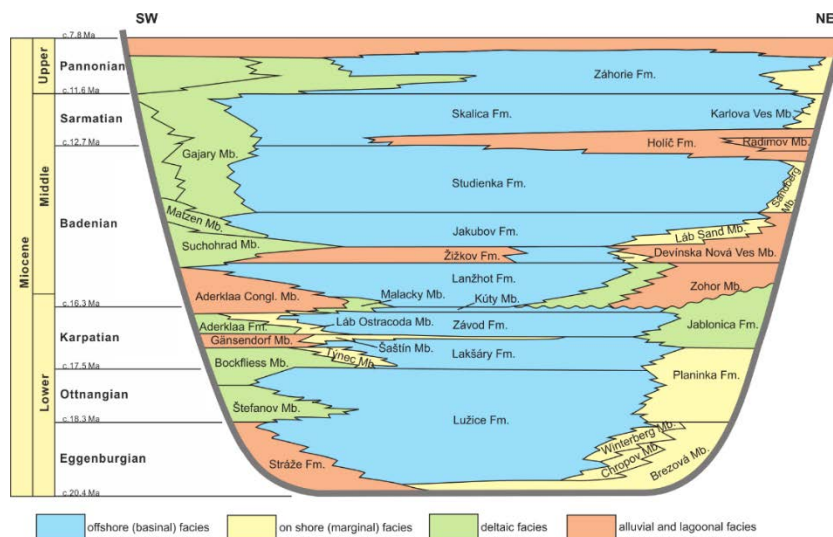


**Figure 1.4.** Miocene depositional system and lithostratigraphic unit names arranged across the Vienna Basin from SW to NE (revised from Baráth et al., 2001; Kováč et al., 2004).

### 1.3 MAIN STRUCTURAL ELEMENTS OF THE VIENNA BASIN

The Vienna Basin has a rhombohedral shape with the left-stepping pattern of en-echelon faults (Royden, 1985). Along the western flank, the Schratzenberg-Steinberg-Bisamberg-Leopoldsdorf Fault systems separated a system of depressions from the western marginal blocks (Poysbrunn, Mistelbach and Mödling Blocks) (Fig. 1.5). A system of grabens are lying along the eastern marginal blocks (the Leitha Mountains and the Male Karpathy Block). The median high zones (the Matzen-Aderklaa, the Wiener herberg and the Enzersdorf highs) are separated by depressions and faults (Arzmüller et al., 2006; Sauer et al., 1992; Wessely et al., 1993).

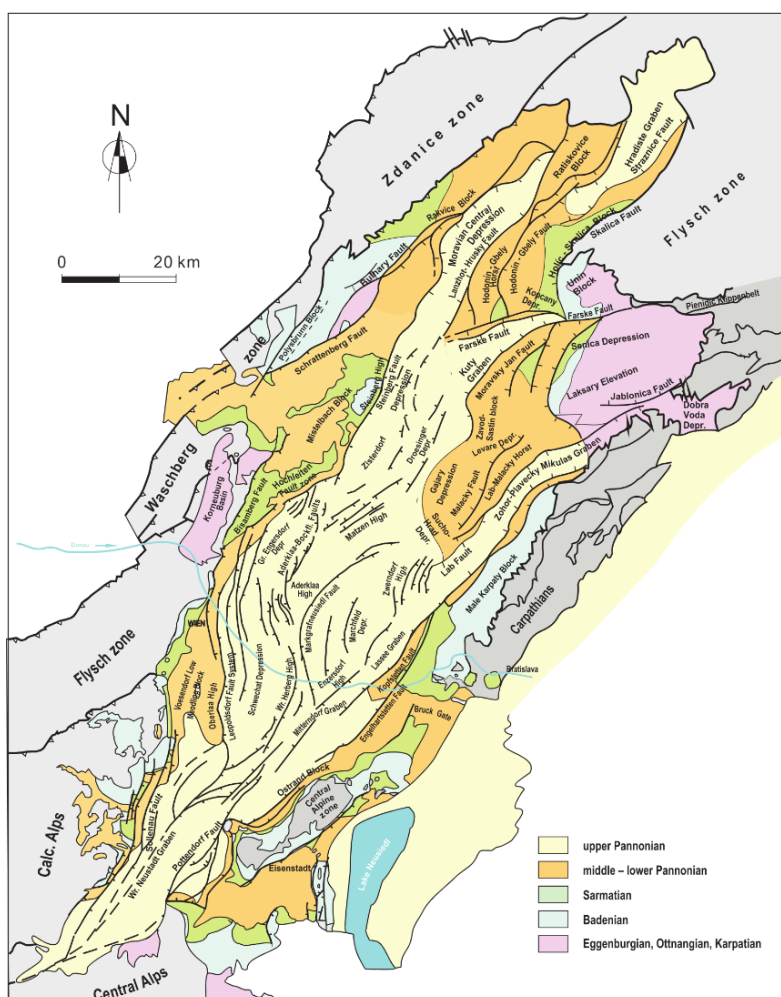


**Figure 1.5.** Map of the Vienna Basin showing surface sediments and main structural elements; faults, highs, horsts, depressions and grabens (revised from Arzmüller et al., 2006).

Geographically, the Vienna basin is subdivided in three parts. The northern part covers the area north of the Kuty graben. The central part extends from the Kuty graben to the Schwechat depression, including the Zistersdorf depression. The southernmost part of the Vienna basin covers the area south of the Schwechat depression, including the Wiener-Neustadt basin and the Mitterndorfer depression (Lankreijer et al., 1995).

This study focuses on the northern and central parts of the Vienna Basin. The parts were dissected into several fault blocks consisting of lower lying depressions, grabens, highs and stable horsts (Fig. 1.5). The most significant tectonic units in the northern and central parts of the Vienna Basin are (Arzmüller et al., 2006; Čekan et al., 1990; Hlavaty, 1996; Wessely et al., 1993):

- **Faults:** Steinberg fault, Schrattenberg fault, Laksary fault, Farske fault, Lanzhot–Hrusky fault, Hodonin-Gbely fault, Láb fault, Leitha fault system
- **Highs and horsts:** Steinberg high (Mistelbach block), Matzen high, Zavod, Šaštín block, Laksary horst, Láb-Malacky horst, Hodonin-Gbely horst
- **Depressions and grabens:** Zisterdorf depression, Moravian Central depression, Leváre depression, Suchohrad depressions, Gajary depression, Zohor-Plavecky Mikulas graben, Kúty graben

## 1.4 DATABASE

A number of geological and geophysical data of the northern and central parts of the Vienna Basin were acquired from the archives of the Dionyz Štur Institute, Bratislava, Slovakia. Data of 201 wells for the northern and central Vienna Basin were arranged for this study (Table 1.1 and Appendix A). Well data in the Austrian region of the central part were obtained from Hölzel (2009). Missing well-data in some areas was corrected by using data from the maps of the Pre-Neogene basement and the Neogene basin fill (Arzmüller et al., 2006; Čekan et al., 1990; Jiříček and Seifert, 1990; Wessely et al., 1993) and interpolated from time-depth conversion of stratigraphic boundaries within seismic reflection data. These interpolated points have been termed as synthetic wells in this study. The wells were used for sediments distribution and isopach mapping. Among them, wells reaching the pre-Neogene

basement were analyzed by decompaction and backstripping techniques to gain subsidence curves and rates.

To analyze subsidence, the porosity-depth relation is evaluated for the Vienna Basin in this study (see Chapter 1.6). Regional water-depth variations were assumed from Sauer et al. (1992) and Seifert (1992) (Fig. 1.6). This study has not incorporated relative sea-level changes in the calculations, since the basin was separated from the world ocean around the early Late Miocene. Additionally, also the regional sea-level changes in the Paratethys were partially in accordance with the global sea-level cycles and superimposed by regional tectonic processes (Haq et al., 1987; Steiniger et al, 1988; Steininger and Wessely, 1999), and the known short-time sea-level fluctuations do not perturb the longer-term subsidence trends.

Block Name	Abb	Numbers	Total
Borský Jur	BJ	4, 5, 6, 7, 8, 16	6
Cunin	Cu	2, 4, 5, 6, 7, 8, 9, 10, 11, 12, 13, 14, 15, 16, 17, 18, 19, 20, 21, 22, 23, 25, 27, 28, 29, 30, 31, 33, 34, 35, 36, 37, 38, 39	35
Dúbrava	Du	1	1
Gbely	Gb	1, 3, 4, 5, 6, 7, 8, 9, 11, 12, 13, 18, 25, 29, 36, 37, 39, 114, 119, 121, 137	21
Kuklov	Kk	3, 4	2
Kúty	Kt	15, 17, 18, 21, 22, 23, 24, 25, 26, 33, 34, 36, 39	13
Láb	Lb	40, 90, 93	3
Lakšárska Nová Ves	LVN	1, 2, 3, 4, 5, 6, 7	7
Lanžhot	Ln	2, 3, 4, 8, 18, 20, 21, 23, 24	9
Lužice	Lu	103, 120	2
Malacky	Ma	20, 22, 64	3
RGL	R	1	1
Rohožník	Ro	1	1
Šaštín	Sa	9, 10, 11, 12	4
Smolinské	Sm	5, 6, 7, 8, 9, 10, 11, 12, 13, 14, 15, 16, 17, 18, 19	15
Studienka	St	1, 2, 3, 4, 5, 6, 8, 11, 14, 15, 31, 32, 33, 34, 35, 36, 37, 38, 39, 40, 41, 42, 43, 44, 45, 83	26
Vysoká	Vy	4, 11, 13, 14, 15, 17, 18, 19, 20, 23	10
Závod	Zv	3, 6, 9, 10, 13, 17, 18, 20, 21, 26, 28, 29, 30, 33, 36, 37, 38, 39, 40, 42, 43, 44, 45, 46, 47, 57, 61, 62, 63, 64, 65, 67, 68, 69, 70, 71, 72, 76, 89, 90, 92, 94, 97	42

**Table 1.1.** Well data obtained from the Dionys Štur Institute, Bratislava, Slovakia. Abb: Abbreviation.

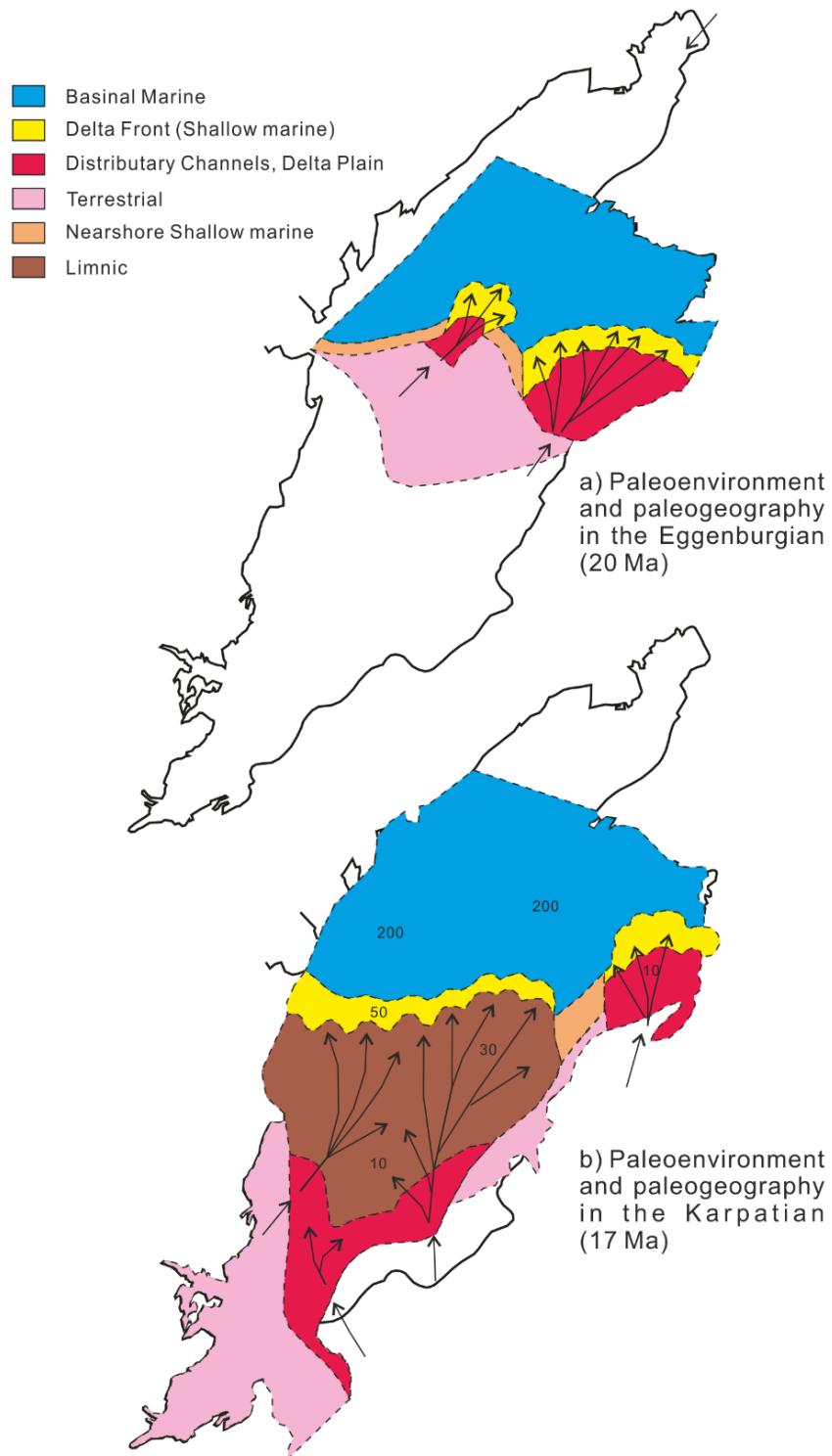
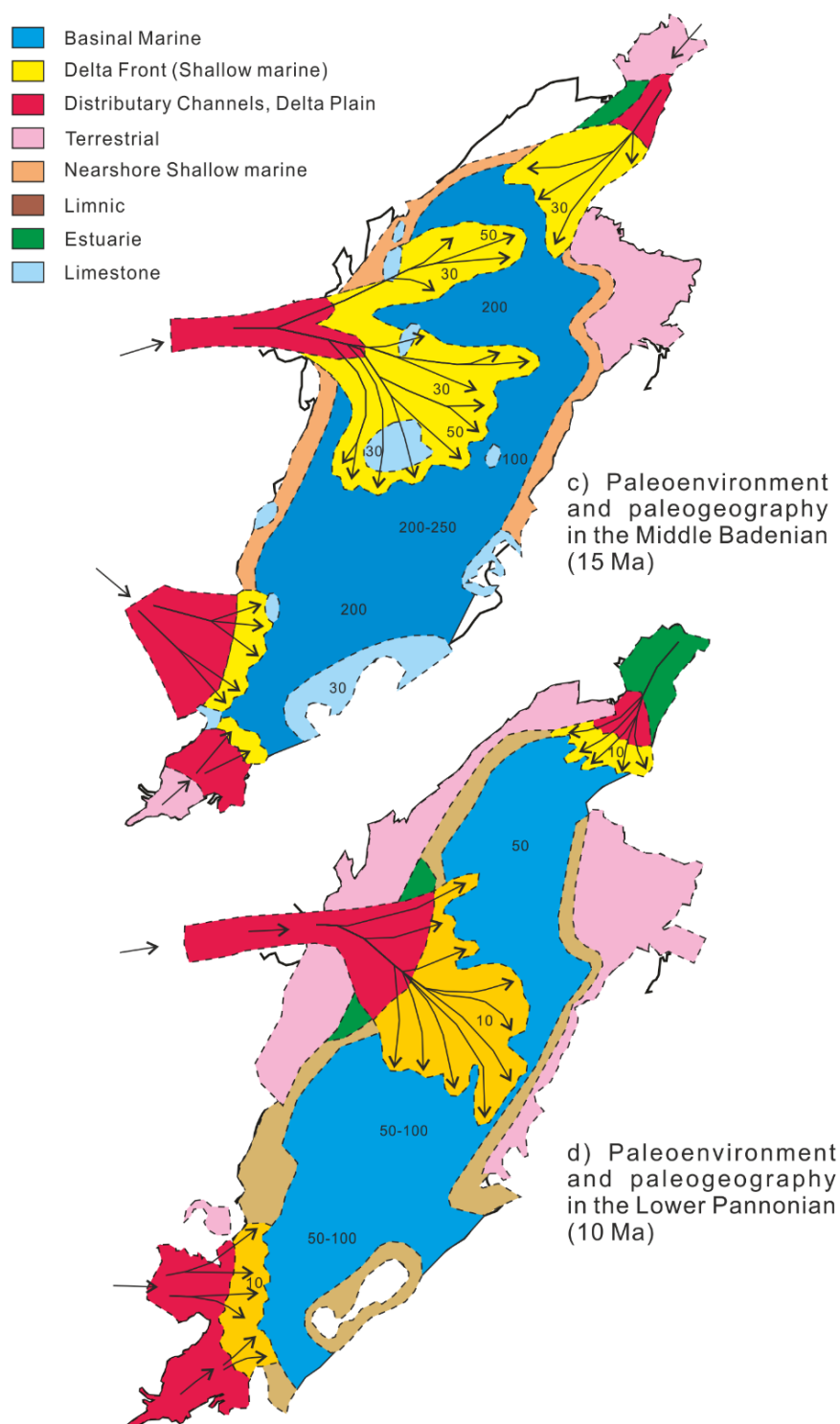


**Figure 1.6.** Paleoenvironment models of the Vienna Basin (revised from Sauer et al., 1992); a) Eggenburgian (20 Ma), b) Karpatian (17 Ma), c) Middle Badenian (15 Ma) and d) Lower Pannonian (10 Ma).

*In the Early Miocene, the Vienna Basin was filled by two deltas coming from the south.*



(continued)

During the Middle Badenian (15 Ma), a new 40x50 km broad delta complex developed on the western flank of the basin carrying sediments from the Molasse area (Sauer et al., 1992).

From the well data, this study arranged the stratigraphic units based on the regional Central Paratethys chronostratigraphy for the Miocene (e.g. Hohenegger et al., 2014; Piller et al., 2007) and regional and local zonations for the Vienna Basin (Fig. 1.3); 1) Eggenburgian-Ottnangian (c. 20.4 – 17.5 Ma), 2) early Karpatian (c. 17.5 – 16.9 Ma) and 3) late Karpatian (c. 16.9 – 16.3 Ma), 4) early Badenian (c. 16.3 – 14.2 Ma), 5) late Badenian (c. 14.2 – 12.8 Ma), 6) Sarmatian (c. 12.8 – 11.6 Ma) and 7) Pannonian (c. 11.6 – 7.8 Ma). The Paratethys was a partly enclosed sea that existed from the Oligocene to the Miocene times to the north of the Alpine mountain belt, and consisted of a chain of basins of various tectonic origin (Piller et al., 2007). The Central Paratethys covered the area from the Bavaria to the Eastern Carpathians (Baldi, 1980).

## 1.5 DECOMPACTION AND BACKSTRIPPING

The stratigraphic column of the basin-fill is not a direct recorder of sediment accumulations rates in the past, because it has been reduced in thickness by the progressive effects of compaction over time. A quantitative analysis of subsidence corrects the stratigraphic column, and provides the time-depth history of any sediment layer and the tectonic subsidence history (Allen and Allen, 2013; Miall, 1999; Steckler and Watts, 1978; Van Hinte, 1978). Subsidence is computed typically at a single location where data from a well can provide detailed data on thickness, lithology, geologic age, porosity, density, paleo-sealevel and paleo-waterdepth (Jin, 1994). Subsidence analysis is processed by decompaction and backstripping techniques, respectively for basement subsidence and tectonic subsidence. The basement subsidence includes the contributions of all factors (e.g. sediment load, waterdepth and sealevel) that affect the subsidence of a basin, while the tectonic subsidence removes these complicate effects from the basement subsidence to reveal the tectonic driving force for subsidence (Allen and Allen, 2013).

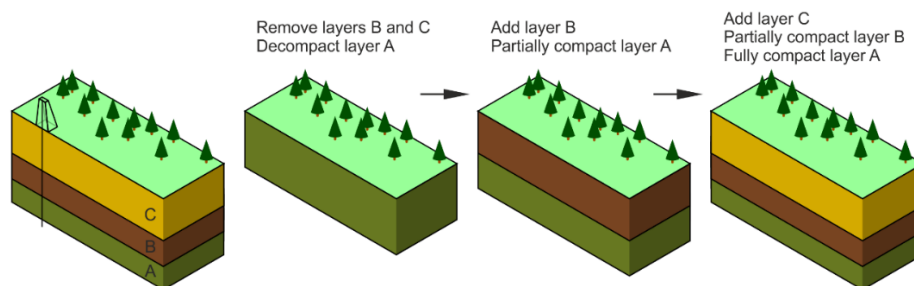


**Figure 1.7.** Concept of the successive stages in the decompaction analysis.

### 1.5.1 Decompaction

The weight of overlying sediments leads to a reduction of porosity and layer thickness in the underlying units, and the resulting compaction is an important process in the quantification of basin subsidence and geometry.

The decompaction technique calculates the thickness of a sediment layer at any time in the past by moving the layer up (Fig. 1.7) using the appropriate porosity-depth relation curve (Allen and Allen, 2013). The porosity-depth relation is exponential (Sclater and Christie, 1980),

$$\phi = \phi_0 e^{-cy}$$

( $\phi$ : porosity,  $y$ : depth,  $\phi_0$ : initial porosity and  $c$ : coefficient)

The porosity-depth curve is strongly influenced by the lithological character of the strata, and, when the porosity-depth relation is not known or unreliable (e.g. Jin, 1994; Lee, 2010), empirical data on  $\phi_0$  and  $c$  (e.g. Sclater and Christie, 1980; see Table 1.2) are used generally. In studying the subsidence in sedimentary basins, it is common to assume that there is no change in the solid volume during burial, so that mechanical compaction of framework grains due to increasing compression from the overlying sediment-water column solely drives porosity reduction (Allen and Allen, 2013).

Lithology	$\phi_0$ (%)	$c$	$\rho_s$
Shale	63	0.51	2.72
Sand	49	0.27	2.65
Shaly Sand	56	0.39	2.68
Chalk	70	0.71	2.71

**Table 1.2.** Initial porosity, coefficient of porosity-depth relation and average density for common lithologies (Sclater and Christie, 1980)

### 1.5.2 Backstripping

The tectonic subsidence, analyzed by backstripping technique, is highly useful to investigate the basin-forming mechanisms without concerning varying sediment load. To gain insights into subsidence rate and tectonic driving force

we need to include a number of modifications or ‘corrections’ to the sediment accumulation rate curve derived by decompaction of the stratigraphic column (Allen and Allen, 2013).

Backstripping is a technique for progressively removing the sedimentary load from a basin, correcting for compaction, paleobathymetry ( $W_d$ ) and sea-level change ( $\Delta_{SL}$ ), in order to reveal the tectonic driving mechanisms of basin subsidence (Miall, 1999). Incorporating the various effects results in the Airy compensated tectonic subsidence (Sclater and Christie, 1980; Steckler and Watts, 1978; Van Hinte, 1978),

$$Z = S \left( \frac{\rho_m - \rho_s}{\rho_m - \rho_w} \right) + W_d - \Delta_{SL} \left( \frac{\rho_m}{\rho_m - \rho_w} \right)$$

(S: sediments thickness,  $\rho_w$ ,  $\rho_s$  and  $\rho_m$ : densities of water, mean sediment and mantle).

### 1.5.3 Dip-Slip Fault Backstripping

To analyze vertical fault displacement through time, this study uses the dip-slip fault backstripping introduced by ten Veen and Postma (1999), ten Veen and Kleinspehn (2000) and Wagreich and Schmid (2002). The method uses basement subsidence curves without sea-level corrections for two stratigraphic profiles from the footwall and hanging wall blocks of synsedimentary faults (Fig. 1.8a). Segments of convergence or divergence record times of dip-slip activity (Wagreich and Schmid, 2002).

The difference in vertical position of two basement subsidence points at a given time  $i$  is expressed as  $\Delta S_i$ . The dip-slip values are calculated by subtracting  $\Delta S_{i-1}$  from  $\Delta S_i$  and divided by the duration of the stratigraphic interval (Fig. 1.8b; see also Hölzel, 2009). The results are presented in step plots of the slip rate vs. time (Fig. 1.8c). The values indicate the sense of dip-slip for relative block movement and, in zero values, fault inactivity or pure strike-slip motion (Wagreich and Schmid, 2002).

Vertical displacement rates of faults (Láb fault, Moravsky Jan fault, Laksary fault, Hodonin-Gbely fault and Lanshot-Hrusky fault) located in the northern and central parts of the Vienna Basin are presented in Appendix B.

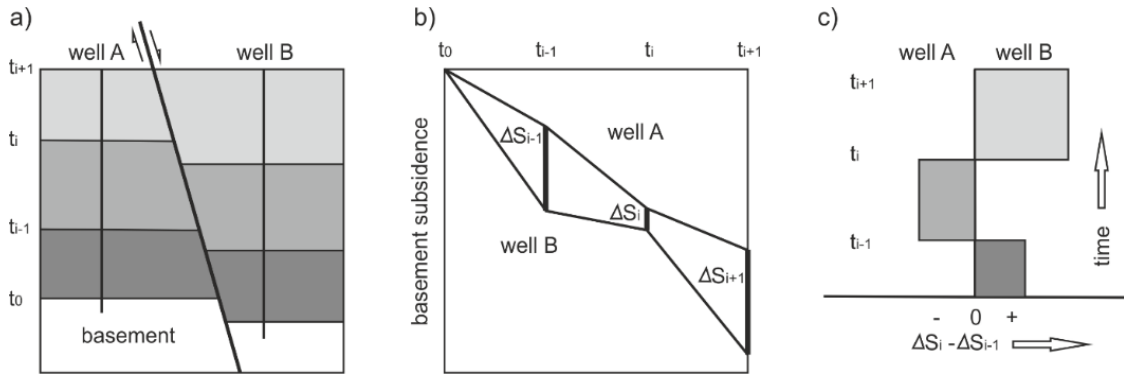


**Figure 1.8.** The dip-slip fault backstripping procedure (revised from Wagreich and Schmid, 2002). a) Two wells A and B on the footwall and the hangingwall of a synsedimentary normal fault, b) Basement subsidence curves of the two wells, and their difference ( $\Delta S$ ), c) Step plot of the apparent dip-slip rates ( $\Delta S_i - \Delta S_{i-1}$ ) vs. stratigraphic time along the fault.

## 1.6 POROSITY-DEPTH RELATION OF THE VIENNA BASIN

The subsidence analysis uses backstripping techniques including sediment decompaction (e.g. Allen and Allen, 2013). To calculate the thickness of a sediment layer at any time in the past (Decompaction), the appropriate porosity-depth curve is necessary (Fig. 1.9).

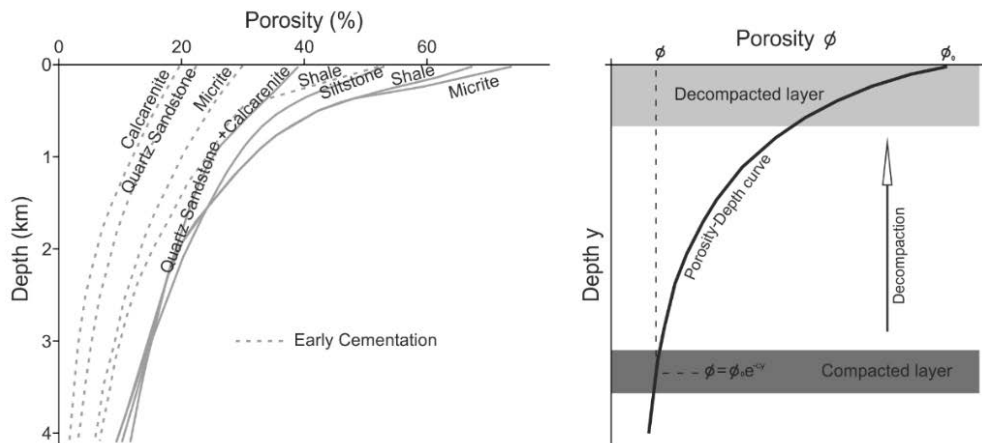


**Figure 1.9.** Empirical porosity-depth curves for different lithologies. Schematic diagram showing decompaction of a sedimentary layer at the surface and at depth (revised from Allen and Allen, 2013; Bond and Kominz, 1984).

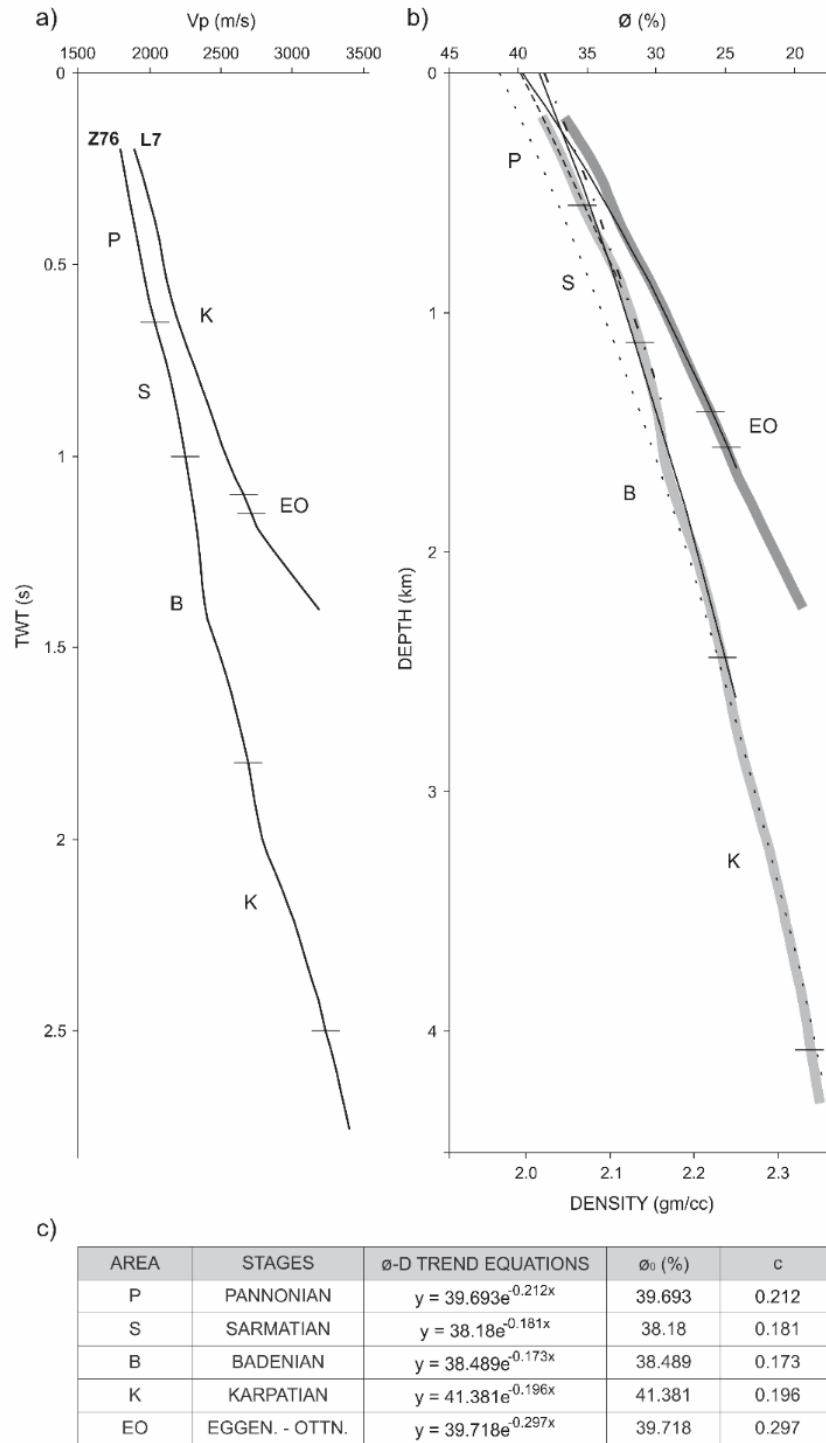


**Figure 1.10.** Porosity-Depth relation evaluated from two wells (Zv76 and LNV7) for the Vienna Basin. a) Porosity&Density-Depth curves with exponential trend lines of each stage, b) evaluated initial porosity ( $\phi_0$ ) and coefficient (c) of each stage.

Previous publications on subsidence in the Vienna Basin (e.g. Hölzel et al., 2008a, b; Lankreijer et al., 1995; Lee et al., 2011) have mainly used empirical porosity-depth relations from literature for specific lithologies of each layer (Tab. 1.2 and Fig. 1.9). However, for a more precise subsidence analysis, this study evaluated the on-site porosity-depth relation of the Vienna Basin based on geophysical data of two wells (Zv76 and LNV7) (Fig. 1.10). Seismic velocity data of the two wells were analyzed by recognizable correlations between seismic velocity-density and density-porosity. A commonly used relation between seismic velocity ( $V_p$ ) and density ( $\rho$ ) is defined by Gardner et al., (1974),

$$\rho = aV_p^{0.25}$$

The relation is simply an approximate average of the relations for a number of sedimentary rock types. The bulk density is a function of the average density of the rock types making up the formation and the relative volumes occupied, as shown by the equation (Allen and Allen, 2013),

$$\rho = \rho_s(1 - \phi) + \rho_v\phi$$

( $\rho_s$  and  $\rho_v$ : average densities of rock matrix and fluid occupying the pore space).

From this analysis, each main stratigraphic unit of the Vienna Basin fill gained an initial porosity ( $\phi_0$ ) and coefficient ( $c$ ) (Fig. 1.10). The initial porosity range of 38.2 – 41.4 % is applicable to the clay contents 0 – 10 % and 60 - 70 % in a microgeometrical model of porosity-clay content in sand-shale mixture (Marion, 1990). It is fitting well to main lithology types (sandy shale and shaly sand) reported in the Vienna Basin (Fig. 1.11).

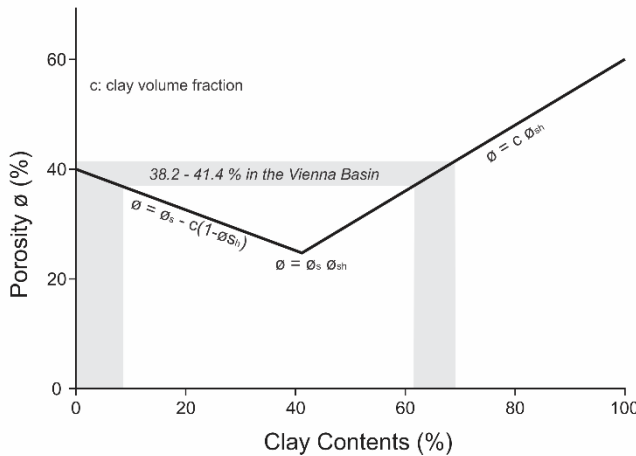


**Figure 1.11.** A micro-geometrical model of porosity-clay content in sand-shale mixture (revised from Marion, 1990). The controlling factor in the model results is the clay volume fraction  $c$  vs. sand porosity  $\phi$ .

## 1.7 THESIS OUTLINE

This thesis investigates the basin internal setting and the basin subsidence evolution of the Vienna Basin, targeting primarily the northern and central parts. The strength of this study results from the integration of a wide range of geological and geophysical data as well as from the interdisciplinary techniques including a custom MATLAB-based 3D modeling software developed as a part of this thesis.

This thesis consists of five chapters, and the introduction chapter is followed by three chapters which correspond to individual papers submitted to peer-review scientific journals.

### **Chapter 1 Introduction**

This chapter introduces general background information including study motivation and objectives for this thesis, geologic overview of the Vienna Basin, geological and geophysical database, and description of decompaction, backstripping and dip-slip fault backstripping techniques. The porosity-depth relation which is analyzed for the Vienna Basin is presented. Further information of well data and dip-slip fault backstripping is available in Appendix.

### **Chapter 2 Program for Basin Analysis: BasinVis 1.0**

This study develops a simple and user-friendly MATLAB-based software for modeling of basin stratigraphic and structural setting and subsidence analysis. BasinVis 1.0 analyzes stratigraphic profile (or well) data and calculate the stratigraphic data for basement and tectonic subsidence. This program is particularly aimed at displaying three dimensional maps to visualize stratigraphic setting and subsidence evolution of study area. The central Vienna Basin, a study area 30 x 40 km, is selected as an example for verification of the results obtained from the program BasinVis 1.0.

*Manuscript (BasinVis 1.0: A MATLAB-based program for sedimentary basin subsidence analysis and visualization) submitted to 'Computers & Geosciences'.*

### **Chapter 3 Quantitative Subsidence Analysis**

This chapter presents a detailed and quantitative analysis of the subsidence history of the northern, central parts and basement highs of the Vienna Basin.

The subsidence was analyzed through the high density of considered boreholes, the geophysical evaluation for more realistic porosity-depth relations and the mapping by employing a 2D interpolation technique. The results are compared with previous studies conducted in the Austrian part of the basin. Main objective of this contribution is to quantify polyphase tectonic subsidence evolution of the Vienna Basin.

*Manuscript (Polyphase tectonic subsidence evolution of the Vienna Basin inferred from quantitative subsidence analysis) submitted to 'International Journal of Earth Sciences'.*

#### **Chapter 4 3D modeling of Depositional setting and Subsidence**

Depositional setting and subsidence evolution of the northern and central parts of the Vienna Basin are modeled with BasinVis 1.0. The modeling of the depositional setting presents 3D sediments distribution models, 2D sediments isopach maps of each stage and cross-section profiles. The modeling of the basement and tectonic subsidence reconstructs 3D subsided depth models and 2D subsidence rate maps for each stage. These models provide insights into the tectonostratigraphic evolution and the paleogeographic effect in the Vienna Basin. This study analyzes basin evolution model of the Vienna Basin focusing particularly on changes in basin configuration through time.

*Manuscript (3D modeling of depositional setting and subsidence evolution in the northern and central Vienna Basin) submitted to 'Austrian Journal of Earth Sciences'.*

#### **Chapter 5 Final Conclusions**

The primary findings of this thesis are presented and ideas for future work are discussed.



## **CHAPTER 2**

# **PROGRAM FOR BASIN ANALYSIS:**

## **BasinVis 1.0**

*This chapter is based on:*

*Lee, E.Y.<sup>1)\*</sup>, Novotny, J.<sup>2)</sup>, Wagreich, M.<sup>1)</sup>, submitted. BasinVis 1.0: A MATLAB®-based program for sedimentary basin subsidence analysis and visualization. Submitted to Computers & Geosciences*

*<sup>1)</sup> Department of Geodynamics and Sedimentology, University of Vienna, Althanstrasse 14, Vienna 1090, Austria*

*<sup>2)</sup> Visualization Research Lab, Department of Computer Science, Brown University, 115 Waterman Street, Providence, RI 02912, USA*

*\* Corresponding author*

## **ABSTRACT**

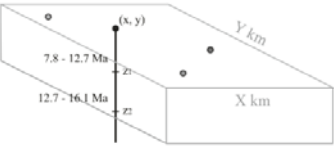
Stratigraphic and structural mapping is highly important to understand the internal setting of sedimentary basins. Subsequent subsidence analysis provides significant insights for basin evolution. This study developed a user-friendly program which allows geologists to analyze and model sedimentary basin data in a simple and straightforward workflow. This program, BasinVis 1.0, is designed to process and visualize stratigraphic setting and subsidence evolution of sedimentary basins from stratigraphic profile data. BasinVis 1.0 is implemented in MATLAB®, a multi-paradigm numerical computing environment, and employs two numerical methods; interpolation and subsidence analysis. Four different interpolation methods (Linear, Natural, Cubic Spline, and Thin-Plate Spline) are provided in this program for surface modeling. The subsidence analysis consists of decompaction and backstripping techniques. BasinVis 1.0 consists of five main processing steps; 1) setup (study area and stratigraphic units), 2) loading stratigraphic profile or well data, 3) stratigraphic setting visualization, 4) subsidence parameter input, and 5) subsidence analysis and visualization. For in-depth analysis, this software provides cross-section and dip-slip fault backstripping tools. The graphical user interface guides users through all process stages and provides tools to analyze and export the results. Interpolation and subsidence results are cached to minimize redundant computations and improve the interactivity of the program. All 2D and 3D visualizations are created by using MATLAB plotting functions, which enables users to fine-tune the results using the full range of available plot options in MATLAB. BasinVis 1.0 is distributed as open source software. Finally, this study demonstrates all functions in a case study of Miocene sediments in the central Vienna Basin.

## 2.1 INTRODUCTION

Sedimentary basins are the fundamental structural units where significant parts of Earth's system sedimentary strata were deposited. Detailed and specialized maps with various geoscientific information (e.g. stratigraphic subsurface, isopach, and structure) has become a prerequisite to understand the depositional and structural setting of a sedimentary basin, especially regarding hydrocarbon and ground water exploration (Allen and Allen, 2013). Furthermore, reconstruction by 2D and 3D modeling is required for the careful and precise study of basin evolution and provides significant insights for basin forming mechanisms. Despite high usefulness of mapping and modeling, several obstacles usually emerge while processing data from sedimentary basins. The main problem is the combination of geologic data with 3D modeling techniques. Geologic data are typically sparsely scattered over a large range of geological time and dimensional space, therefore the data have to be modeled by adequate interpolation methods. However, data interpolation usually requires critical programming knowledge and considerable time to process and model. While large (commercial) software suites take this into account, these programs are often expensive, complicated or both and therefore hard to access for academic earth scientists and students.

This study focused on developing a simple and user-friendly program that allows geologists to analyze and model sedimentary basin data. The developed software, BasinVis 1.0, is particularly aimed at stratigraphic and subsidence 2D/3D modeling of sedimentary basins with stratigraphic profile or well data, interpolation methods, and subsidence analysis techniques. This program interpolates input data (three dimensional depth data), and displays 3D models to visualize stratigraphic setting of each stratigraphic unit and basin scale. It calculates the stratigraphic data for subsidence analysis which has been used widely in basin studies since Van Hinte (1978), and produces graphs and interpolated-models for basement subsidence, tectonic subsidence, and their respective rates. The cross-section and dip-slip fault backstripping functions of this program provide insights into the internal basin structure and vertical fault displacement. In this study four different interpolation methods are available; Linear, Natural, Cubic Spline, and Thin-Plate Spline interpolation. The outputs are useful in the understanding of internal setting and stratigraphic and tectonic evolution of a basin.

Several publications studied programming and algorithms for basin subsidence analysis (e.g. Friedinger, 1988; Hölzel et al., 2008a; Jin, 1994; Springer, 1993; Stam et al., 1987). Different from the previous studies, this study chooses MATLAB® as a numerical computing environment for programming and provides 2D/3D visualization function. MATLAB® is a software package developed by MathWorks Inc. and designed to perform mathematical calculations, to analyze and visualize data, and to facilitate the writing of new software programs (Trauth and Sillmann, 2013). MATLAB is a powerful tool for software development and the language is relatively easy to learn. It contains a large collection of functions from different scientific and technical fields such as image and signal processing and statistics that access state-of-the-art libraries for matrix and sparse matrix computation (Schwanghart and Kuhn, 2010). During the last few years it has been extensively and widely used in academic, research, and industrial fields. In the Earth sciences, various MATLAB-based programs have been developed to process, analyze, and visualize data (e.g. Chen et al., 2013; Lanari et al., 2014; Monnet et al., 2003; Ricard and Chanu, 2013; Witten, 2002; Witten, 2004).

Parameter	Symbol	Description	Example																				
Study Area Location Depth Geologic Age	X, Y, Z x, y z <sub>1</sub> , z <sub>2</sub> , ... Ma, ka, yr	a size of mapping and modeling area x, y coordinators top depth of each stratigraphic unit geologic age of each stratigraphic unit																					
Initial Porosity Coefficient Densities	$\phi_0$ c $\rho_s$ $\rho_m$ $\rho_w$	initial porosity of porosity-depth relation (%) coefficient of porosity-depth relation ( $\times 10^{-5}$ ) average density of sediment grain ( $\text{g/cm}^3$ ) average density of mantle ( $3.3 \text{ g/cm}^3$ ) average density of water ( $1.0 \text{ g/cm}^3$ )	from Sclater and Christie (1980) <table border="1"> <thead> <tr> <th></th><th><math>\phi_0</math></th><th>c</th><th><math>\rho_s</math></th></tr> </thead> <tbody> <tr> <td>Shale</td><td>63</td><td>0.51</td><td>2.72</td></tr> <tr> <td>Sand</td><td>49</td><td>0.27</td><td>2.65</td></tr> <tr> <td>Shaly Sand</td><td>56</td><td>0.39</td><td>2.68</td></tr> <tr> <td>Chalk</td><td>70</td><td>0.71</td><td>2.71</td></tr> </tbody> </table>		$\phi_0$	c	$\rho_s$	Shale	63	0.51	2.72	Sand	49	0.27	2.65	Shaly Sand	56	0.39	2.68	Chalk	70	0.71	2.71
	$\phi_0$	c	$\rho_s$																				
Shale	63	0.51	2.72																				
Sand	49	0.27	2.65																				
Shaly Sand	56	0.39	2.68																				
Chalk	70	0.71	2.71																				
Water-depth Sea-level	$W_d$ $\Delta_{SL}$	paleowaterdepth paleosealevel																					

**Table 2.1.** Required input data in BasinVis 1.0. Study area, location, depth and geologic age data are needed for setup stage. Initial porosity, coefficient, densities, paleowaterdepth and paleosealevel data are needed for subsidence analysis.  $3.3 \text{ g/cm}^3$  and  $1.0 \text{ g/cm}^3$  are used generally for average densities of mantle and water respectively.

## 2.2 INTERPOLATION METHODS

This section introduces the provided interpolation methods and details about the properties of their reconstructed surfaces. Since data locations are often distributed sparsely over the study area, this study uses a set of four surface interpolation methods for irregular data points. This study samples the interpolants on a tight grid covering the study area (gridded interpolation) to integrate it with MATLAB 3D surface plotting functions. The methods differ in the smoothness class of their interpolated surfaces. Three methods – linear, natural and cubic spline interpolation – can be classified as Local Neighborhood approaches, while the forth one – Thin plate spline interpolation – is a global approach (Albrecht, 2007; Mitas and Mitasova, 1999). This study lists them with increasing surface smoothness:

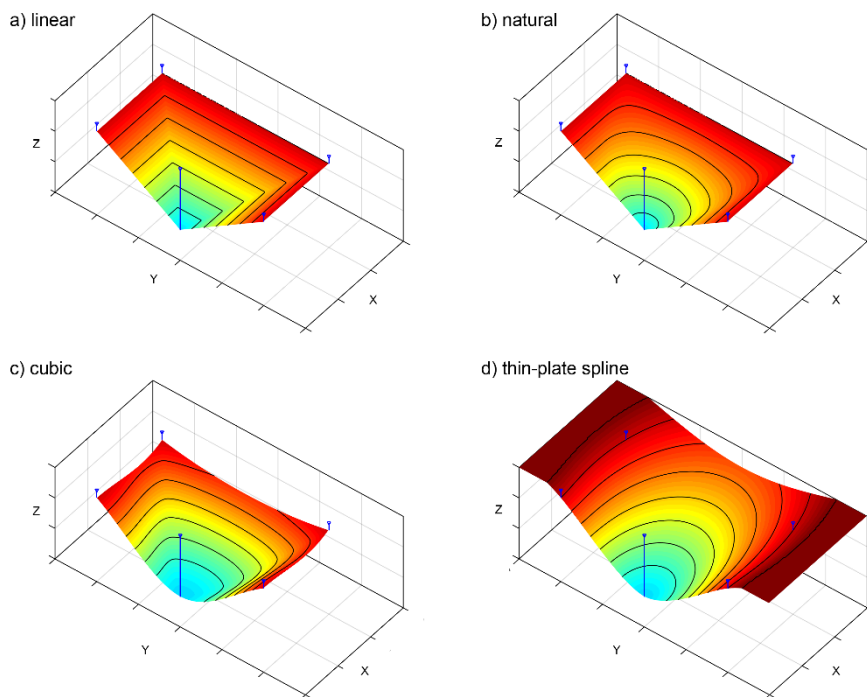


**Figure 2.1.** Interpolation methods and their continuity class shown on a simple example with five data points; a) linear ( $C^0$ , discontinuities at edges and data locations), b) natural ( $C^1$ , discontinuities only at data locations), c) cubic spline ( $C^2$ , no discontinuities) and d) thin-plate spline ( $C^2$ , no discontinuities and extrapolation). Application examples of each method are shown in the Figures 2.2, 2.10 and 2.15.

### 2.2.1 Linear Interpolation

Linear interpolation is based on a triangulated irregular network (TIN) created from  $x$  and  $y$  coordinates of data points using Delaunay tessellation. Including  $z$  coordinates of data points into this network creates a 3 dimensional triangle mesh. The interpolation function within a given triangle is defined as

$$f_{linear}(x, y) = b_1 z_1 + b_2 z_2 + b_3 z_3$$

where  $b_1$ ,  $b_2$  and  $b_3$  are the barycentric coordinates of point  $(x, y)$  within the corresponding triangle and  $z_1$ ,  $z_2$  and  $z_3$  are the depth values at the corner points of the triangle (Amidror, 2002). The surface of this mesh has  $C^0$  continuity within the convex hull of the data points in the X-Y plane (Watson and Philip, 1984) and features sharp edges and peaks. The differentiability class  $C^k$  of a surface defines that the  $k$ th derivative of the surface exists and is continuous. The interpolated surface is obtained by sampling the 3D planes described by the triangles at each 2D point of the sampling grid (Fig. 2.1a).

### 2.2.2 Natural Interpolation

Natural neighbor interpolation calculates the weighted average of multiple data points surrounding each sample location. Neighbors and weights are obtained by inserting a sample point into the Voronoi tessellation of all data point coordinates in the X-Y plane. This is described by the interpolation function (Sibson, 1981),

$$f_{natural}(x, y) = \sum_{i=1}^n w_i z_i$$

where  $n$  is the number of natural neighbors of the point  $(x, y)$ ,  $w_i$  are the weights based on the Voronoi tessellation and  $z_i$  are the corresponding depth values. The resulting surface is  $C^1$  continuous, which means it smooth in all areas except directly at the data points (Bobach and Umlauf, 2006). It models the physical behavior of a rubber sheet fixed to the locations of the data points (Mitas and Mitasova, 1999) (Fig. 2.1b).

### 2.2.3 Cubic Spline Interpolation

Like the linear interpolation, the cubic spline approach is based on a TIN created by Delaunay tessellation. The surface in each triangle is interpolated by a

bivariate cubic spline function. To achieve  $C^2$  continuity, functions are constrained to match the surface positions and gradients of their neighboring triangles along each edge. Multiple solutions for this piecewise optimization problem have been proposed (Lai, 2008; Watson, 1992). In this software this study uses the MATLAB implementation of the solution discussed in Yang, 1985 (Fig. 2.1c).

#### 2.2.4 Thin-Plate Spline Interpolation

The surfaces created by the presented local interpolation approaches are only defined within the convex hull of data points and do not allow extrapolation of the data to the borders of the study area. To address this problem, this study included the thin-plate spline (TPS) approach, which is not based on initial triangulation. The TPS models the bending behavior of a thin metal sheet passing through all data points. This method calculates parameters and weights of the thin-plate spline function  $f_{TPS}$  (Whaba, 1990) that minimize the error function  $E_f$  and the surface roughness measure  $R_f$  for the provided data points,

$$f_{TPS}(x, y) = t(x, y) + \sum_{i=1}^p w_i \varphi(\|(x_i, y_i) - (x, y)\|)$$

$$\arg \min_f \left( \overbrace{\sum_{i=1}^p (z_i - f(x_i, y_i))^2}^{E_f} + \lambda \overbrace{\iint_{\mathbb{R}^2} (f_{xx}^2 + 2f_{xy}^2 + f_{yy}^2) dx dy}^{R_f} \right)$$

where  $t$  is a trend function that captures surface variations;  $p$  is the number of data points;  $x_i, y_i$  and  $w_i$  are the positions and weights at given data points; and  $\varphi$  is the radial basis function of the biharmonic spline,  $\varphi(r) = r^2 \log r$ . In the approach this study uses the summed squared error at data point locations as error function  $E_f$  and the roughness measure of the second-order bivariate TPS  $R_f$  (Iske, 2004).  $\lambda$  is a positive regularization parameter that controls the surface smoothness. The lower bound  $\lambda = 0$  results in an exact interpolation, higher values generate smoother approximation surfaces that are not guaranteed to pass through data points. The resulting surface has  $C^2$  continuity and inter- and extrapolates the data points over the entire study area (Fig. 2.1d).

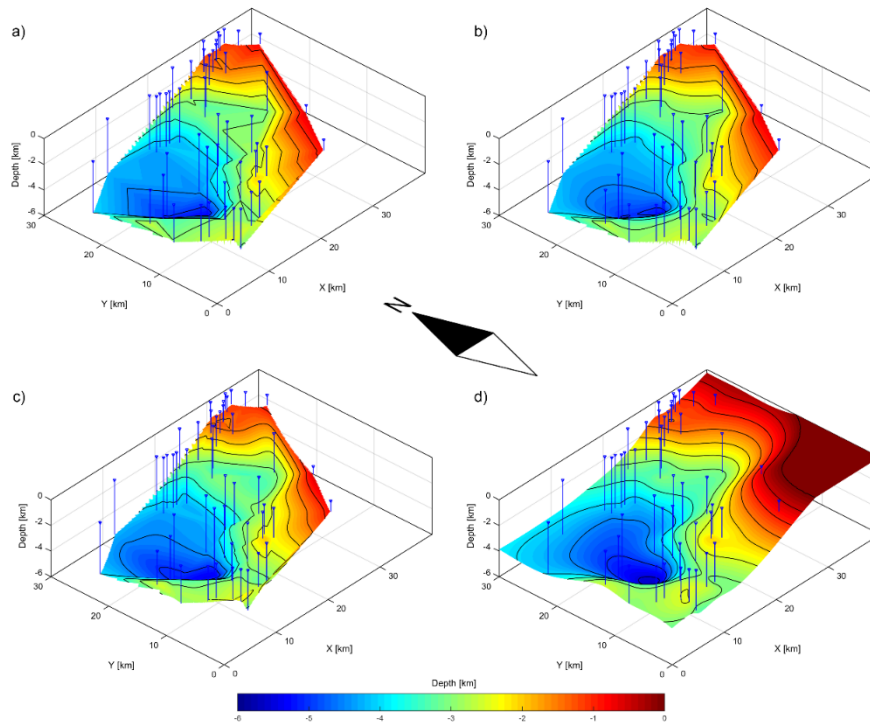


**Figure 2.2.** Interpolation methods; a) linear, b) natural, c) cubic spline and d) thin-plate spline. The example shows the top depth mapping of the Pre-Neogene Basement in the case study area.

The four interpolation methods listed above are implemented in BasinVis 1.0 based on functions of the MATLAB Curve Fitting Toolbox. Users may choose the best method based on the geological characteristics of their data and their research goals. The interpolation functions of BasinVis 1.0 are in a modular way. This allows researchers with MATLAB programming experience to extend the software with custom interpolation methods.

## 2.3 EXAMPLE APPLICATION DATA BACKGROUND

The Vienna Basin located in the central Europe (Fig. 2.3a) was selected as an example for the evaluation of BasinVis 1.0. It is one of the most explored and studied basins worldwide and therefore an ideal place to assess the functions of this program. A number of data is available to analyze and visualize stratigraphic setting and subsidence evolution, and previous publications provide comparison points for the results of BasinVis 1.0.

The Miocene evolution of the Vienna Basin is divided into two major basin stages; Early Miocene piggy-back basin and Middle – Late Miocene pull-apart basin (Decker, 1996; Royden, 1985) (Fig. 2.3c). The Vienna Basin started with the E-W trending piggy-back depressions formed on top of the Alpine thrust belt during the Early Miocene (c. 20 – 17 Ma). Around the end of the Early Miocene (c. 17 – 16), the region became a sinistral pull-apart structure formed by Miocene lateral extrusion of the Eastern Alps, and the accommodation of the basin was filled with enormous amounts of sediment (up to 6 km thick). From c. 8 Ma, the basin halted subsidence and experienced basin inversion.

The area modeled in this study covers 30x40 km<sup>2</sup> of the central Vienna Basin, lying mainly on the hanging wall of the prominent Steinberg fault (Fig. 2.3a). The area also contains the negative flower structure of the Leitha fault system (Decker, 1996; Hinsch et al., 2005b).

For the case study, a total of 110 wells reaching Miocene sediments fills were arranged in the study area (Fig. 2.3b). 95 wells in the Slovak part were acquired from the Dionyz Štur Institute, Slovakia and 7 wells in the Austrian part from Hölzel (2009). 8 synthetic wells were created from seismic sections and published maps for interesting areas where no public well data were available. Particularly, 32 wells reaching the pre-Neogene basement were selected for subsidence analysis. This study used  $\phi_0$  and  $c$  evaluated geophysically for the Vienna Basin (Fig. 1.10).  $W_d$  and  $\Delta_{SL}$  variations of the region were assumed from paleoenvironment models of Sauer et al. (1992) and Seifert (1992) (Fig. 1.6).

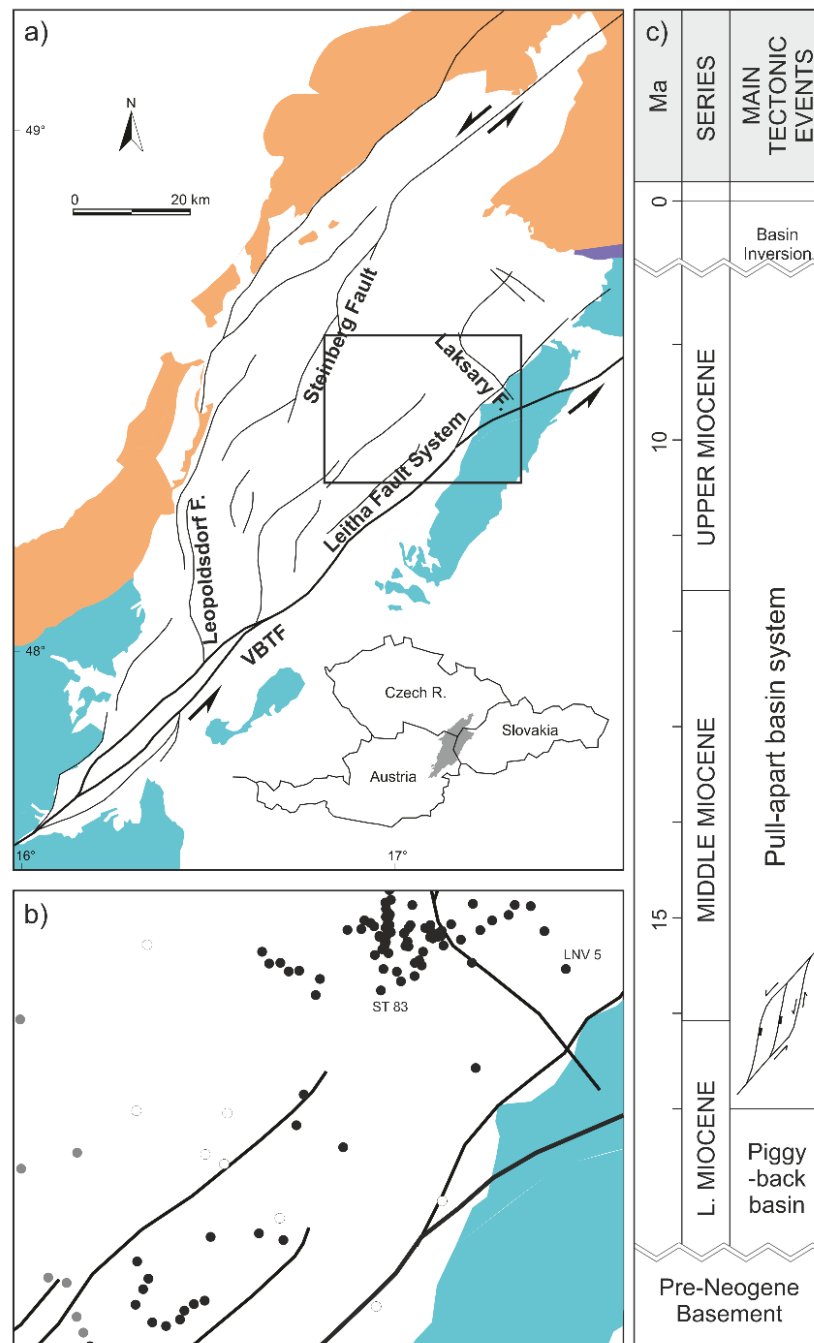


**Figure 2.3.** a) Structural outline of the Vienna Basin and location of the study area, b) locations of the studied wells (black dot: wells from the Dionyz Štur Institute, gray dot: wells from Hölzel (2009), and white dot: synthetic wells), c) General tectonic evolution of the Vienna Basin (Decker, 1996; Hölzel, 2009; Wessely et al., 1993).

## 2.4 PROGRAM FRAMEWORK

BasinVis 1.0 is implemented entirely in MATLAB® version 8.4 (R2014b) and requires the ‘Symbolic Math’ and ‘Curve Fitting’ Toolboxes (Math, Statistics, and Optimization package). It can be operated under Microsoft Windows (XP or higher), Mac OS X (10.7.4+ or higher), and recent Linux distributions (e.g. Ubuntu 14.04).

Figure 2.4 outlines the main scripts and functions within the workflow of BasinVis 1.0 and describes their high-level goals. The program is started by running the ‘mainwindow.m’ script in the program folder, which opens the main program window.

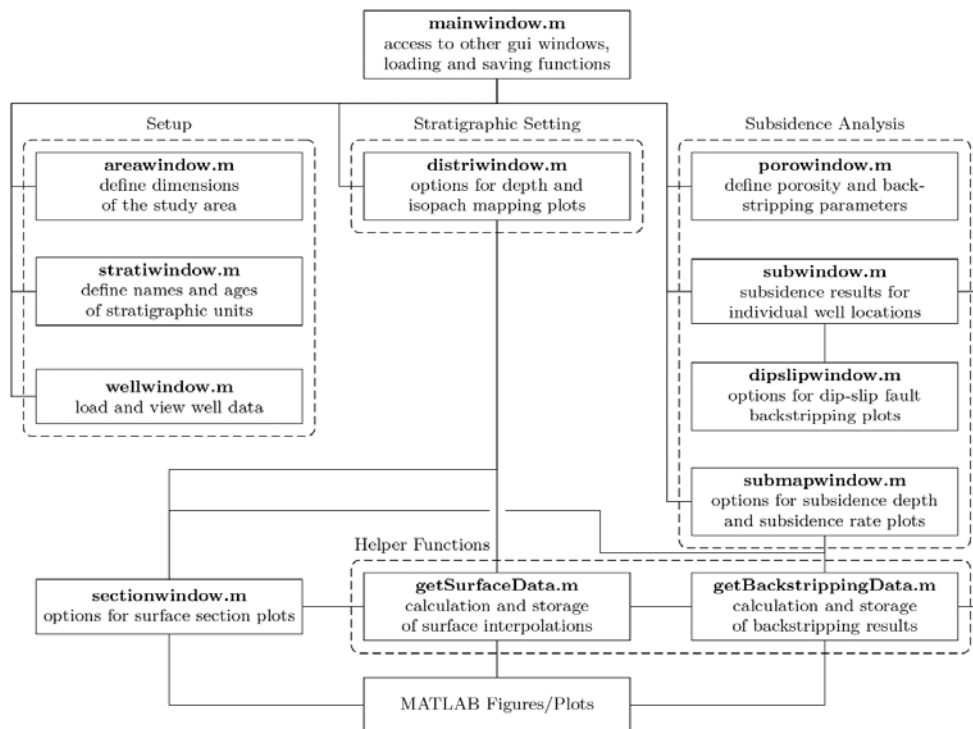


**Figure 2.4.** Workflow chart of BasinVis 1.0's functions.

The main window (Fig. 2.5) acts as central hub to all functions and process stages of BasinVis 1.0. Function buttons (Study Area, Stratigraphic Units, Well Data Input, Stratigraphic Modeling, Parameter Input, Subsidence Analysis, Subsidence Modeling) are arranged to follow the order of the work flow and are enabled as soon as all required data for the individual operations have been entered.



**Figure 2.5.** Main menu of the program, BasinVis 1.0.

### 2.4.1 Setup

In the setup stage a new project is initialized by defining the extent of the study area (Fig. 2.6), the stratigraphic unit names and their corresponding geologic ages (Fig. 2.7). The study area is used as boundary for all interpolation and visualization results.

This study uses the stratigraphic unit names and the geologic ages based on the regional Central Paratethys chronostratigraphy for the Miocene and regional and local zonations for the Vienna Basin (e.g. Hohenegger et al., 2014; Piller et al., 2007); EO (Eggenburgian-Ottnangian), LKA (Lower Karptian), UKA (Upper Karpatian), LBA (Lower Badenian), UBA (Upper Badenian), SA (Sarmatian), PA (Pannonian).

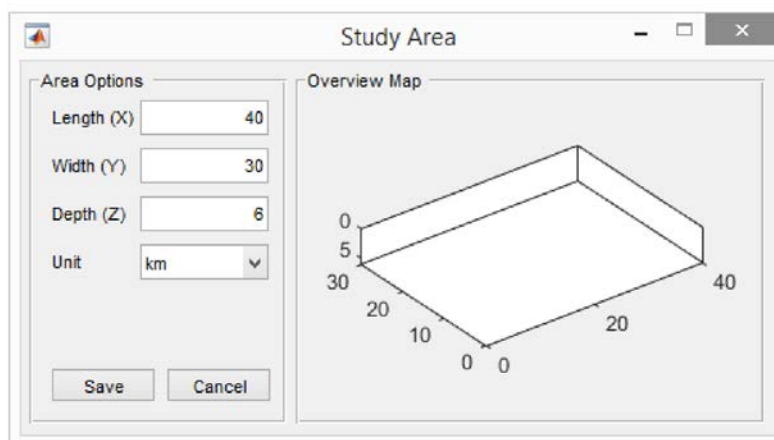
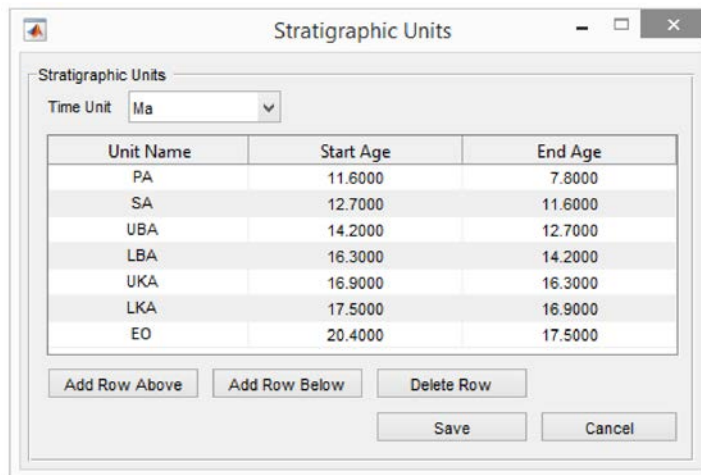


**Figure 2.6.** Setup of the extent of the study area. (See Figure 2.3b for the location).

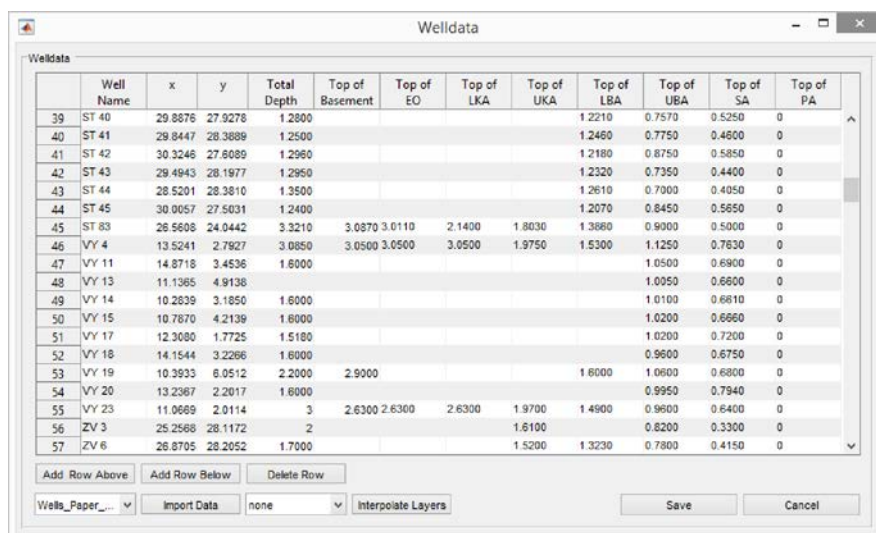


Stratigraphic Units

Time Unit:

Unit Name	Start Age	End Age
PA	11.6000	7.8000
SA	12.7000	11.6000
UBA	14.2000	12.7000
LBA	16.3000	14.2000
UKA	16.9000	16.3000
LKA	17.5000	16.9000
EO	20.4000	17.5000

**Figure 2.7.** Setup of the stratigraphic unit and their corresponding geologic ages.



Welldata

	Well Name	x	y	Total Depth	Top of Basement	Top of EO	Top of LKA	Top of UKA	Top of LBA	Top of UBA	Top of SA	Top of PA
39	ST 40	29.8876	27.9278	1.2800					1.2210	0.7570	0.5250	0
40	ST 41	29.8447	28.3889	1.2500					1.2460	0.7750	0.4600	0
41	ST 42	30.3246	27.6089	1.2960					1.2180	0.6750	0.5850	0
42	ST 43	29.4943	28.1977	1.2950					1.2320	0.7350	0.4400	0
43	ST 44	28.5201	28.3810	1.3500					1.2610	0.7000	0.4050	0
44	ST 45	30.0057	27.5031	1.2400					1.2070	0.8450	0.5650	0
45	ST 63	26.5608	24.0442	3.3210	3.0870	3.0110	2.1400	1.8030	1.3680	0.9000	0.5000	0
46	VY 4	13.5241	2.7927	3.0850	3.0500	3.0500	3.0500	1.9750	1.5300	1.1250	0.7630	0
47	VY 11	14.8718	3.4536	1.6000						1.0500	0.6900	0
48	VY 13	11.1365	4.9138							1.0050	0.6600	0
49	VY 14	10.2839	3.1850	1.6000						1.0100	0.6610	0
50	VY 15	10.7870	4.2139	1.6000						1.0200	0.6660	0
51	VY 17	12.3080	1.7725	1.5180						1.0200	0.7200	0
52	VY 18	14.1544	3.2266	1.6000						0.9600	0.6750	0
53	VY 19	10.3933	6.0512	2.2000	2.9000				1.6000	1.0600	0.6800	0
54	VY 20	13.2387	2.2017	1.6000						0.9950	0.7940	0
55	VY 23	11.0669	2.0114	3	2.6300	2.6300	2.6300	1.9700	1.4900	0.9600	0.6400	0
56	ZV 3	25.2568	28.1172	2				1.6100		0.8200	0.3300	0
57	ZV 6	26.8705	28.2052	1.7000				1.5200	1.3230	0.7800	0.4150	0

**Figure 2.8.** Well Data input. Each profile is defined by name, location relative to the study area and a list of the top depths for the previously set stratigraphic units.

The 'Welldata' window is used to input stratigraphic profile information manually or to load it from a Microsoft Excel data source (Fig. 2.8). Each profile is defined by name, location relative to the study area and a list of the top depths for the previously set stratigraphic units. If a unit does not exist at a given profile location it has to be reported at the same depth as its overlying layer. In practice, not every profile reaches the basement layer and in some cases not every boundary

between sedimentary layers is reported with a depth value. To accommodate for these cases we allow empty depth value fields, indicating that these depths will be interpolated in the subsequent processes.

### 2.4.2 Stratigraphic setting and Visualization

BasinVis 1.0 provides a simple user interface to generate a variety of 2D and 3D data plots. We use MATLAB implementations of four interpolation techniques and store surface results in a regular grid representation. Results can be visualized as combination of multiple plots; well locations, contours and surfaces in 2D and 3D. The user interface provides access to a set of basic plot options (Fig. 2.9). Figure 2.10 shows example visualizations of the stratigraphic unit LKA of our study area. Well locations are marked by blue lines, and the interpolated 3D top-depth surface is drawn with a colormap encoding its depth. The optional 2D contour plot below the surface plot shows the sediments thickness of the layer at the study area.

All visualizations are generated in standard MATLAB plot windows, giving users access to advanced plot options to customize visualization results. The surface plots of our case study use a user-defined color map to demonstrate this option. Additionally we use an axis scaling factor for the z-axis to emphasize surface features. Visualizations can be exported to the wide range of image formats supported by MATLAB.

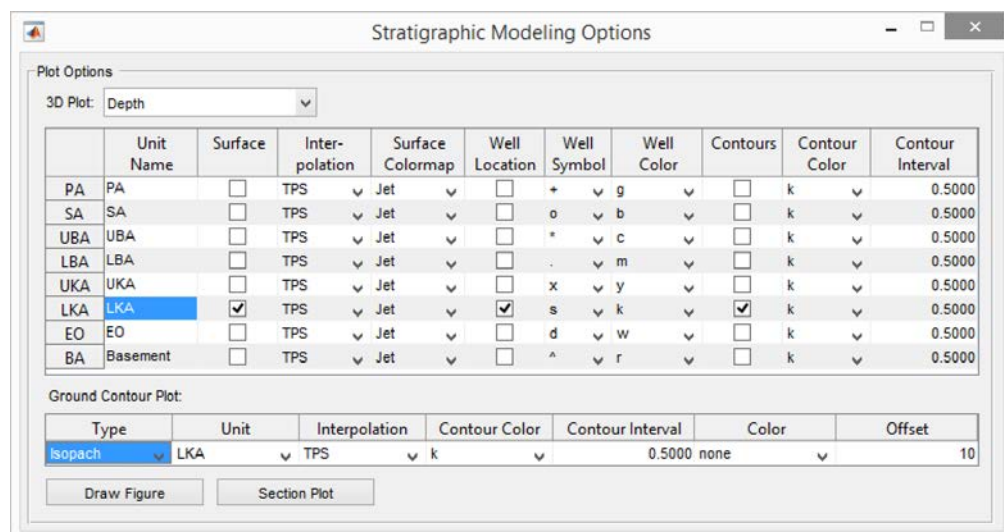


**Figure 2.9.** Stratigraphic modeling interface.

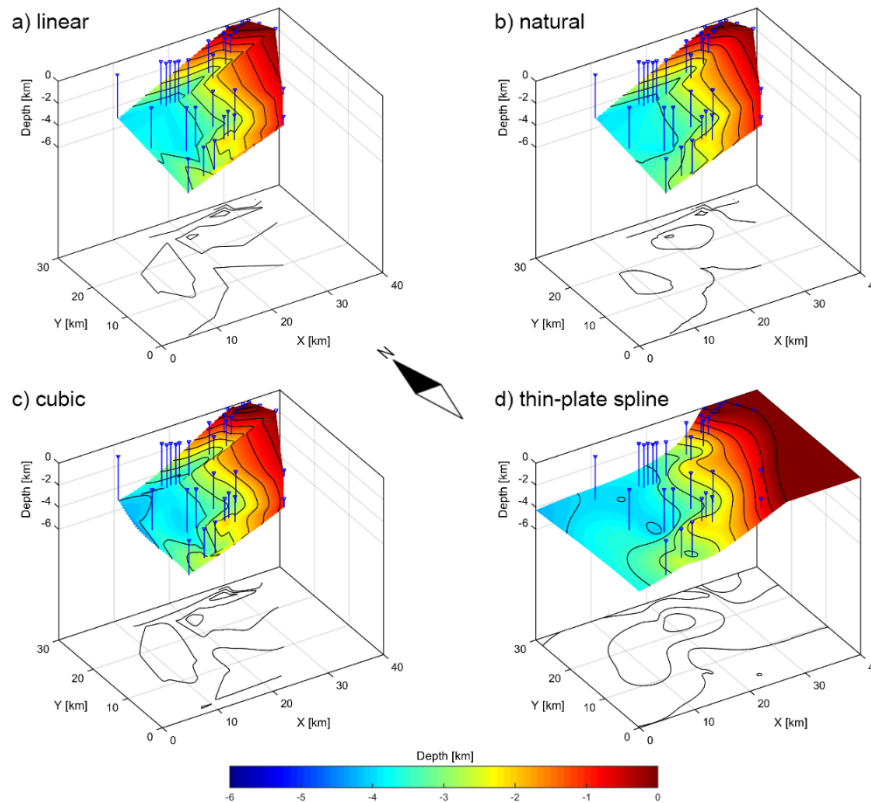


**Figure 2.10.** Stratigraphic setting visualization; a) linear, b) natural, c) cubic spline and d) thin-plate spline. Example stratigraphic visualization of the stratigraphic unit LKA deposited during 17.5 – 16.9 Ma; 3D top-depth distribution surface model (above) and 2D sediments isopach map (below).

By default, stratigraphic setting models are generated by directly interpolating the layer depth data at well locations. While this is a very straight forward method, it is possible that the resulting layer depth surfaces intersect each other in areas with insufficient data or extreme depth changes. To mitigate this problem this study also offers an interpolation mode that combines thickness interpolations (Isopach) of all overlaying layers to generate the depth surface of a given layer. This mode prevents layer intersections, but due to the combination interpolation errors may increase, especially in the lowest layers.

### 2.4.3 Subsidence analysis and Visualization

The 'Subsidence Parameters' window handles the input of additional parameters required for the subsidence analysis (see Chapter 1.5 for the calculation methods). Default values are required for each stratigraphic unit. However, these values can be adjusted individually for each well, if more accurate data is available at each well (Fig. 2.11).

The 'Subsidence Analysis' window allows users to inspect numerical subsidence results at individual well locations in a table representation (Fig. 2.12). Additionally basement and tectonic subsidence depth and rates can be explored in 2D plots. Displayed example is the subsidence analysis results for the well ST 83, which penetrates all stratigraphic layers and the basement (Fig. 2.13).

	Init. Porosity	c	Waterdepth	Sealevel	Sed. Density
PA	0.3972	0.2970	0.0500	0	2.6800
SA	0.4138	0.1960	0.1000	0	2.6800
UBA	0.3849	0.1730	0.1000	0	2.6800
LBA	0.3849	0.1730	0.1000	0	2.6800
UKA	0.3818	0.1810	0.2000	0	2.6800
LKA	0.3818	0.1810	0.1000	0	2.6800
EO	0.3969	0.2120	0.0500	0	2.6800

**Figure 2.11.** Subsidence parameters input; Initial porosity, coefficient (c), waterdepth, sealevel and average sediment density. Example parameter data for a well, ST 83 (see Figure 2.3b for location of the well ST 83).

	7.8 Ma	11.6 Ma	12.7 Ma	14.2 Ma	16.3 Ma	16.9 Ma	17.5 Ma
PA	0.5	0.42402	0.52593	0.46827	0.39107	1.0163	0.099132
SA	0.9	0.92962	0.97192	0.84193	1.373	1.1044	
UBA	1.386	1.361	1.3293	1.7094	1.4583		
LBA	1.803	1.7084	2.245	1.8717			
UKA	2.14	2.6017	2.3247				
LKA	3.011	2.8795					
EO	3.087						
Base Sub	3.0870	2.6795	2.3247	1.8717	1.4583	1.1044	0.0991
Base Sub Rate	0.1072	0.3226	0.3020	0.1969	0.5898	1.6755	0.0342
Tect Sub	1.5530	1.3777	1.1838	1.0539	0.8021	0.6866	0.0917
Tect Sub Rate	0.0461	0.1763	0.0866	0.0961	0.2759	0.9914	0.0316

**Figure 2.12.** Subsidence analysis numerical result of a well ST 83 (see Figure 2.3b for location of the well ST 83).

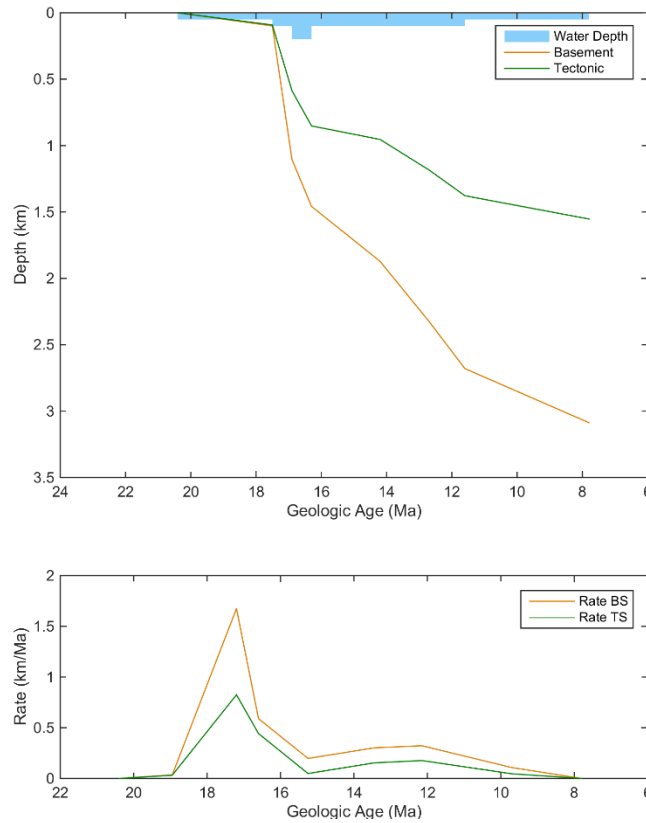


**Figure 2.13.** Subsidence analysis. 2D graph plots for basement and tectonic subsidence depths (km) and rates (km/Ma) from the well ST 83 (see Figure 2.3b for location of the well ST 83).

3D subsidence modeling can be created by interpolating basement and tectonic subsidence data at different geologic ages. It has to be noted that only wells penetrating the basement layer are used in this process. To generate surface results, this study provides the same set of interpolation and plotting methods as used in the stratigraphic setting analysis (Fig. 2.14 and 2.15). The optional 2D contour plot below the subsidence plot shows the subsidence rate during each geologic age stage. An additional mask option allows users to define basin borders, excluding outside regions from the surface interpolation process. Masks can be defined individually for each layer to accommodate for changes in the basin structure.

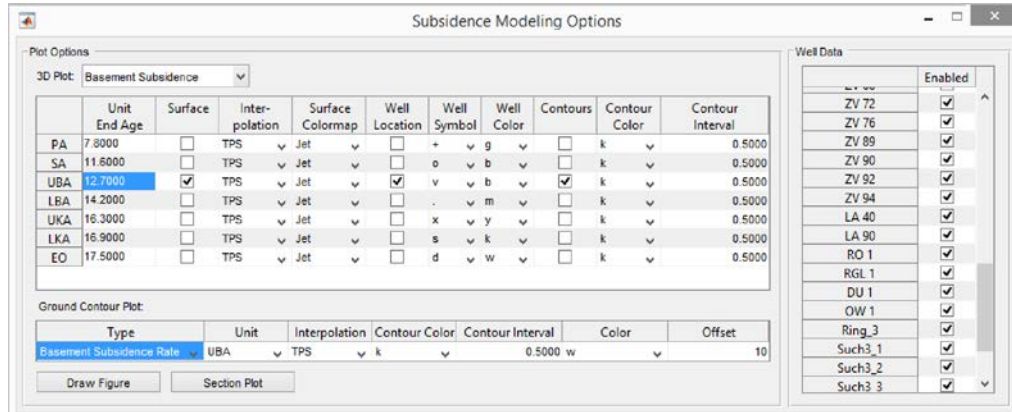


**Figure 2.14.** Subsidence modeling interface.

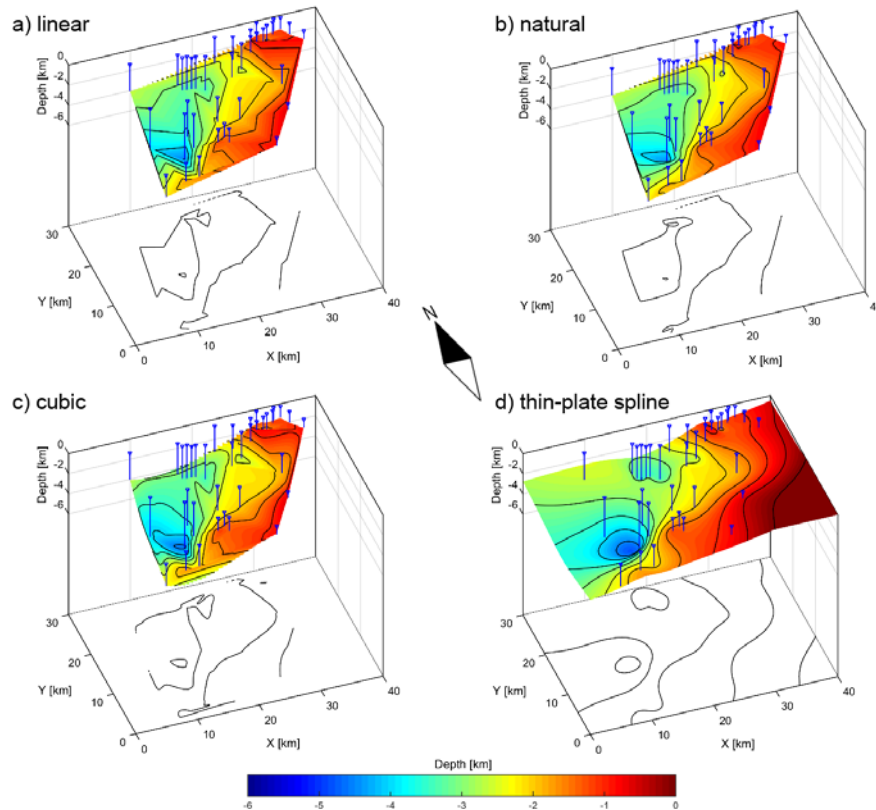


**Figure 2.15.** Subsidence modeling visualization; a) linear, b) natural, c) cubic spline, and d) thin-plate spline. Example subsidence visualization for subsided basement depths (km) at 12.7 Ma (above) and basement subsidence rates (km/Ma) during 14.2 – 12.7 Ma (below).

### 2.4.4 Cross-section

To aid users in the analysis of specific regions, this study provides the 'Cross-section Plot' window, which enables them to create 2D section plots. Section locations can be defined as axis-aligned line (parallel to the x or y-axis) by selecting a single point on a 2D map of the study area or as arbitrary line by selecting a point pair (Fig. 2.16).

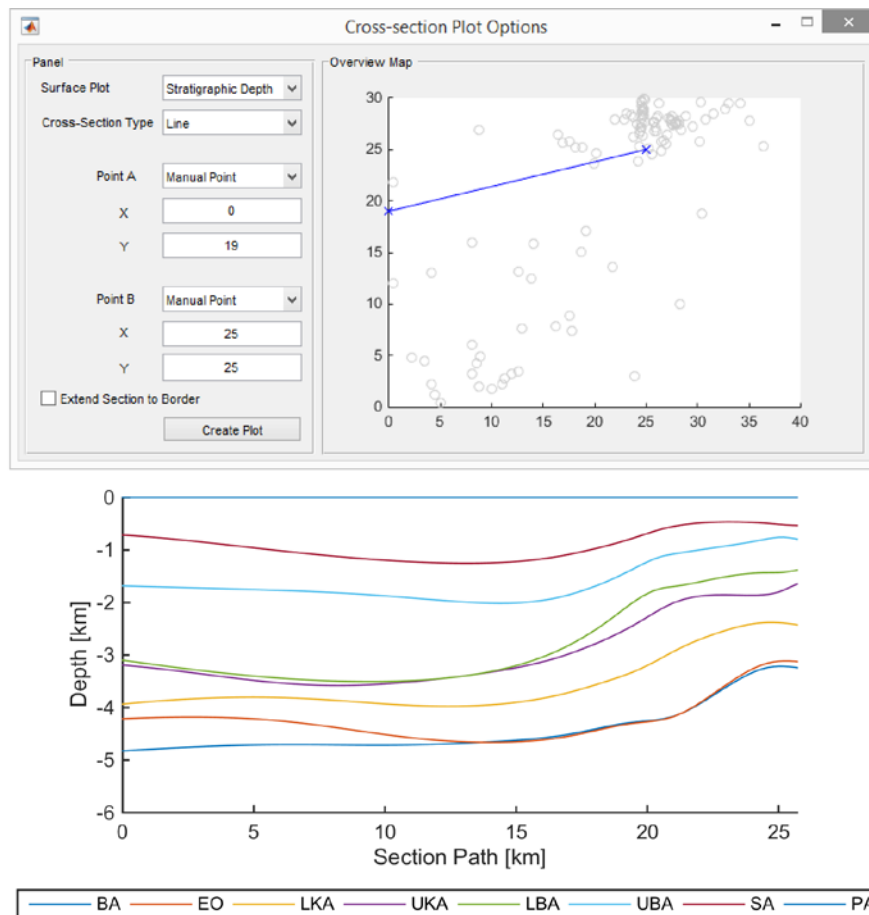


**Figure 2.16.** Cross-section plot option with preview of the section location and generated section plot.

### 2.4.5 Dip-slip Fault Backstripping

The fault backstripping function can be accessed through the 'Dip-Slip Fault Backstripping' window (see Chapter 1.5.3 for the calculation method). Guided by a preview map, users select a pair of well locations eligible for dip-slip backstripping and can generate step or line plots of the vertical fault displacement rates between them (Fig. 2.17).

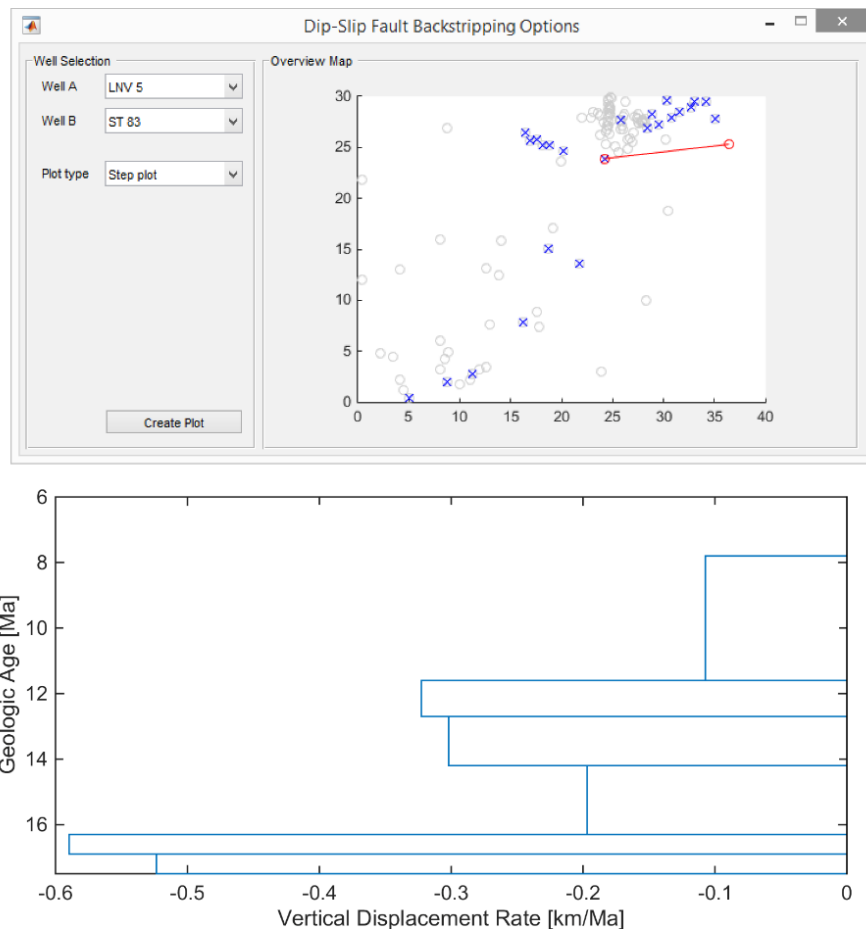


**Figure 2.17.** Dip-slip fault backstripping of the Laksary fault between the wells LNV 5 and ST 83 (see Figure 2.3b for well locations).

## 2.5 DISCUSSION AND CONCLUSIONS

This MATLAB-based program, BasinVis 1.0, was designed to analyze and visualize stratigraphic setting and subsidence evolution of a sedimentary basin. It performs the goal, and provides geologists with an easy-to-learn and user-friendly program for sedimentary basin analysis. The structure of the program allows researchers with programming experience to edit and extend the functionalities of the software if needed.

### 2.5.1 Evaluation of Example Application

This study compared the results of BasinVis 1.0 with previous stratigraphy, structure and subsidence studies conducted in the central Vienna Basin (e.g. Hölzel, 2009; Jiříček and Seifert, 1990; Kováč et al., 2004; Lankreijer et al., 1995). The final results match those of preceding works and in several cases provide even better model representations (e.g. Lee and Wagreich, submitted; Chapter 3). Although the interpretation introduces uncertainty into detailed model visualizations, especially in the western part due to the lack of the stratigraphic profile data, they are highly useful to understand overall geologic trends and characteristics of each geologic stage.

The top depth subsurface model of the Pre-Neogene basement of the Vienna Basin (Fig. 2.2) is reflecting the structural trend of the basement and is comparable with previous maps (e.g. Wessely et al., 1993). The top-depth surface and isopach models of a stratigraphic unit LKA (Fig. 2.10) show features of the shallow and NE-SW trending piggy-back basin. The displayed subsidence results of the well ST 83 (Fig. 2.13) represent a typical subsidence pattern of the central Vienna Basin, with shallow piggy-back subsidence and abruptly increasing pull-apart subsidence. The subsidence model of the pull-apart system is visualized as interpolating the subsidence depths and rates at 12.7 Ma (Fig. 2.15). In the models, subsidence is deeper along the major faults (Fig. 2.3a) and data reflect regional highs and lows formed during the pull-apart tectonic events.

### **2.5.2 Unsatisfactory parts**

Unsatisfactory surface depth mapping results were mainly found near or at fault structures. The provided interpolation methods including TPS currently do not completely integrate the displacement and timing of faults. Resulting surfaces are therefore smoothing out the sharp features at these locations. A similar problem can be found in the paleo-environmental features (e.g. delta, valley), because the gradually changing interpolation results fail to capture sudden local changes in sediment thickness due to changing sedimentary systems. This problem can be mitigated by increasing the number of stratigraphic profiles. However, this study found that using data at important locations was more effective.

### **2.5.3 Further Study Plan**

To advance BasinVis 1.0, a subsequent study will evaluate the software on example data from various sedimentary basins. This will help to verify and extend usability, efficiency, and potential of the program. Besides studying sedimentary basins, BasinVis 1.0 is applicable to other geological and non-geological studies which need surface reconstruction. This study plans to improve the program by including geostatistic-based interpolation methods and improved modeling interfaces. Furthermore, this study plans to include additional analysis functionalities such as fault displacements.

BasinVis 1.0 is an open-source project and available for download at <http://geologist-lee.com/basinvis.html>. The software is under active development and authors encourage users to contribute program extensions to the system.

## CHAPTER 3

# QUANTITATIVE SUBSIDENCE ANALYSIS

*This chapter is based on:*

*Lee, E.Y.<sup>1)\*</sup>, Wagreich, M.<sup>1)</sup>, submitted. Polyphase tectonic subsidence evolution of the Vienna Basin inferred from quantitative subsidence analysis. Submitted to International Journal of Earth Sciences.*

<sup>1)</sup> *Department of Geodynamics and Sedimentology, University of Vienna, Althanstrasse 14, Vienna 1090, Austria*

*\* Corresponding author*

## ABSTRACT

This study analyzes a detailed and quantitative subsidence history in the northern and central parts of the Vienna Basin to understand its Neogene tectonic subsidence evolution. 201 wells were used to arrange stratigraphic setting, and 89 wells reaching the pre-Neogene basement were analyzed for basement and tectonic subsidences. The main results of this study are generated by using the MATLAB-based program, BasinVis 1.0 for the basin analysis and visualization. Due to the special position of the Vienna Basin, the tectonic subsidence was influenced by the regional tectonic evolution of surrounding units – the Eastern Alps, the Western Carpathians and the Pannonian Basin system. In the Early Miocene, subsidence was shallow and NE-SW trending, indicating the development of piggy-back basins. During the late Early Miocene data show abruptly increasing subsidence, which initiated the Vienna pull-apart basin system. From the Middle Miocene, the subsidence was decreasing overall, however the tectonic subsidence curves show regionally different patterns. This study suggests that a major tensional regime change, from transtension to E-W extension, caused laterally varying tectonic subsidence across the Vienna Basin. From the late Middle Miocene to the Late Miocene, the tectonic subsidence occurred dominantly along the regional active normal faults, and corresponds to the E-W trending extension. This study arranged the tectonic subsidence history of the Vienna Basin to five phases; 1) E-W trending piggy-back subsidence (Early Miocene), 2) NE-SW transtensional subsidence (late Early Miocene), 3) NW-SE to E-W transitioning extensional subsidence (Middle Miocene), 4) E-W extensional subsidence (late Middle - Late Miocene) and 5) NE-SW transtensional subsidence (Quaternary).

### 3.1 INTRODUCTION

The Vienna Basin (central Europe) is situated on top of the Alpine fold-and-thrustbelt, located at the junction between the Eastern Alps, the Carpathians and the Pannonian Basin system (Fig. 3.1). It is interpreted as a classical thin-skinned pull-apart structure formed during Miocene lateral extrusion of the Eastern Alps (e.g. Mann et al., 1983; Royden, 1985). The rhombic basin is about 200 km long and 60 km wide, and formed mainly along the sinistral Vienna Basin transfer system (Decker, 1996; Decker and Peresson, 1996; Royden, 1985; Strauss et al, 2006; Wessely, 1988). This more than 300 km long strike-slip fault system is one of the most conspicuous crustal structures between the Eastern Alps and the Carpathians (Decker et al., 2005).

The basin has been studied intensively starting with classical paleontological-stratigraphical papers and then continuing since the beginning of hydrocarbon exploration at about 100 years ago. Studies focused mainly on the southern and central parts (Austrian part) of the basin for a variety of reasons. However, a comprehensive detailed study crossing the borders of Austria, Slovakia and Czech Republic is still missing. The northern and central parts (Czech and Slovakian parts) are highly important to understand the overall stratigraphic and structural evolution of the basin, because these parts contain up to 6 km of the Miocene sedimentary rocks, several complex structures, and the Steinberg Fault, one of the most prominent structure feature of the basin (e.g. Decker, 1996).

This study analyzed a more detailed regional subsidence history of the northern and central parts of the basin to understand the tectonic evolution. Several publications studied the subsidence history of the Vienna Basin (e.g. Hölzel et al., 2008a, b; Lankreijer et al., 1995; Lee et al., 2011; Royden et al., 1983; Sclater et al., 1980; Wagreich and Schmid, 2002). However these studies either cover the basin locally or focus more on surrounding areas with sparse well data. Compared to other publications on this topic, this study covers an extensive region of the basin and provides a more accurate analysis through the high density of considered boreholes, the geophysical evaluation for more realistic porosity-depth relations, and the mapping by employing a 3D interpolation technique. Furthermore the results of this study are compared with previous studies conducted in the southern part.

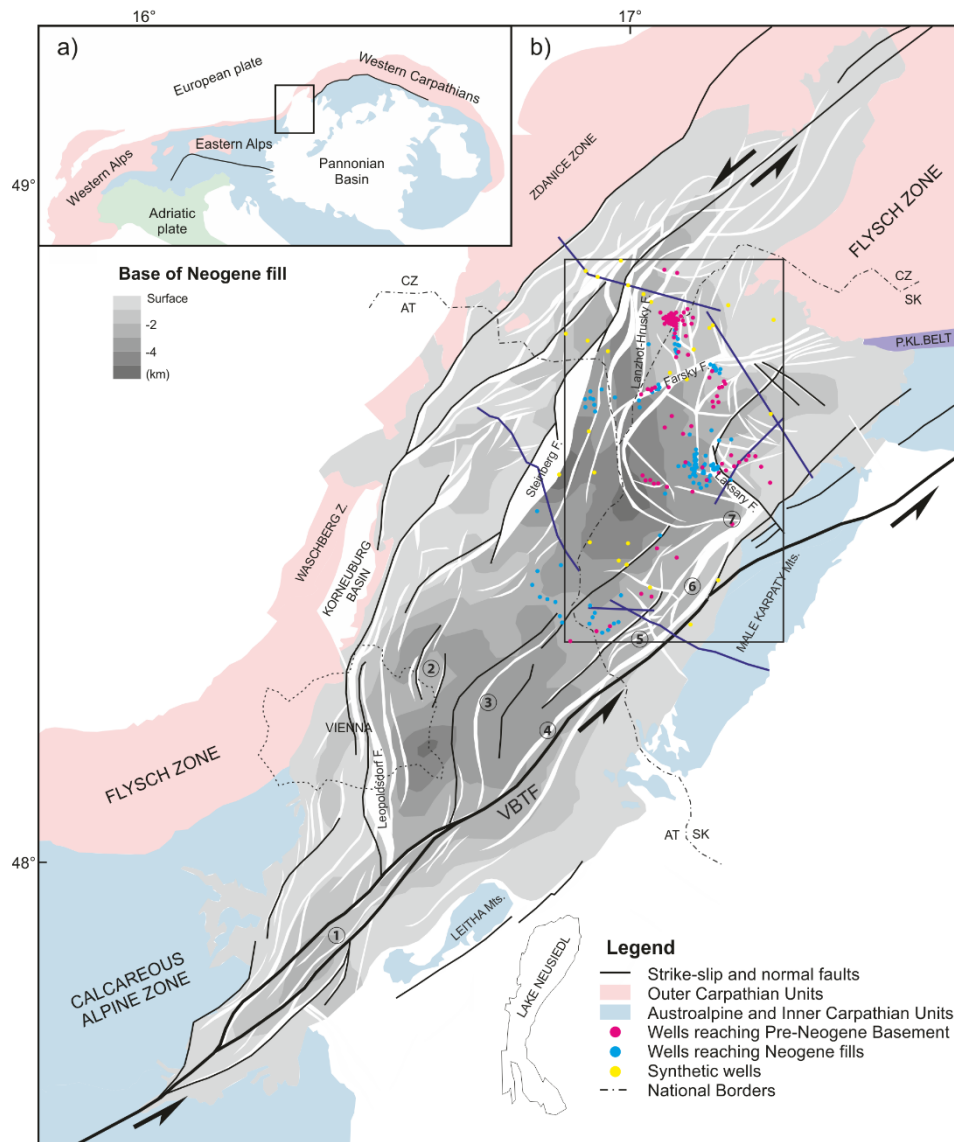


**Figure 3.1.** a) Tectonic sketch map of the East Alpine-West Carpathian region. b) The structure map of the Vienna Basin showing the faulted pre-Neogene basement surface and the base depth of the Neogene fill (revised from Arzmüller et al., 2006; Wessely et al., 1993). AT: Austria, SK: Slovakia, CZ: Czech Republic. Locations of wells, cross-sections and mapped area are shown in the basin. Letters L1 – C4 denote well groups distinguished in this study. Quaternary basins (①-⑦; see Figure 1.1) are arranged along the Vienna Basin transfer fault system (VBTF) (Beidinger and Decker, 2011).

### 3.2 DATA BACKGROUND

A number of well, seismic, and geophysical data of the northern and central parts of the Vienna Basin were acquired from the archives of the Dionyz Štur Institute, Slovakia. A total of 201 wells were arranged for this study (Tab. 1.1 and Fig. 3.1), and used for sediments distribution and isopach mapping. Among them, 89 wells reaching the pre-Neogene basement (partly shown in Fig. 3.2) were analyzed by decompaction and backstripping techniques (see Chapter 1.5) to gain subsidence curves and rates. Missing stratigraphic profile data in some areas were corrected by using data from the maps of the Pre-Neogene basement and the Neogene basin fill (Arzmüller et al. 2006; Čekan et al. 1990; Jiříček and Seifert 1990; Wessely et al. 1993) and interpolated from time-depth conversion of stratigraphic boundaries within seismic reflection data. These interpolated points have been termed synthetic wells. For a more precise subsidence analysis, this study used the on-site porosity-depth relation of the Vienna Basin based on geophysical well data. Regional water-depth variations were assumed from Sauer et al. (1992) and Seifert (1992) (Fig. 1.6).

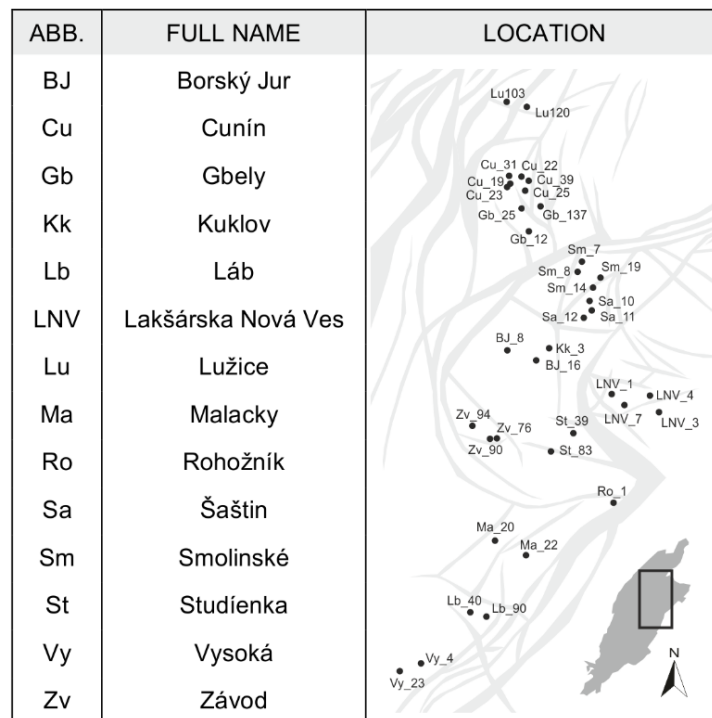


**Figure 3.2.** Abbreviations (ABB), full names and locations of wells presented in figure 3.6, 3.7 and 3.8.

### 3.3 SEDIMENTS DISTRIBUTION AND ISOPACH MAPPING

Sediments of Eggenburgian to early Karpatian age (Early Miocene) are disconformably overlying the eroded surface of various Alpine-Carpathian tectonic units (Fig. 3.3), and are restricted to small depressions (Fig. 3.4a and b) in the northern and central Vienna Basin. The depressions are distributed NE-SW trending along the synsedimentary faults by the N/NW moving Alpine thrust belt, and are classified as piggy-back basins (Decker, 1996; Fodor, 1995). The Luzice Formation of the Eggenburgian - Ottnangian is gradually spreading from the depocenters in the northern part and represents various marine depositional environments (Kováč et al., 2004). The sediments recorded in the southwestern part of the study area (Fig. 3.4a) are correlated with the terrigenous fluvial Bockfliess Formation continuing in the Austrian part of the Vienna Basin. The Bockfliess Formation has a thickness of up to 800 m and was deposited until the early Karpatian (Jiříček and Seifert, 1990; Kováč et al., 2004). The lower Karpatian sediments are thicker (up to 1,000 m) and more evident NE-SW trending than the older ones (Fig. 3.4b).

During the late Karpatian, tectonic kinematics changed from a piggy-back basin to a pull-apart basin (Decker and Peresson, 1996; Fodor, 1995; Hinsch et al., 2005a), and the area of sedimentation widened far to the South (Fig. 3.4c). Nearly the whole area of today's Vienna Basin was covered with sediments, and was bordered by newly formed synsedimentary faults (Fodor, 1995; Jiříček and Seifert, 1990; Jiříček and Tomek, 1981). The major depocenters were located between the Steinberg Fault and the Laksary Fault and along the Leitha Fault system which consists of strike-slip faults and negative flower structures activated along the southeastern margin of the basin (Kováč et al., 2004) (Fig. 3.3). There was no sedimentation on the northern edge rim and the Laksary horst in the study area. According to Arzmüller et al. (2006), Baráth et al. (2003), Jiříček and Seifert (1990) and Kováč et al. (2004), the northern and northeastern margins are distinctly erosive and lack preserved marginal facies by a period of nearly total regression occurred in the Vienna Basin. Due to the regression, considerable thickness of the upper Karpatian sediments is missing in the northeastern part of the basin.

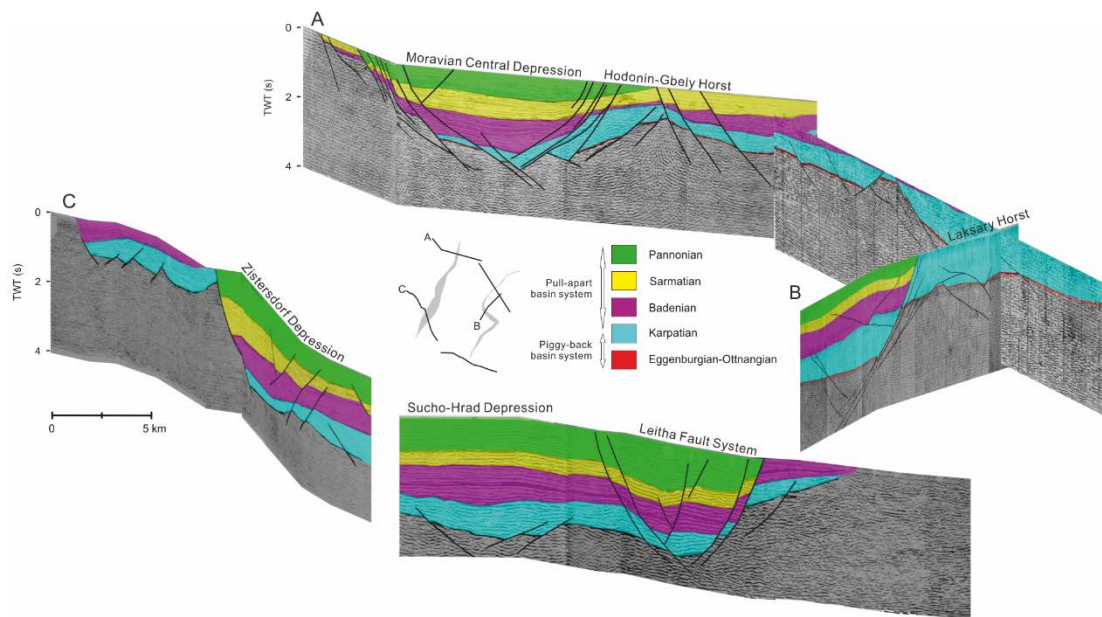


**Figure 3.3.** Seismic sections across the study area (See Figure 3.1 for location). Section A and C were revised from Čekan et al. (1990), and section B was acquired from the archives of the Dionyz Štur Institute, Slovakia. These sections were modeled by Blender which is an open-source 3D computer graphics software.

During the Badenian, the Vienna Basin was dissected into several fault blocks, resulting in lower lying strongly subsiding depocenters, and higher and more stable horst blocks. The faults are related to growth strata (Hölzel, 2009) (Fig. 3.3). The lower to middle Badenian sediments transgressed unconformably on various layers of the Lower Miocene and the flysch substratum in the northern area (Hamilton et al., 2000) and the sedimentation reached most of the central part (Fig. 3.4d). The upper Badenian sediments were distributed more widely and thicker than the lower and middle Badenian ones (Fig. 3.4e).

Although the Sarmatian began by regression of the sea (Fig. 1.3), the deposition blanketed the Badenian sequences without major depositional breaks (Fig. 3.3). The Sarmatian sediments covered a large part of study area with the total thickness generally varying between 200 – 600 m, and a tectonically controlled depocenter is found along the Steinberg Fault (Fig. 3.4f).

Sedimentation during Pannonian time shows considerable similarities to the Sarmatian one. However, the depocenter in the study area was wider and deeper along the Steinberg Fault and shifted slightly to the southwest (Fig. 3.4g). Considering uplift and erosion during the latest Pannonian and Pliocene, the Pannonian sediments would be thicker than the present-day preserved thickness.

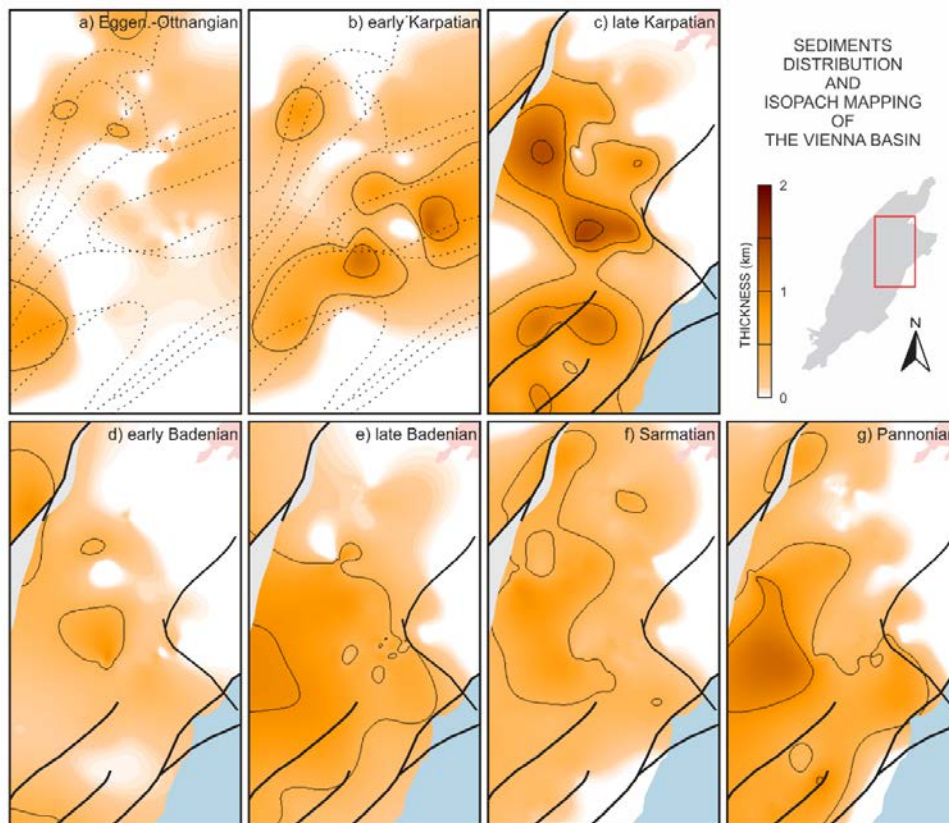


**Figure 3.4.** Sediments distribution and isopach maps of each stage; a) Eggenburgian-Ottnangian (c. 20.4 – 17.5 Ma), b) early Karpatian (c. 17.5 – 16.9 Ma), c) late Karpatian (c. 16.9 – 16.3 Ma), d) early Badenian (c. 16.3 – 14.2 Ma), e) late Badenian (c. 14.2 – 12.8 Ma), f) Sarmatian (c. 12.8 – 11.6 Ma), and g) Pannonian (c. 11.6 – 7.8 Ma). The Alpine-Carpathian nappe borders are shown with dotted lines for a - b, and major faults (Steinberg fault, Laksary fault and Leitha fault system) with black solid lines for c - g.

### 3.4 SUBSIDENCE ANALYSIS

About 90 wells reaching the pre-Neogene basement have been investigated and sorted into 10 groups. The sorting of wells was based on their position regarding fault blocks, and the positions of wells and groups are indicated in Fig. 3.1b. The 10 groups were named after their position and blocks. Four groups in the northern part are N(North)1-4, and four groups in the central part are C(Center)1-4. Two groups situated at basement highs are L1-2 which follow the first letter of their block names (Lužice and Lakšárska Nová Ves).

Subsidence curves and rates of selected wells are presented in this study. The model graph shows how the results are presented for subsidence history of each group (Fig. 3.5). The graphs represent the basement subsidence curves with dashed lines and the tectonic subsidence curves and rates with solid lines.

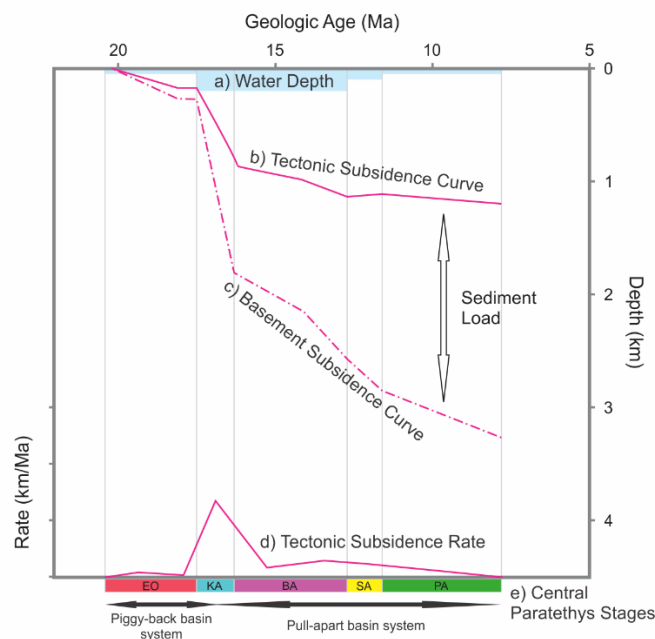


**Figure 3.5.** Model of subsidence graphs in this study; a) assumed average water-depth (Sauer et al., 1992; Seifert, 1992), b) tectonic subsidence curve (solid line), c) basement subsidence curve (dashed line), d) tectonic subsidence rate (solid line) and e) Central Paratethys stages; EO: Eggenburgian-Ottnangian, KA: Karpatian, BA: Badenian, SA: Sarmatian and PA: Pannonian.

### 3.4.1 SUBSIDENCE TREND OF THE NORTHERN PART

Wells of N1-4 are located in the northern Vienna Basin (Fig. 3.1b). The common trend is the stepwise subsidence patterns of the basement subsidence with two increasing stages and of the tectonic subsidence with one increasing stage. Total subsided depths of each group are deepening from N1 to N4 approaching to the central part of the Vienna Basin (Fig. 3.6).

The subsidence of N1-4 started during the Eggenburgian – Ottnangian. It was rather shallow and showed basement subsidence of up to 300 m. This minor subsidence is indicating the main piggy-back basin phase.

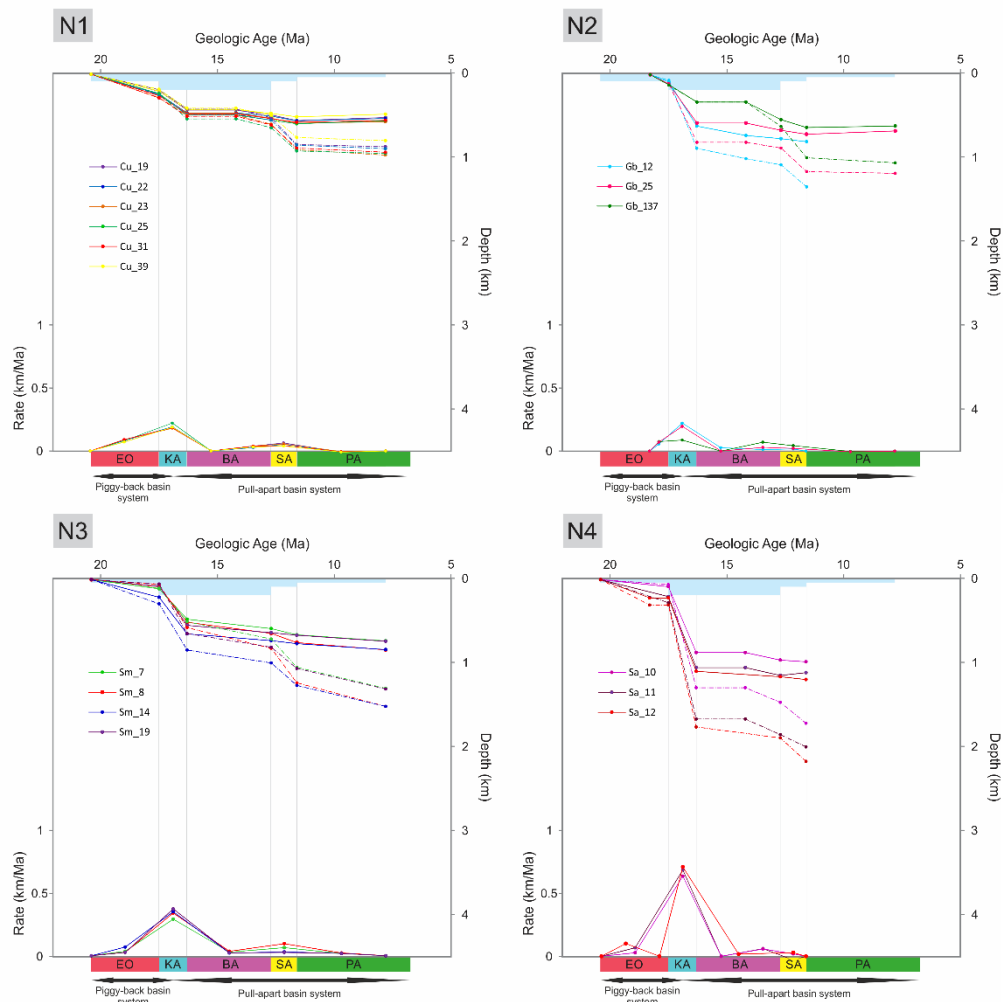


**Figure 3.6.** Subsidence curves and tectonic subsidence rates of group N1-4. For abbreviations of wells see Figure 3.2.

For Karpatian times, the subsidence curves document a rapid increase in both basement and tectonic subsidences (Fig. 3.6). The Karpatian data of wells in this group were not separated precisely between the lower and upper stages, and this made it hard to compare subsidence rates between the early and late Karpatian. In the northern part, the lower Karpatian sediments were thinner than the upper ones (Jiříček and Seifert, 1990) (Fig. 3.5b and c). Therefore, the recorded increasing Karpatian subsidence is interpreted as a combination of minor piggy-back and major pull-apart tectonics.

For the Badenian, tectonic subsidence was low and almost stationary with few notable changes (Fig. 3.6). During the early Badenian, wells in the northern part show only minor subsidence, because lower Badenian sediments were not reported in the region. From the late Badenian to the Sarmatian, wells of N1-4 show slightly increasing tectonic subsidence. At this time, however, the basement depth was increasing significantly without obvious tectonic effects, therefore this high basement subsidence is interpreted as a result of significant sediment loading.

Most subsidence curves of N1-4 continued until the Pannonian, however Gb12 in the N2 and wells in N4 stopped subsiding at the end of the Sarmatian (Fig. 3.6). Some wells also show decreasing tectonic subsidence during the Sarmatian - Pannonian. This study considers that this resulted from uplift and erosion by the basin inversion of the late Pannonian – Pliocene.

### **3.4.2 SUBSIDENCE TREND OF THE CENTRAL PART**

Group C1-4 are located broadly in the central part of the basin, and comprise data from hanging wall blocks along major faults (Fig. 3.1b). C1 and C2 are lying on the hanging wall between the Steinberg Fault and the Laksary Fault. In C2, the Závod (Zv) wells are closer to the Steinberg Fault and the Studienka (St) wells are located near the Laksary Fault. C3 and C4 are situated near the Leitha Fault System along the southeastern border of the Vienna Basin. The subsidence patterns of this group are highly dependent on the development of the major tectonic driving faults.

Most wells of C1-3 started to subside during the piggy-back basin time and exhibited quite shallow subsidence with thin sediments (up to 170 m) in the

Engenburiian – Ottnangian (Fig. 3.7). However, C4 recorded no sediments for this time, and subsided only from the late Karpatian initiating the pull-apart tectonics.

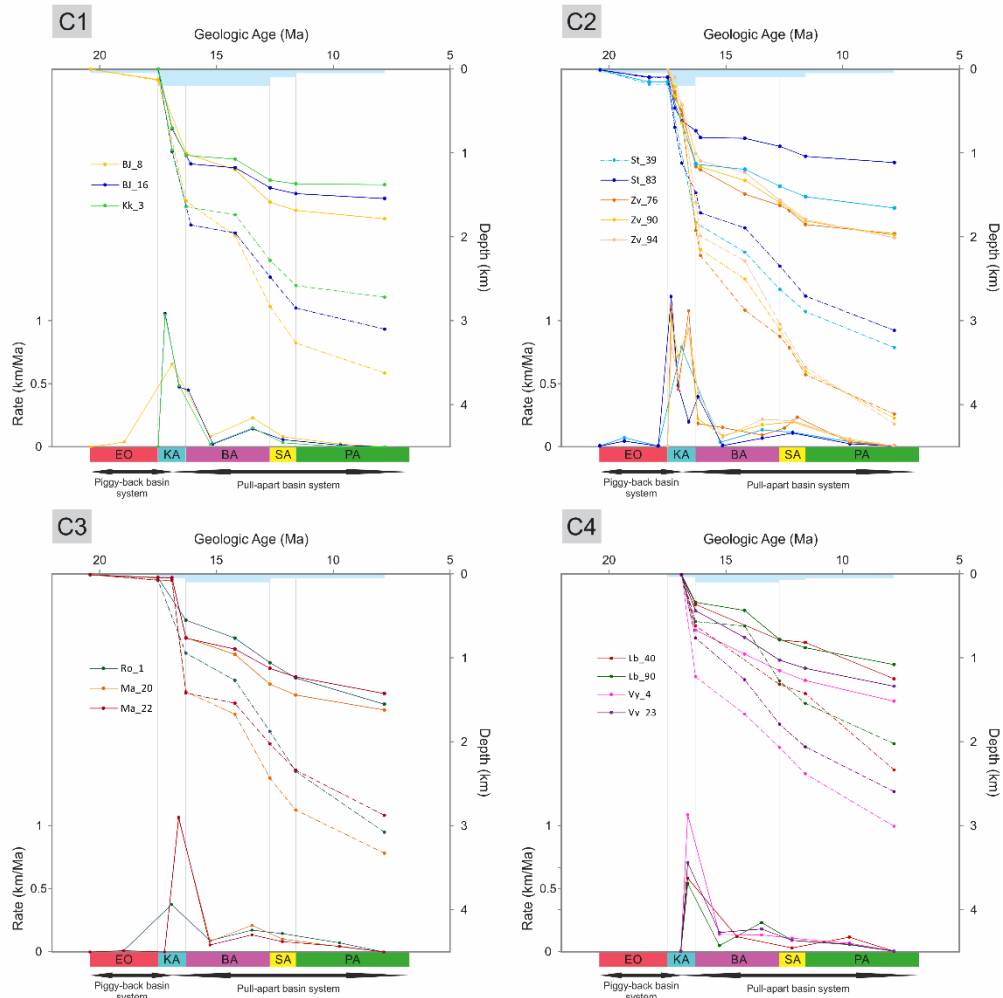


**Figure 3.7.** Subsidence curves and tectonic subsidence rates of group C1-4. For abbreviations of wells see Figure 3.2.

After the major Karpatian subsidence pulse, C1 and the Studienka wells of C2 almost stopped subsiding with thin sedimentation during the early Badenian. However, the Závod wells of C2 and C3-4 continued the tectonic subsidence slowly during this time (Fig. 3.7). In the late Badenian, C1-4 show increasing tectonic subsidence more evidently than N1-4.

While C1 has a stationary tectonic subsidence pattern during the Sarmatian, which is similar with the northern part, C2-4 display continuous tectonic subsidence until the Pannonian (Fig. 3.7). With the exception of some wells of C2, Sarmatian and Pannonian tectonic subsidence was minor compared to the late Badenian subsidence. Since the late Badenian, the basement subsided enormously (up to 2 km). However, it was mostly affected by sediment loading, not much by tectonic effects as shown by only minor tectonic subsidence.

### 3.4.3 SUBSIDENCE TREND OF THE BASEMENT HIGHS

The groups L1 and L2 are located each in the northern basement high and the Laksary horst (Fig. 3.1b). The subsidence curves of L1-2 show strong differences compared to the subsidence patterns of the other groups in this study.

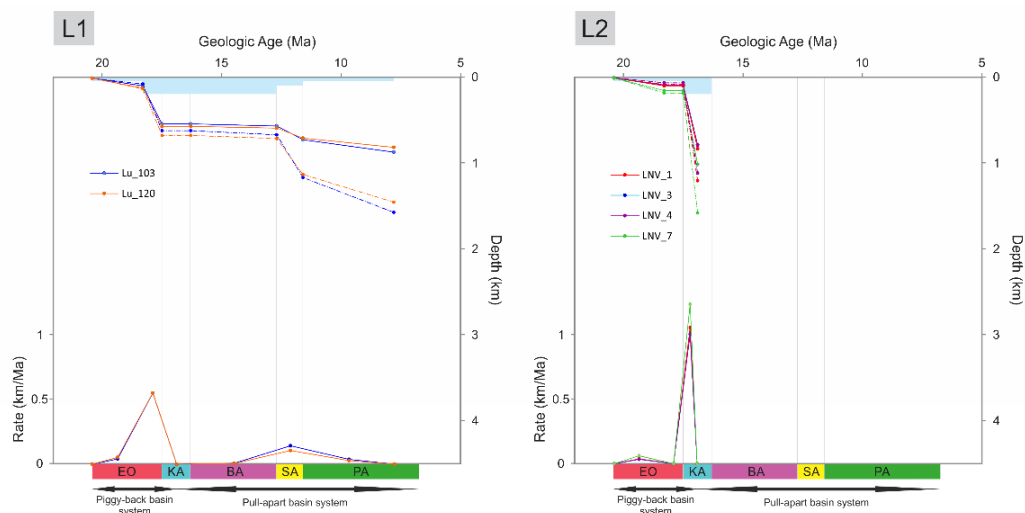


**Figure 3.8.** Subsidence curves and tectonic subsidence rates of group L1-2. For abbreviation of wells see Figure 3.2.

After the shallow subsidence of the Eggenburgian - Ottnangian, L1 had no significant Karpatian and Badenian subsidences at all, and L2 had subsided until the early Karpatian (Fig. 3.8). This may be due to the fact that L1-2 areas subsided mainly during the piggy-back phase time (although by some reasons group L1 subsided again from the Sarmatian).

The late Karpatian is a highly important time in the Vienna Basin, because the structural type of the basin changed from piggy-back to the pull-apart basin by onset of transtensional tectonic movement. However, the late Karpatian and subsequent Badenian sediments are not found in the areas of L1-2. This supports the idea that the areas of L1-2 were not affected by these transtensional tectonics, and, in contrast to most parts of the basin, underwent transpressional stress during the time. According to Fodor (1995) and Jiříček and Tomek (1981), in the Badenian, depocenters and subsidence moved to the south, and a significant angular discordance in the northern sedimentation area indicates uplift and deformation. The basin inversion was due to local transpressional tectonics where sinistral-slip transferred toward the northeast.

### **3.5 TECTONIC SUBSIDENCE RATE MAPPING**

Tectonic subsidence shows the idealized subsidence history of a basin that would have existed if only water, and no sediment, filled the subsiding depression. This enables the evaluation and classification of the general tectonic driving force for subsidence at different positions within a single basin (Allen and Allen, 2013; Xie and Heller, 2009). To understand regional tectonic trends in the study area, the tectonic subsidence rates were interpolated in Figure 3.9 for each major stratigraphic units.

During the piggy-back basin time, the Eggenburgian – Ottnangian tectonic subsidence was rather limited in the northern part (Fig. 3.9a). The subsidence rate was distributed with NE-SW trending, which is reflecting the Alpine-Carpathian thrusting. The trend is more evident in the subsidence rate map for the early Karpatian (Fig. 3.9b).

During the late Karpatian, the tectonic subsidence pattern changed abruptly (Fig. 3.9c) as a result of the principal change in the basin type. The tectonic subsidence rate increased rapidly over the area except for the northern basement high and the Laksary horst. This increase is strongly related to movement along the NE-SW trending strike-slip and normal faults. The faulted areas subsided considerably, especially in the hanging wall of the Steinberg Fault and along the negative flower structure of the Leitha Fault system.

After this large scale subsidence phase, the tectonic subsidence rate decreases markedly in the early Badenian (Fig. 3.9d). Rates decreased to zero abruptly in the northern part, whereas the central part is characterized by ongoing weak tectonic subsidence. These slow subsidence rates increased again during the late Badenian along the Steinberg Fault (Fig. 3.9e), and the central part including the the Spannberg ridge subsided widely. During the Sarmatian, the tectonic subsidence continued and its subsiding area spread to the north along the Steinberg Fault (Fig. 3.9f). The tectonic subsidence rate decreased again in the Pannonian (Fig. 3.9g), remaining weak near the two major tectonic driving faults.

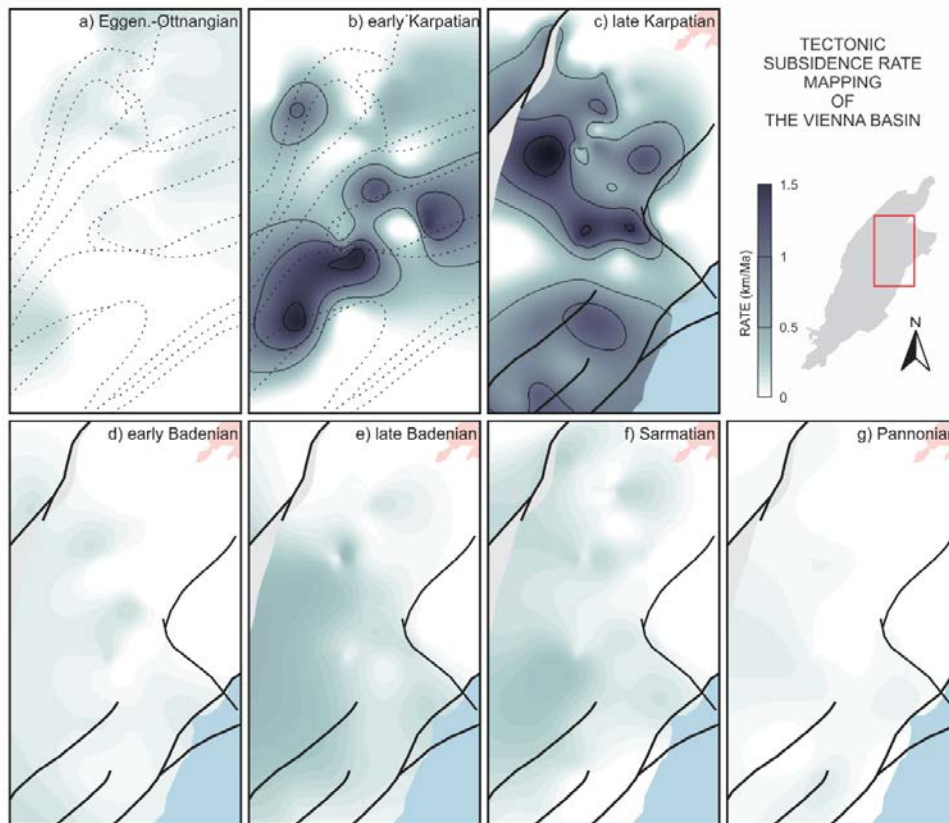


**Figure 3.9.** Maps of tectonic subsidence rate of each stage; a) Eggenburgian-Ottnangian (c. 20.4 – 17.5 Ma), b) early Karpatian (c. 17.5 – 16.9 Ma), c) late Karpatian (c. 16.9 – 16.3 Ma), d) early Badenian (c. 16.3 – 14.2 Ma), e) late Badenian (c. 14.2 – 12.8 Ma), f) Sarmatian (c. 12.8 – 11.6 Ma) and g) Pannonian (c. 11.6 – 7.8 Ma). The Alpine-Carpathian nappe borders are shown with dotted lines for a - b, and major faults (Steinberg fault, Laksary fault and Leitha fault system) with black solid lines for c - g.

### 3.6 TECTONIC SUBSIDENCE OF THE SOUTHERN PART

In order to enhance the understanding of the regional subsidences, the tectonic subsidence trends resulted in this study were compared with the previous works conducted in the Austrian part; the southern part of the central Vienna Basin (Lankreijer et al., 1995) and the southern part (Hölzel et al., 2008b).

The previous works have a few minor differences in methodological details, compared to this study. They used empirical depth-porosity relation from literature for specific lithologies of each layer. And they also used largely the same Central Paratethys chronostratigraphy and the local zones refined since the 1990s but did not include recent age refinements (e.g. Hohenegger et al., 2014). Hölzel et al. (2008b) focused on the pull-apart evolution and thus analyzed subsidence from the Badenian Lower Lagenid Zone and excluded decompaction effects of the Lower Miocene sediments. The decompacted depth and the time factor are the most influential parameters in subsidence analysis, and can cause different amount and timing of subsidence rates between studies. However their work is still valuable for comparing overall and regional subsidence trends.

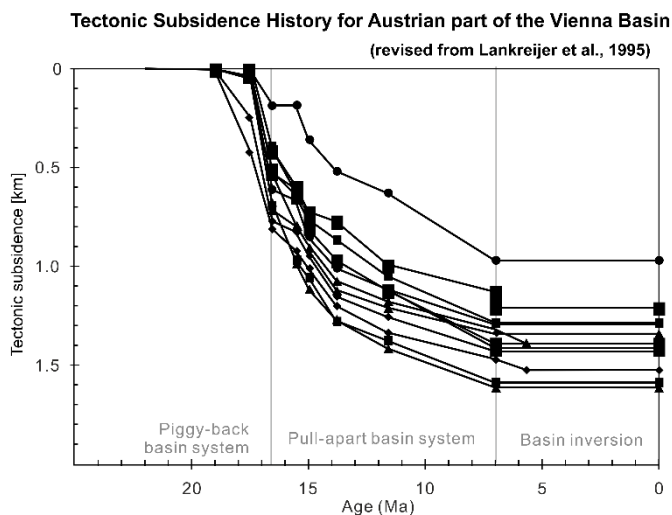


**Figure 3.10.** Tectonic subsidence history for the Austrian part (the southern part of the central Vienna Basin) (revised from Lankreijer et al., 1995).

Lankreijer et al. (1995) presented the subsidence history of the southern part of the central Vienna Basin, located in the Austria (Fig. 3.10). The study described that the tectonic subsidence changed gradually from one subsidence mode to the other. And, the subsidence curve has a concave shape, which is steeper in areas located more

to the south. Despite of the differences in methodological details, this trend is quite similar with the tectonic subsidence trend of the central part in this study.

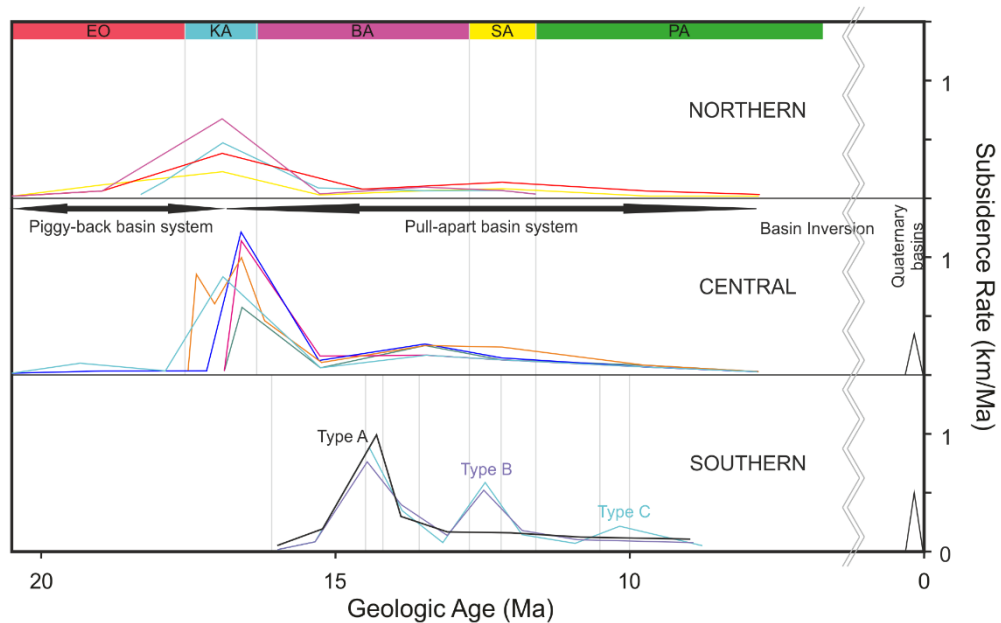


**Figure 3.11.** Tectonic subsidence rates of the northern, central and southern parts of the Vienna Basin. Rates of the southern part are from Hölzel et al. (2008b). The tectonic subsidence rates of the Quaternary basins were assumed from Quaternary sediments data of Decker et al. (2005), Beidinger and Decker (2011), Salcher (2008) and Salcher et al. (2012).

The tectonic subsidence rates were arranged to the northern, central and southern parts of the Vienna Basin (Fig. 3.11). The subsidence rates of the southern part were taken from Hölzel et al. (2008b). In the southern part three types of the tectonic subsidence have been characterized, representing combinations of three main identified subsidence phases (Hölzel et al., 2008b) (Fig. 3.11). Type A which is dominant in the southern part exhibits a high rate only in the Upper Lagenid Zone (early to middle Badenian, see Hohenegger et al., 2014) that decreases continuously through the rest of the Miocene. Type B includes an additional subsidence peak within the early Sarmatian, and Type C includes two peaks within the early Sarmatian and the middle Pannonian.

### 3.7 QUATERNARY BASIN SUBSIDENCE

The Quaternary reactivation of the Vienna Basin is related to NE-SW extension since c. 250 - 300 ka (Salcher, 2008) at a releasing bend along the Vienna Basin transfer fault (VBTF) (Fig. 3.12). Earthquake data depict moderate seismicity concentrated along the slow-moving (1-2mm/y; Grenerczy et al., 2000; Decker et al., 2005) sinistral fault system at the southern boundary of the Vienna basin, and the seismicity proves the continued activity of the fault zone (Beidinger and Decker, 2011; Decker et al., 2005). The small Quaternary basins are filled mainly by fluvial sediments up to 150 m thick (Fig. 3.12) which are unconformably overlying Miocene sediments (Beidinger and Decker, 2011; Decker et al., 2005; Hinsch et al., 2005b). This study calculated the tectonic subsidence rates of the Quaternary basins (Fig. 3.11) using the Quaternary sediments data (e.g. Kullman, 1966; Beidinger and Decker, 2011).

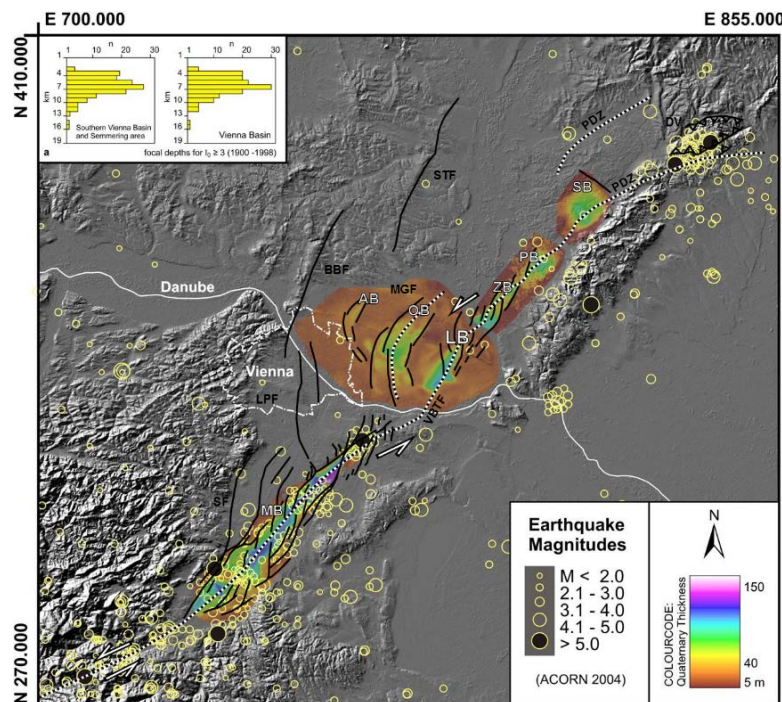


**Figure 3.12.** Thickness of Quaternary deposits and earthquake epicenters (ACORN, 2004) draped over a shaded digital elevation model of the Vienna Basin (revised from Beidinger and Decker, 2011). Quaternary thickness data digitized from Kullman (1966). Focal depths from Reinecker and Lenhardt (1999). MB: Mitterndorf Basin, LB: Lassesee Basin, ZB: Zohor Basin, PB: Pernek Basin, SB: Sološnica Basin, SF: Sollenau Fault, LPF: Leopoldsdorf Fault, MGF: Markgrafneusiedl Fault, BBF: Bisamberg Fault, STF: Steinberg Fault, DV: Dobra Voda, VBTF: Vienna Basin Transfer Fault.

### 3.8 DISCUSSION

The tectonic subsidence of strike-slip basins are mainly episodic, short lived (typically  $< 10$  Ma), and end abruptly with commonly very high tectonic subsidence rates ( $> 0.5$  km/Ma) compared to all other basin types (Allen and Allen, 2013; Xie and Heller, 2009). The high tectonic subsidence rates of the late Karpatian time in the Vienna Basin, which was caused by the evolution of the master strike-slip faults, occurred in only short time of c. 0.6 Ma. The tectonic subsidence curves reflect generally the typical 'concave-up' shape pattern displayed in basins in strike-slip zones (Fig. 3.13).

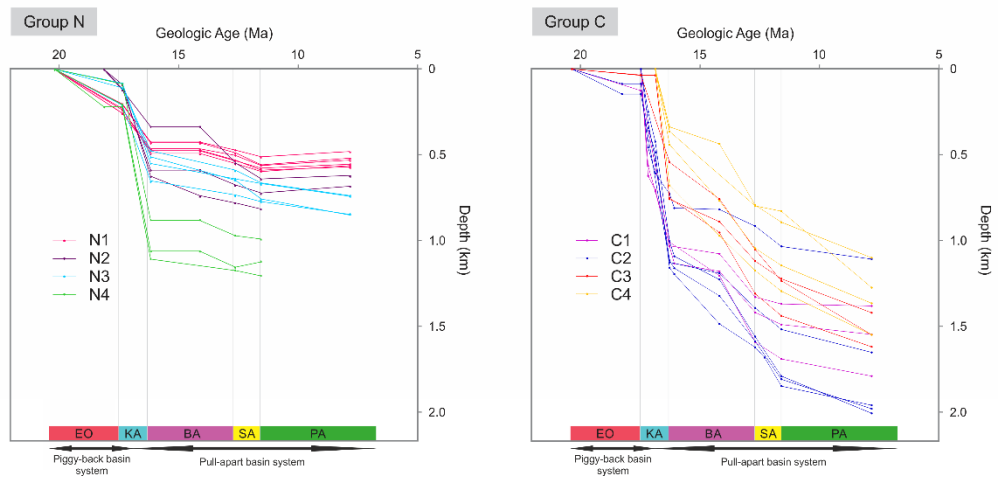


**Figure 3.13.** Tectonic subsidence curves of the Northern (N1-4) and Central (C1-4) parts.

#### 3.8.1 Different tectonic subsidence patterns between the northern part and the central part

After the strong subsidence phase, this study found that the tectonic subsidence nearly stops in the northern part, whereas the central part is characterized by a gradually decreasing pattern (Fig. 3.13). The significant subsidence difference between the parts was recorded already in previous works (Lankreijer et al., 1995; Royden, 1985). There were two major suggestions to explain the different subsidence decrease patterns observed in the Vienna Basin.

Royden (1985) interpreted the Vienna Basin as a typical example of how thin-skinned extension can create a sedimentary basin. The work stated that post-extensional (or thermal) subsidence within the basin is impossible, because the extension and the associated strike-slip faulting were restricted to shallow levels, and thus no significant gradually decreasing thermal subsidence phase is present. Royden (1985) analyzed subsidence curves of the basin for two different cases; (1) for the northeastern part, where most of the subsidence and sedimentation is of Early Miocene age or older, and (2) for the south-central part, where most of the subsidence is of the Middle to Late Miocene age. The study, however, analyzed uncorrected subsidence curves neglecting compaction of sediments, and failed to explain tectonically why subsidence happened locally in different times.

The other model by Lankreijer et al. (1995) proposed a post-rift (thermal) subsidence for the central part. According to these authors, the Vienna Basin comprises a non-uniform extensional basin changing from thin-skinned extension in the northern part to whole lithospheric extension in the central part. Lankreijer et al. (1995) also suggested that the deep-rooted strike-slip and normal faults reactivated pre-existing fault planes which penetrated locally into the overlying thrust belt and created a new structural regime (Picha, 1996; Wessely, 1988). However, there is no major thermal anomaly arguing for backing up the lithospheric extension and the heat flow is uniformly low in the basin (Cloetingh and Ziegler, 2007; Dövényi and Horváth, 1988; Sachsenhofer, 2001). Additionally, in such a small size basin, the coexistence of two extension types seems highly speculative.

### **3.8.2 Badenian Tectonic subsidence**

In details of the Badenian subsidence rates, the high rate of the Upper Ladinid Zone observed in the southern part is missing in the rest of the Vienna Basin, and in the central and northern parts the late Badenian subsidence rate is higher than the early Badenian (Upper Ladinid Zone) one (Fig. 3.11). Hölzel et al. (2008b) explained this differential subsidence mainly with a paleoenvironmental effect caused by the Spannberg ridge which was uplifted at the end of the Karpatian (Hölzel et al., 2010). The ridge largely restricted sedimentation in the southern part during the Early Badenian. Consequently, only non-marine

sediments are known from the southern part of the Vienna Basin during this time interval (e.g. Seifert, 1996). Subsequently, the ridge was buried in the late Badenian, and caused sedimentation to spread to the central part. This study suggests that the regional difference of the Badenian tectonic subsidence was caused by a Badenian paleostress change. The differential tectonic subsidence means the major fault activity successively advanced toward north during the Badenian. This is in accordance to Weissenböck (1996), who showed that the synsedimentary fault activity in the basin displays a time-transgressive trend from south to north during that time. The Middle Miocene evolution was characterized by a combination of strike-slip (transtension) and extensional faulting rather than a pure strike-slip or pure tensional regime (Fodor, 1995). The differential subsidence can be related to a change of the major tensional regime shifting from transtension to E-W directed extension toward the Late Middle Miocene.

### **3.8.3 Sarmatian – Pannonian Tectonic Subsidence**

The Sarmatian - Pannonian subsidence occurred dominantly along the Steinberg Fault in the northern and central parts (Fig. 3.9f). In the southern part, the Bockfliess and Markgrafneusiedl Faults were the major active faults in this time (Hinsch et al., 2005a). This subsidence corresponds to the E-W trending extension found in the western parts of the Pannonian Basin system for the late Sarmatian – early Pannonian (Huisman et al., 2001). The changing tectonic regime is supported by that the transpressional area (the northern basement high; group L1) subsided again from the Sarmatian onwards (Fig. 3.8). Similar extension is also reported in neighboring basins – the Styrian Basin and the Danube Basin (Kováč et al., 1999; Sachsenhofer et al., 1997; Vass et al., 1990).

This study supposes that during the Middle – Late Miocene the Vienna Basin experienced tectonic subsidences by the Badenian transitioning tensional and the Sarmatian-Pannonian E-W trending extensional regimes. However the tectonic subsidence events were much more evident in the central and southern parts than in the northern part (Fig. 3.11). The difference can be connected to the location of the major driving faults of the Vienna Basin. The faults evolved mainly during the late Karpatian are found mostly in the central and southern parts (Fig. 3.1b). The extensional activities of the Eastern Alps and the Pannonian Basin

System influenced the major driving faults, which caused the stronger tectonic subsidence in the central and southern parts.

#### **3.8.4 Uncertainty of Pannonian subsidence**

The Pannonian subsidence was shallow and regionally restricted in the study area (Fig. 3.9g). However, subsidence results calculated in this study may be biased due to the fact of missing significant parts of the youngest sedimentary column. The latest Pannonian and Pliocene E-W compressional event resulted in basin inversion and sediment deformation (Decker and Peresson, 1996; Peresson and Decker, 1997a, 1997b). Uplift of more than 200 m is assumed (Strauss et al., 2006), which eroded Pannonian sediments. Therefore it is possible that the Pannonian subsidence has been underestimated due to missing thickness data. In addition, this study found that in some of well data Quaternary deposits have not been separated from Pannonian sediments. Along the still active Vienna Basin transfer fault (Fig. 3.1), the Pannonian subsidence observed in C3-4 thus also partly includes Quaternary subsidence reported in Beidinger and Decker (2011).

### **3.9 CONCLUSIONS**

The special position of the Vienna Basin caused that the tectonic subsidence history reflects the regional tectonic evolution of surrounding units. The central and southern parts have more distinct tectonic subsidence during the Middle – Late Miocene due to the location of the major driving faults. The tectonic subsidence history of the Vienna Basin can be arranged to five subsidence phases;

#### **E-W trending piggy-back subsidence (Eggenburgian – early Karpatian; Early Miocene)**

In the Early Miocene, the piggy-back basin started to subside in front of the N- and NW- thrusting active Alpine sheets. The subsidence was shallow and NE-SW trending in the northern and central parts, and became stronger and broader in the early Karpatian.

**NE-SW transtensional subsidence (late Karpatian)**

High subsidence during the late Karpatian was accelerated and further enlarged mainly by sinistral strike-slip duplexes and by listric faults connected to strike-slip faults. The transtensional subsidence affected most parts of the basin except the northern basement high and the Laksary horst which are considered as transpressional regime areas.

**NW-SE to E-W transitioning extensional subsidence (Badenian; Middle Miocene)**

During the Badenian, the tectonic subsidence history varies laterally across the Vienna Basin. While the southern part subsided in the early Badenian, the central part subsided in the late Badenian and the northern part also recorded only slight tectonic subsidence during that time. This study suggests that this differential tectonic subsidence was caused by the major extension regime changed from transtension to E-W directed extension.

**E-W extensional subsidence (Sarmatian – Pannonian)**

The tectonic subsidence of the Sarmatian – Pannonian was concentrated along the major driving faults. It was related to fault activity corresponding to the E-W trending extension of the western parts of the Pannonian Basin system.

**NE-SW transtensional subsidence (Quaternary)**

In the Quaternary the Vienna Basin has been reactivated, and resulted in small basins subsided along the Vienna Basin transfer fault.



## **CHAPTER 4**

### **3D MODELING OF DEPOSITIONAL SETTING AND SUBSIDENCE**

*This chapter is based on:*

*Lee, E.Y.<sup>1)</sup>\*, Wagreich, M.<sup>1)</sup>, submitted. 3D modeling of depositional setting and subsidence evolution in the northern and central Vienna Basin. Submitted to Austrian Journal of Earth Sciences.*

*<sup>1)</sup> Department of Geodynamics and Sedimentology, University of Vienna, Althanstrasse 14, Vienna 1090, Austria*

*\* Corresponding author*

## ABSTRACT

This study analyzed and modeled 210 wells using a MATLAB-based basin modeling program (BasinVis 1.0) for the depositional setting and the subsidence evolution of the northern and central Vienna Basin. The depositional setting for each stage was modeled to 3D sediments distribution models, 2D sediments isopach maps and cross-section profiles. Subsidence modeling resulted in 3D subsided depth surface models and 2D subsidence rate maps of the basement and tectonic subsidences of each stage. The results were compared with previous studies to understand the comprehensive basin evolution. The models provided insights into the integrated and extensive basin evolution of the Vienna Basin, which is closely related with the regional stress change and the paleoenvironmental setting. In the piggy-back basin phase, the deposition and subsidence were shallow and E-W trending, and restricted to small depressions. In the late Early Miocene, the Vienna Basin changed to a pull-apart basin system with wider and deeper deposition and subsidence by sinistral strike-slip faults. The sediments deposited during the Early Miocene were supplied through the small deltaic system entering from the south. After shallow deposition and subsidence of the early Middle Miocene, the development of the Vienna Basin was controlled and accelerated mainly by NE-SW trending synsedimentary normal faults, especially the Steinberg fault. From the middle Middle to Late Miocene, enormous amount of sediments eroded from the Molasse area were supplied by a broad paleo-Danube delta complex on the western flank of the basin. The Late Miocene was characterized by the slowing down of basement and tectonic subsidences.

## 4.1 INTRODUCTION

The Vienna Basin is a Neogene basin of about 200 km length and 55 km width, situated between the Eastern Alps, the Western Carpathian, and the Pannonian Basin (Fig. 4.1). Along the NW flank the basin is separated by the thrust sheets of the Waschberg Zone from the Molasse Foreland Basin, which extends parallel to the Alpine-Carpathian units (Weissenböck, 1996). Due to its special location, the basin has experienced a complex tectonic and depositional history ranging from piggy-back basins in the Early Miocene to a large pull-apart basin in the Middle – Late Miocene, and small pull-apart basins in the Quaternary. The basin is dissected into several fault blocks consisting of lower lying depressions, grabens, highs and stable horsts

The Vienna Basin is one of the most extensively studied basins due to fundamental research and hydrocarbon exploration in the region over the last 150 years. The Neogene sedimentary succession is documented by numerous boreholes (more than 6,000 wells; the deepest to a total depth of 8,553 m) and a dense network of two- and three-dimensional seismic profiles (Arzmüller et al., 2006; Kováč et al., 2004). Various aspects of the structural and depositional setting of the basin have been analyzed in publications by Beidinger and Decker (2011), Brix and Schultz (1993), Čekan et al. (1990), Hölzel et al. (2010), Jiríček and Seifert (1990), Kováč et al. (2004), Lankreijer et al. (1995), Picha (1996), Sauer et al. (1992), Seifert (1992), Wessely et al. (1993).

The Vienna Basin is spreading across three Central European countries (Fig. 4.1); Slovakia and Czech Republic in the north to Austria in the south. For a variety of reasons, intensive studies have been mainly focused on the southern and central parts of the Vienna Basin. To understand the comprehensive basin evolution, this study focuses more on the northern and central parts of the Vienna Basin, and compares the results with previous studies conducted in the southern part.

This study analyzed and modeled stratigraphic, structural and subsidence setting in the northern and central parts of the basin. This comprehensive study benefits from an extensive database of the Miocene sedimentary infill of the Vienna Basin. The dataset offers ideal information for integrated and extensive modeling of depositional setting and subsidence evolution. Three dimensional modeling can provide insights into the tectonostratigraphic evolution of the Vienna Basin.

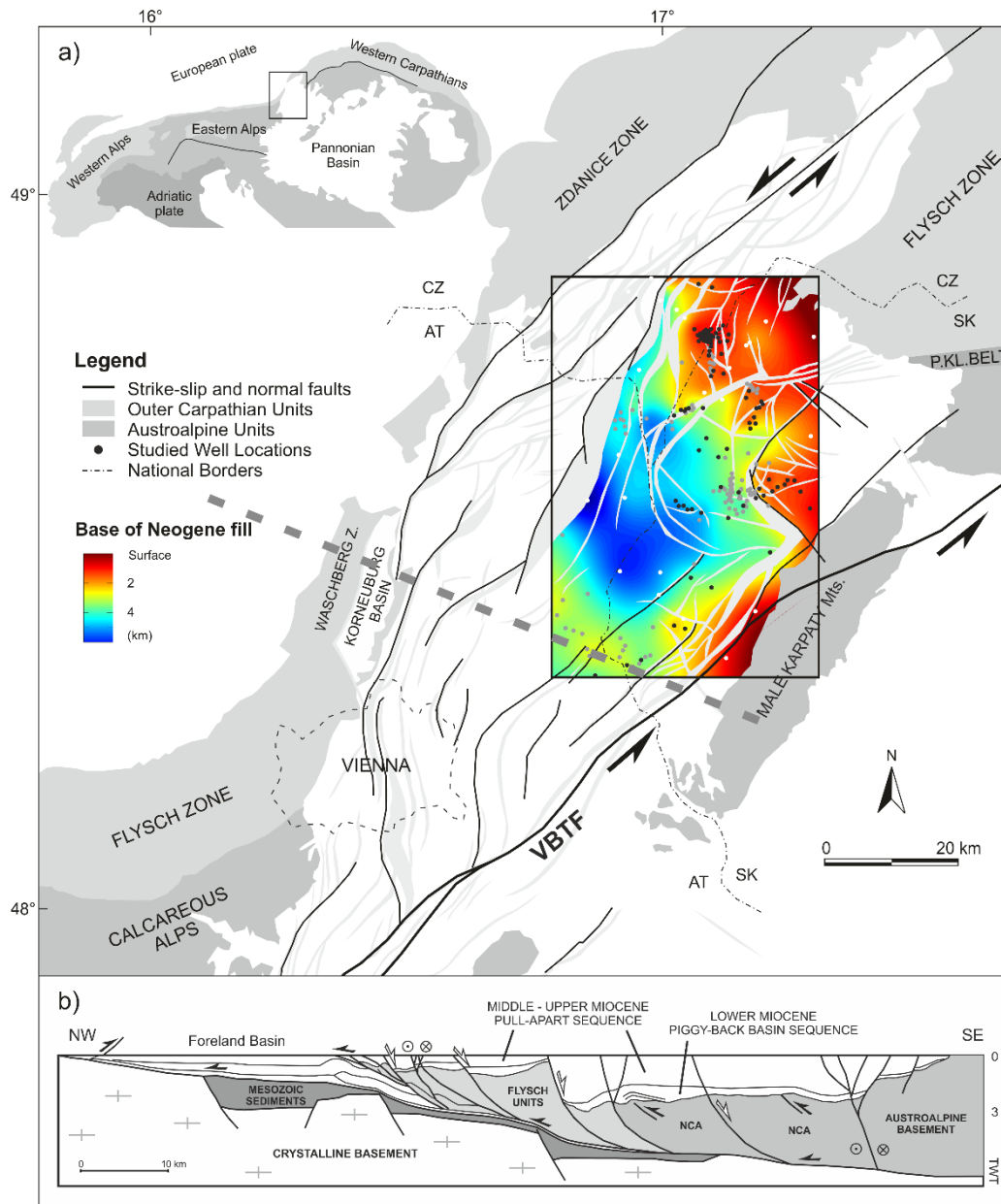


**Figure 4.1.** a) Tectonic sketch map and faulted pre-Neogene basement surface map of the Vienna Basin located at the junction between the Eastern Alps, the Western Carpathians and the Pannonian Basin system (revised from Arzmüller et al., 2006; Wessely et al., 1993). The base depth map of the Neogene fill, shown in the study area of this chapter, is modeled in this study. Locations of wells (black dot: wells reaching the pre-Neogene basement, gray dot: wells reaching the Miocene basin fill and white dot: synthetic wells) and a cross-section are shown. AT: Austria, SK: Slovakia, CZ: Czech Republic, VBTF: Vienna Basin Transfer Fault. b) Geologic cross-section through the Vienna Basin and the adjacent Molasse Foreland Basin (revised from Beidinger, 2013).

## 4.2 DATA AND METHODS

The modeled area extensively covers 40 x 60 km in the northern and central parts of the Vienna Basin. The depositional setting was analyzed using sediments thickness data of 210 wells including 9 wells of the Austrian part (Fig. 4.1). 24 synthetic wells were used for missing well-data in some areas, and the wells were mainly acquired from time-depth conversion of stratigraphic boundaries within seismic reflection data. Among them, 104 well data were selected for modeling the basement and tectonic subsidences.

These data were evaluated and modeled with BasinVis 1.0 (Lee et al., submitted; see Chapter 2), for depositional setting models (3D sediments distribution model, 2D sediments isopach map and cross-section profiles) and subsidence evolution models (3D subsidence depth model and 2D subsidence rate map for basement and tectonic subsidences). During the modeling and mapping, the Male Karpaty Mts., the flysch part and the Steinberg high (Mistelbach block) are not considered in the study area were subsequently removed by using the mask function of BasinVis 1.0.

The subsidence models were calculated by the decompaction and backstripping techniques (see Chapter 1.5). For the subsidence analysis, regional water-depth variations were assumed from Sauer et al. (1992) and Seifert (1992) (Fig. 1.6). This study has not incorporated relative sea-level changes in the calculations, since the basin was separated from the world ocean around the early Late Miocene. Additionally, also the regional sea-level changes in the Paratethys were partially in accordance with the global sea-level cycles and superimposed by regional tectonic processes (Haq et al., 1987; Steininger et al, 1988; Steininger and Wessely, 1999), and the known short-time sea-level fluctuations do not perturb the longer-term subsidence trends. This study used  $\phi_0$  and  $c$  of the porosity-depth relation (Fig. 1.10) evaluated geophysically for the Vienna Basin (Lee and Wagreich, submitted).

In some wells of the selected 104 wells, the Karpatian and Badenian data were not subdivided into lower and upper substages or zones, which made it hard to analyze detailed subsidences for the early Karpatian and the early Badenian. And, direct interpolation in areas with insufficient data caused intersecting surface or extreme depth change. To mitigate the problems, this study interpolated the missing depth data combining thickness interpolations (Isopach) of all overlaying layers, and

subsequently this study analyze the data for subsidence models. This leads to the fact that the tectonic subsidence rate mapping of this study is partly different from the rate mapping of Chapter 3 which is interpolated by a straight forward method of the BasinVis 1.0.

The depositional setting and subsidence are modeled in seven successive stages; 1) Eggenburgian-Ottangian (c. 20.4 – 17.5 Ma), 2) early Karpatian (c. 17.5 – 16.9 Ma), 3) late Karpatian (c. 16.9 – 16.3 Ma), 4) early Badenian (c. 16.3 – 14.2 Ma), 5) late Badenian (c. 14.2 – 12.8 Ma), 6) Sarmatian (c. 12.8 – 11.6 Ma) and 7) Pannonian (c. 11.6 – 7.8 Ma).

### 4.3 3D MODELING OF DEPOSITIONAL SETTING

Depositional setting of the study area was modeled to 3D sediments distribution models, 2D sediments isopach maps and cross-section profiles. In 3D sediments distribution models, areas in which no sedimentation occurred were excluded from the model. 2D sediments isopach maps are showing locations of the major faults (Steinberg fault, Laksary fault and Leitha-Láb fault system) to help understanding the sedimentation trend of each stage. Cross-section profiles are images exported from the depositional setting modeled with BasinVis 1.0 in the study area. The important structural elements of the Vienna Basin (Fig. 4.2) were documented in the cross-section profiles.



**Figure 4.2.** A map of main structural elements of the study area in the northern and central parts of the Vienna Basin (revised from Arzmüller et al., 2006; see Figure 1.5 for a map of the whole Vienna Basin).

### **4.3.1 Depositional setting of the Piggy-back basin system**

During the Eggenburgian – Ottnangian, the sediments were largely shallow, distributed with an overall thickness of less than 500 m (Fig. 4.3A), and were deposited in small depressions (Fig. 4.5). Thicker (up to 800 m) depositional packages are recorded in the southwestern part of the study area. These intervals correlated to the Bockfliess Formation which is a deltaic-brackish complex (Fig. 1.6a) deposited from the Ottnangian to the early Karpatian.

The Lower Miocene deposition is related to the tectonic opening of depocenters mainly in the northern part of the basin, and the sediments filled the small depressions formed along the NE-SW synsedimentary faults by the N- to NW-propagating Alpine-Carpathian thrustbelt (Beidinger, 2013; Decker, 1996; Fodor, 1995). The NE-SW trending depressions are more evident in the early Karpatian depositional setting (Fig. 4.3B), and thick sediments (up to 1,000 m) concentrate in the depressions of the central part.

According to Kováč et al. (2004) and Sauer et al. (1992), during the Early Miocene, the northern part of the Vienna Basin was marine, while the central part was characterized by deposition of huge lacustrine-deltaic formations and the southern depositional area was fully continental (Fig. 1.6a and b).

### **4.3.2. Depositional setting of the Pull-apart basin system**

From the late Karpatian, the area of sedimentation widened to the South, and covered nearly the whole study area except the northern edge rim and the Laksary horst (Fig. 4.3C). On the Laksary horst, no sediments have been deposited since the late Karpatian (Fig. 4.5J). The major depocenters (Zohor-Plavecký Mikuláš graben and Leváre depression) were located along the Leitha-Láb fault system which consists of strike-slip faults and negative flower structures activated along the southeastern margin of the basin, and also between the Steinberg fault and the Laksary fault (Fig. 4.3C). The deposition was bounded by synsedimentary fault blocks and structural ridges (e.g. Spannberg ridge, Matzen ridge and Laksary horst). Voluminous sediments eroded from the Alps were supplied due to the development of deltaic system entering the Vienna Basin from the south (Fig. 1.6b) and the transgression onset correlates with a global sea-level rise (Kováč et al., 2004; Sauer et al., 1992).

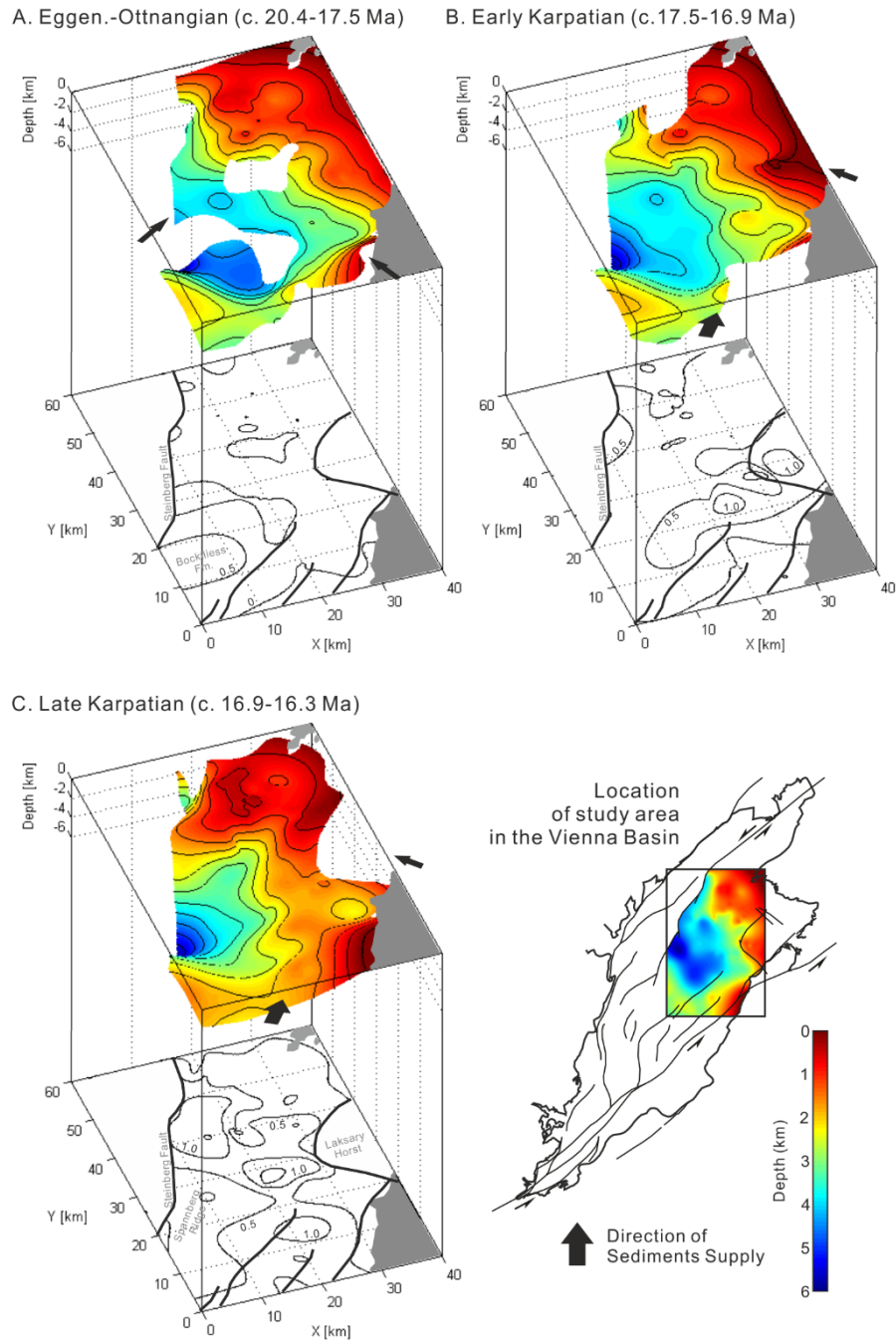


**Figure 4.3.** Depositional setting models of the Early Miocene basin system. 3D top-depth sediments distribution models (above) and 2D sediments isopach maps (below). The major faults and contour lines (0.5km) are shown with black solid lines in the isopach maps. A: Eggenburgian-Ottangian (c. 20.4 – 17.5 Ma), B: early Karpatian (c. 17.5 – 16.9 Ma) and C: late Karpatian (c. 16.9 – 16.3 Ma).

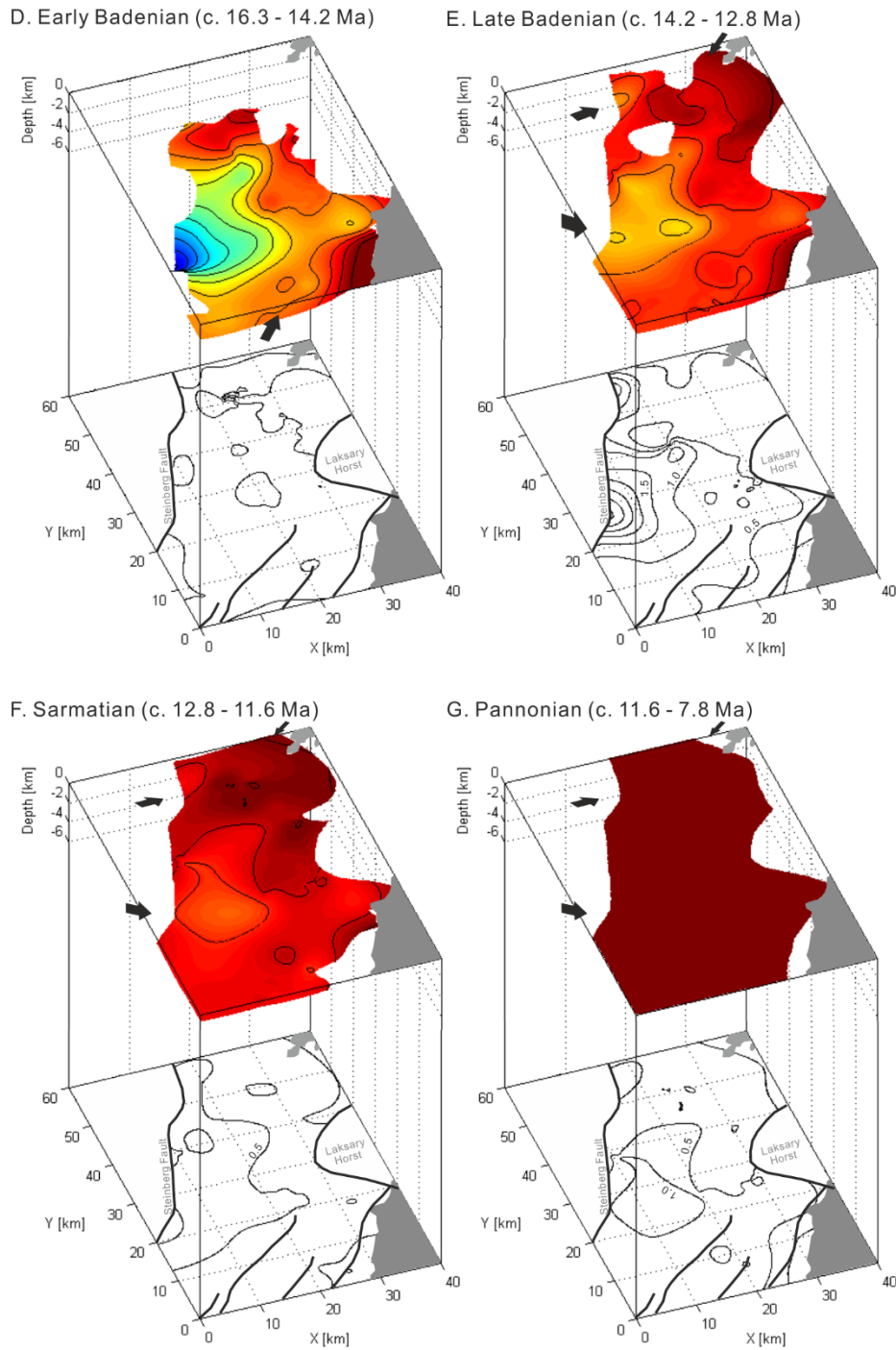


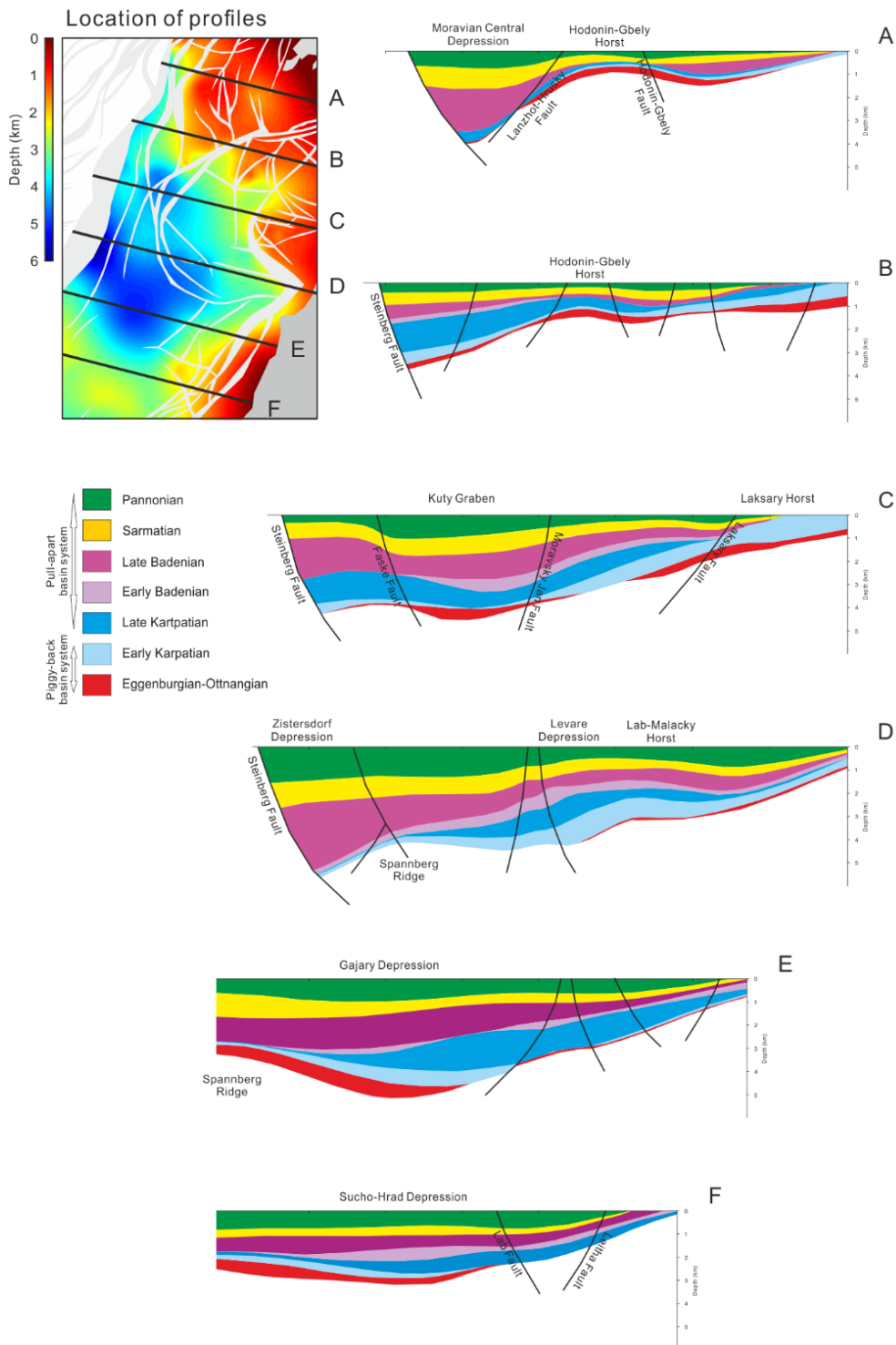
**Figure 4.4.** Depositional setting models of the Middle-Late Miocene basin system. 3D top-depth sediments distribution models (above) and 2D sediments isopach maps (below). The major faults and contour lines (0.5km) are shown with black solid lines in the isopach maps. D: early Badenian (c. 16.3 – 14.2 Ma), E: late Badenian (c. 14.2 – 12.8 Ma), F: Sarmatian (c. 12.8 – 11.6 Ma) and G: Pannonian (c. 11.6 – 7.8 Ma). The top depth of the Pannonian unit is assumed as 0 km.

The early Badenian deposition was thin (0 - 500 m in thickness) and confined to the central part of the Vienna Basin (Fig. 4.4D). The early Badenian sediments transgressed unconformably on various stratal units of the Lower Miocene and were onlapping on the northern slope of the Spannberg/Matzen ridges that were uplifted during the late Karpatian (Fig 4.5H). According to Kováč et al. (2004), the sediments extent of the early Badenian in the Slovak part of the Vienna Basin is approximately identical with the paleo-shoreline.

During the late Badenian, the sedimentation was distributed more widely and thicker than the former ones (Fig. 4.4E), forming westward thickening wedges which are bounded to the west by synsedimentary faults (Fig. 4.5D). The configuration of the Vienna Basin was mainly influenced by NE-SW and NNE-SSW oriented normal faults, and growth strata were developed along the normal faults, especially the Steinberg fault. Thick sedimentary units are related mainly to the paleo deltas (Fig. 1.6c). Around the middle Badenian, paleogeographic changes developed a new 40 x 50 km broad paleo-Danube delta complex on the western flank of the basin, carrying sediments from the Molasse area into the Vienna Basin. This also created some smaller local deltas in the SW and NE corners of the basin (Sauer et al., 1992). The areas exhibiting the highest thickness were the Zisterdorf depression and the Moravian-Central depression.

The Sarmatian sedimentation covers a large part of the study area and extends farther northward than the Badenian one (Fig. 4.4F). The deposits attain a varying thickness between 200 – 600 m, with a depocenter along the Steinberg Fault. The sedimentation continued without major depositional break across the Sarmatian/Pannonian boundary in the central part of the basin (Fig. 4.5), despite of the regression and salinity decrease by the separation of the Paratethys (Jiricek and Seifert, 1990; Kováč et al., 2004; Sauer et al., 1992).

Compared to the Sarmatian sedimentation, the Pannonian deposition has a wider and deeper depocenter along the Steinberg Fault, and the depocenter shifted to the southwest in the study area (Fig. 4.4G). The main delta system developed during the Badenian had continued transporting sediments from the Molasse area into the shallowing basin (Fig. 1.6d). Considering the uplift and erosion during the latest Pannonian and Pliocene, the Pannonian sediments were probably thicker than the present-day preserved thickness.



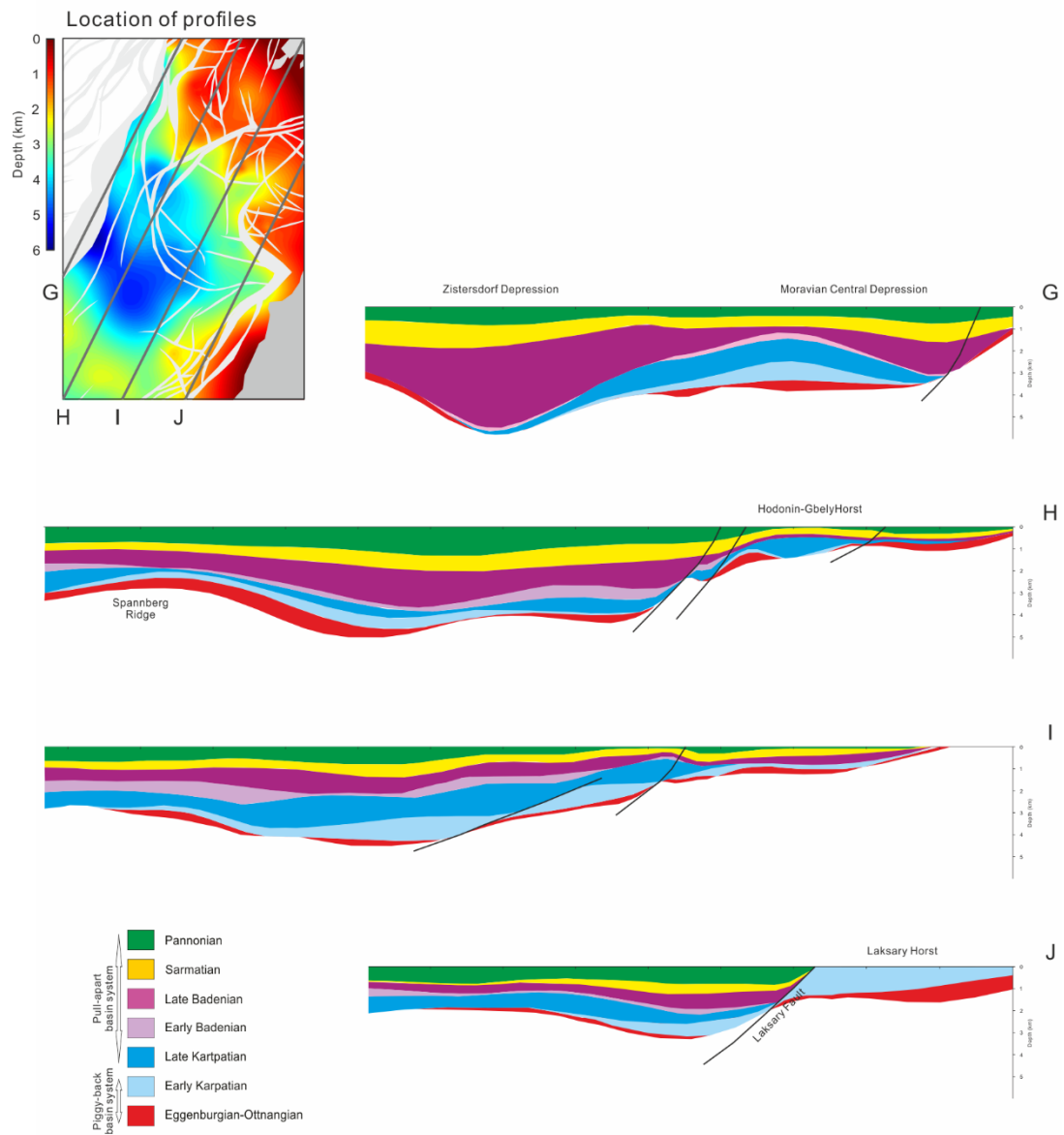


**Figure 4.5.** Cross-section profiles across the study area, exported from the cross-section function of BasinVis 1.0. Assumed locations of the main structural elements.

## **4.4 3D MODELING OF SUBSIDENCE EVOLUTION**

In this study, modeling of the basement subsidence presents 3D subsided depth surface models and 2D subsidence rate maps of the pre-Neogene basement at each stage. Modeling of the tectonic subsidence shows 3D tectonically subsided depth models and 2D tectonic subsidence rate maps of each stage to help understanding stepwise basement and tectonic subsidence trends of each stage. 2D subsidence rate maps are showing locations of the Alpine-Carpathian nappe borders for the piggy-back basin system and of the major faults (Steinberg fault, Laksary fault and Leitha-Láb fault system) for the pull-apart basin system,

### **4.4.1 Subsidence evolution of the Piggy-back basin system**

During the Eggenburgian – Ottnangian, the basement and tectonic subsidences were shallow showing low rates (Fig.4.6A). The basin subsidence spread over the study area, however, was localized in EW trending small areas. These minor and local subsidences trends are indicating the complex piggy-back basin structural features of the Vienna Basin, formed on top of the nappes of the moving Alpine-Carpathian thrustbelt in Early Miocene. The relatively high basement and tectonic subsidence area, found regionally at the southwestern corner of the study area, is correlating with the location of the deltaic-brackish complex (Bockfliess Formation) reported in the depositional setting model of the Eggenburgian – Ottnangian (Fig. 4.3A).

In the early Karptian, the study area shows increasing basement subsidence (up to 1.5 km deep) and tectonic subsidence (up to 0.5 km deep) in the northern and central Vienna Basin, and the subsidences took place in a more NE-SW trending structural confinement (Fig. 4.6B). In this stage, high tectonic subsidence rates (0.5 – 1.0 km/Ma) are found in a NE-SW trending area continuing from the Laksary horst to Leváre and Gajary depressions of the central part and an area near the proto-Steinberg fault in the northern part.

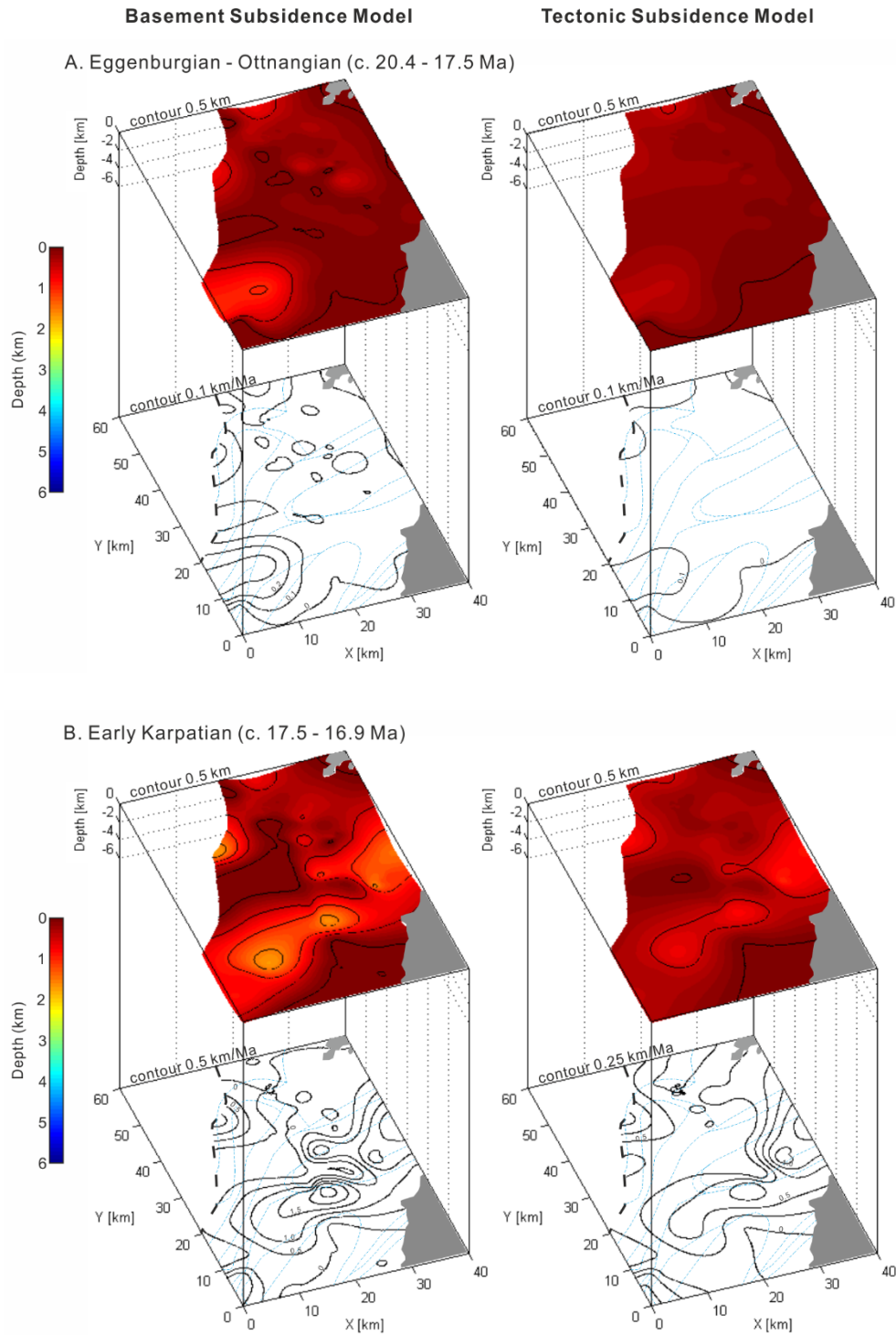


**Figure 4.6.** Basement subsidence (left) and tectonic subsidence (right) models of the Eggenburgian-Ottangian (A) and the early Karpatian (B). 3D subsided depth surface models (above) and 2D subsidence rate maps (below). The Alpine-Carpathian nappe borders are shown with blue dotted lines, and the location of the Steinberg fault with black broken lines.

#### 4.4.2 Subsidence evolution of the Pull-apart basin system

From the late Karpatian, the thrust movement of the Alpine-Carpathian thrustbelt died out, and the initial pull-apart effects were caused between two convergent left-lateral strike-slip fault segments (Decker, 1996; Royden, 1985; Sauer et al., 1992). This stage is intensely crucial in the development of the Vienna Basin, because the structural type of the basin changed from the piggy-back to the pull-apart basin.

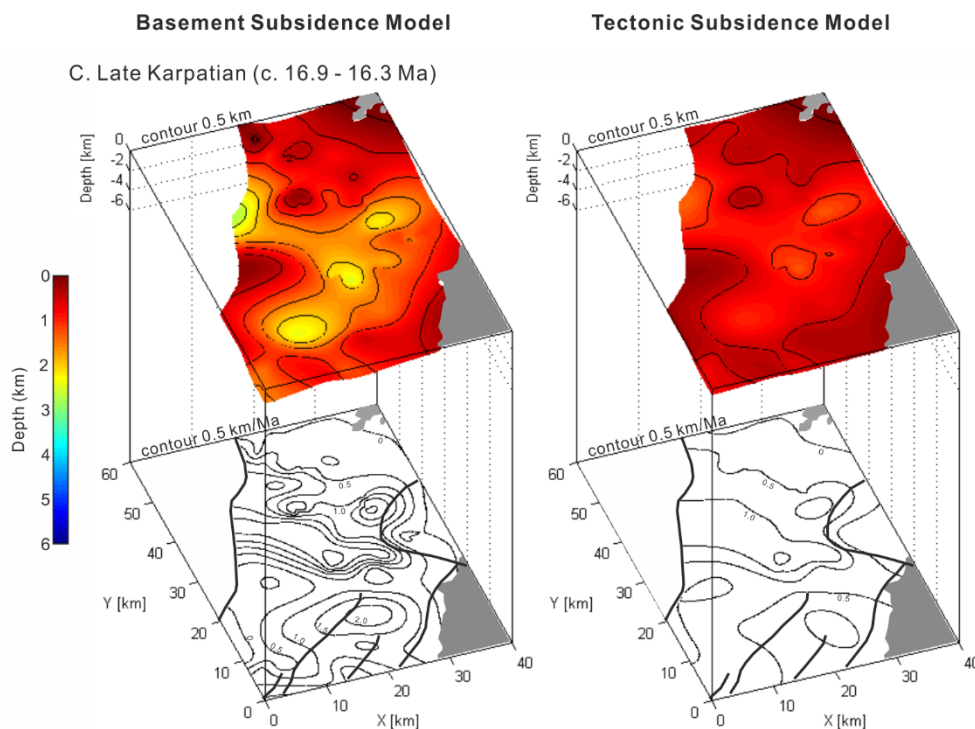


**Figure 4.7.** Basement subsidence (left) and tectonic subsidence (right) models of the late Karpatian. 3D subsided depth surface models (above) and 2D subsidence rate maps (below). The major faults are shown with black solid lines in the rate map.

Due to the onset of transtensional tectonic movement, the basement and tectonic subsidence were considerably high in the study area, especially faulted areas between the Steinberg fault and the Laksary fault and along the Leitha-Láb fault system (Fig. 4.7). The subsidence was bounded by the synsedimentary fault blocks, the en-echelon fault system and the structural ridges (e.g. Stannberg

Ridge), as the tectonic style of the basin changed to a left-lateral strike-slip movement (Decker and Peresson, 1996; Fodor, 1995; Hinsch et al., 2005a; Jiříček and Tomek, 1981; Jiříček and Seifert, 1990; Weissenböck, 1996).

The rapid increase of the subsidence rates is also strongly related to movement along the NE-SW trending negative flower strike-slip structures and normal faults. However the tectonic subsidence rate is relatively low or decreasing in the northern basement high, the Laksary horst, and the Spannberg ridge. It is supposed that these areas were not affected by the transtensional tectonics, and, in contrast to most parts of the basin, underwent transpressional stress during the time (Lee and Wagreich, submitted). According to Fodor (1995) and Jiříček and Tomek (1981), a significant angular unconformity in the northern part indicates uplift and deformation, and the basin inversion was due to local transpressional tectonics where sinistral-slip transferred toward the northeast.

After the high rate of the late Karpatian subsidence, the basement and tectonic subsidences decreased markedly in the early Badenian, showing low subsidence rates (Fig. 4.8D). Relatively high rates of the basement subsidence are indicated in the Kutý graben and the Leváre depression. The tectonic subsidence almost stopped in this stage, with low tectonic subsidence rate (0 – 0.1 km/Ma).

From the late Badenian, high basement and tectonic subsidences commenced along the Steinberg Fault (Fig. 4.8E). The Spannberg ridge uplifted during the late Karpatian also subsided from this time onwards. However, the high rate (more than 0.5 km/Ma) of the tectonic subsidence is more restricted to the Zisterdorf depression. The Steinberg fault was synsedimentary subsiding with large displacement of 5 – 6 km, and most activity has occurred since the late Badenian. However, the increase of the basement depth was much bigger than the tectonic subsidence effect, therefore this high basement subsidence is resulted partly from sediment and water loading.

During the Sarmatian, the basement subsided mainly in the hanging wall region of the Steinberg fault (Fig. 4.9F). The highest rates (0.5 – 1.0 km/Ma) of basement subsidence are found in the Zisterdorf depression, the Gajary depression and the Sucho-Hrad depression. Compared to the late Badenian subsidence, the Sarmatian subsidence area shifted slightly to the south in the study area.

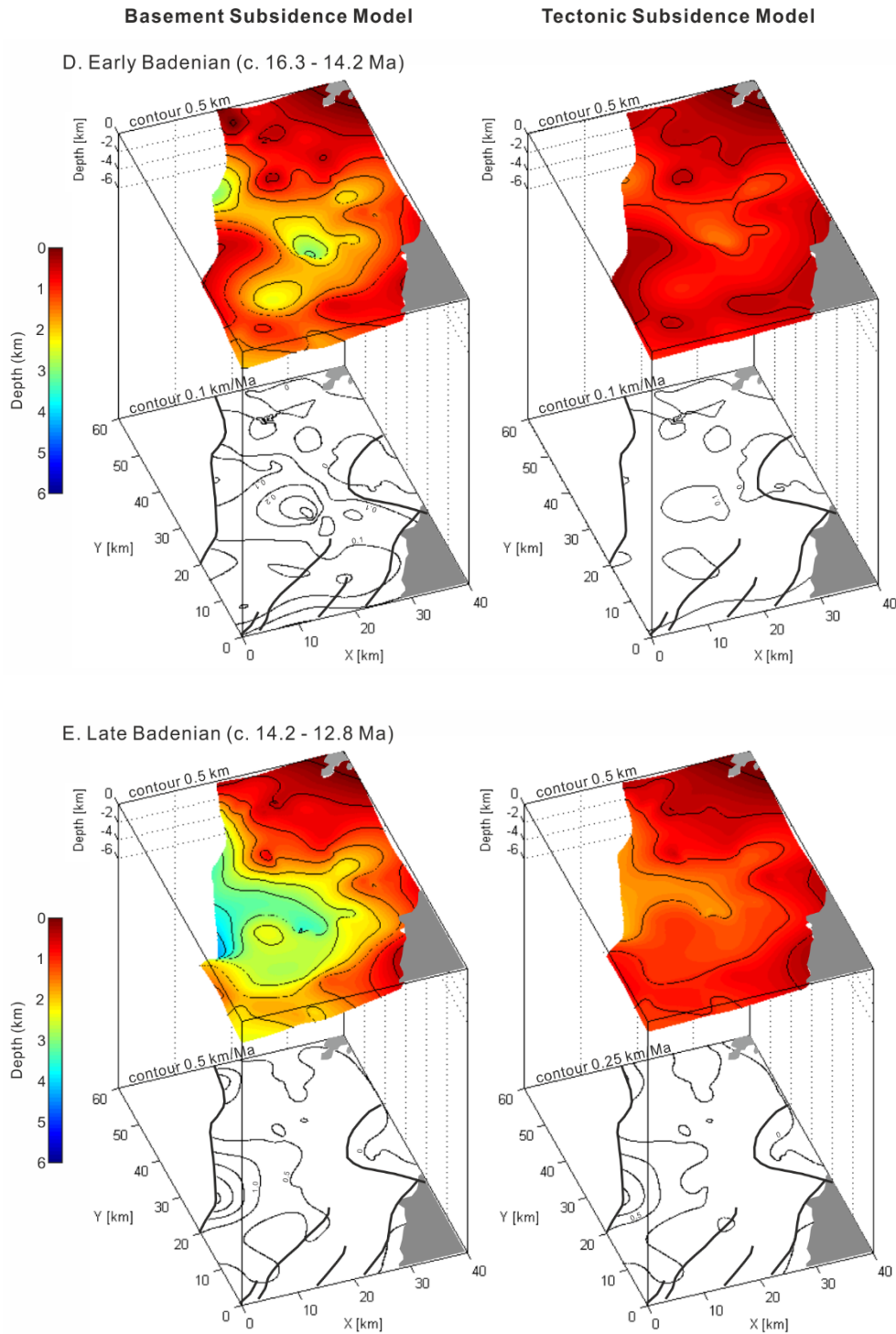


**Figure 4.8.** Basement subsidence (left) and tectonic subsidence (right) models of the early Badenian (D) and the late Badenian (E). 3D subsided depth surface models (above) and 2D subsidence rate maps (below). The major faults are shown with black solid lines in the rate map.

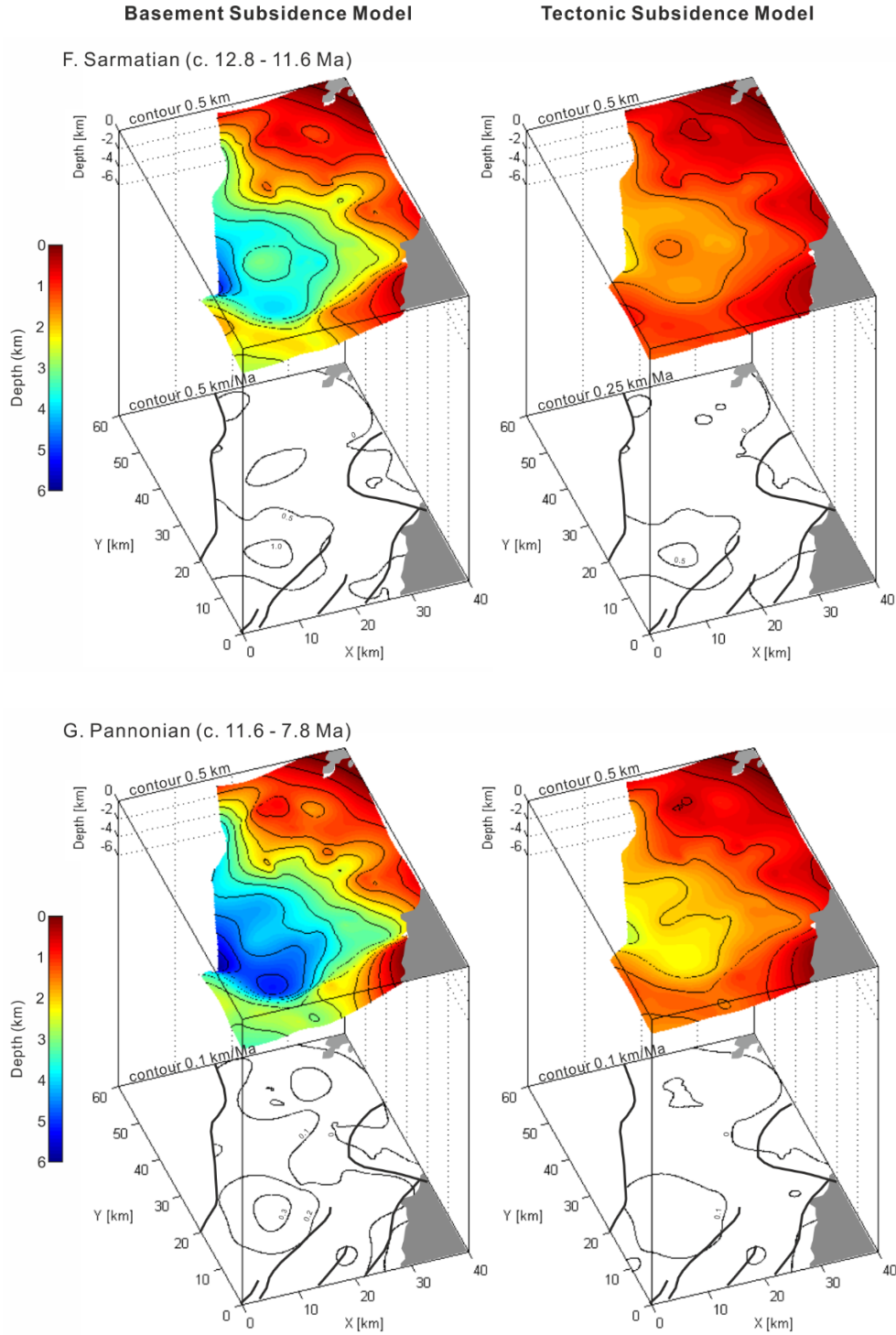


**Figure 4.9.** Basement subsidence (left) and tectonic subsidence (right) models of the Sarmatian (F) and the Pannonian (G). 3D subsided depth surface models (above) and 2D subsidence rate maps (below). The major faults are shown with black solid lines in the rate map.

The Late Miocene is characterized by the slowing down of basement and tectonic subsidence (Fig. 4.9), especially in the northern part of the Vienna Basin. Basement and tectonic subsidence during the Pannonian time show similarities to the Sarmatian ones, with subsidence mainly in the hanging wall of the Steinberg fault (Fig. 4.9G), however, the Pannonian subsidence rates are much lower.

It is possible that the Pannonian subsidence has been underestimated due to missing (eroded) strata and thickness data in this study. Uplift of more than 200 m resulting from the latest Pannonian and Pliocene E-W compressional event caused basin inversion (Fig. 1.3), sediment deformation and erosion of Pannonian sediments (Decker and Peresson, 1996; Peresson and Decker, 1997a, 1997b; Strauss et al., 2006). In addition, Lee and Wagneich (submitted) found that Quaternary deposits (see Figure 1.2 and 3.12 for locations and sediments thickness of Quaternary basins) have not been separated from Pannonian sediments in well data, thus the Pannonian subsidence also partly includes Quaternary vertical faulting displacement along the Vienna Basin transfer fault (e.g. Beidinger and Decker, 2011).

## **4.5 DISCUSSION AND CONCLUSIONS**

This study presented the Early to Late Miocene basin evolution of the Vienna basin with modeling the depositional setting and the basement and tectonic subsidences. The results demonstrate that the basin evolution in the Vienna Basin is closely coupled with changes of the basin structural setting, the regional stress field and the paleogeography and resulting regional sediment supply (Fig. 4.10).

The piggy-back basin system of the Vienna Basin was a depositional edifice superimposed on top of the N- to NW- propagating and moving Alpine-Carpathian thrustbelt which died out during the late Early Miocene (Beidinger, 2013; Decker, 1996; Sauer et al., 1992). Because of the tectonic setting, the Early Miocene setting of the Vienna Basin overlapped with the final stage of the thrusting. The Early Miocene kinematic of the Vienna Basin is characterized by the combination of synsedimentary thrusting and wrench faulting (Beidinger, 2013; Decker, 1996). During the Early Miocene piggy-back basin system (c. 20.4 – 16.9 Ma), the deposition

and subsidence from the Eggenburgian to the Ottnangian were shallow. Slowly subsiding areas in the E-W trending small depressions of the northern and central parts predominate. The early Karpatian basin setting was deeper and NE-SW trending. According to Fodor (1995), the Eggenburgian depocenters concentrated at the junction area of the Eastern Alps-Western Carpathians. Successively, the Ottnangian – early Karpatian depocenters migrated southward along sinistral strike-slip or oblique thrusts, therefore the early Karpatian depressions spread more to south and NE-SW trending. This can be also related to an apparent counterclockwise rotation of the Alpine thrust front between the Eggenburgian and the Karpatian, resulted from the eastward increase of the cumulative in-sequence thrust distance (Beidinger, 2013; Beidinger and Decker, 2014). The NE-SW trending strikes sub-parallel to the Leitha-Láb strike-slip fault system in the study area, which, however, is not genetically related to the Malacky negative flower structure. The Lower Miocene depressions were filled with sediments supplied from the small deltaic system entering from the south (Sauer et al., 1992; Seifert, 1992).

During the late Karpatian (c. 16.9 – 16.3 Ma), the Vienna Basin evolved into a pull-apart basin opened by the lateral extrusion tectonics of the Eastern Alps and between two left-stepping segments of the sinistral strike-slip fault system (Royden, 1985, 1988; Decker, 1996). The sinistral Vienna Basin fault system controlling the basin extended from the Eastern Alps into the flysch units of the Western Carpathians (Decker, 1996). The area of sedimentation and subsidence widened and deepened, depressions developed by synsedimentary faults, and the principal rhombin shape of the basin formed. The generated sinistral border faults transferred the left slip from southwest to northwest, and the nappe emplacement could continue north of the basin (Fodor, 1995). Thus, in the study area, this transtensional tectonic regime shifted the depocenters towards the south, and deep subsiding areas were activated mainly by the Leitha-Láb fault system and the Steinberg fault, while the northern part was relatively stationary regarding subsidence. The voluminous accommodation space created by strike-slip faulting was filled with sediments eroded from the Alps, developing of broad deltaic system entering from the south and west (Sauer et al., 1996; Seifert, 1992).

In the study area, the early Badenian (c. 16.3 – 14.2 Ma) deposition was abruptly thin and confined in a narrow area, due to the nearly stopped tectonic subsidence.

In contrast, high tectonic subsidence rate of the early Badenian (the Upper Laidenid Zone) is observed in the southern part (Hölzel et al., 2008b). There are three suggestions trying to explain this regional difference of the early Badenian subsidence;

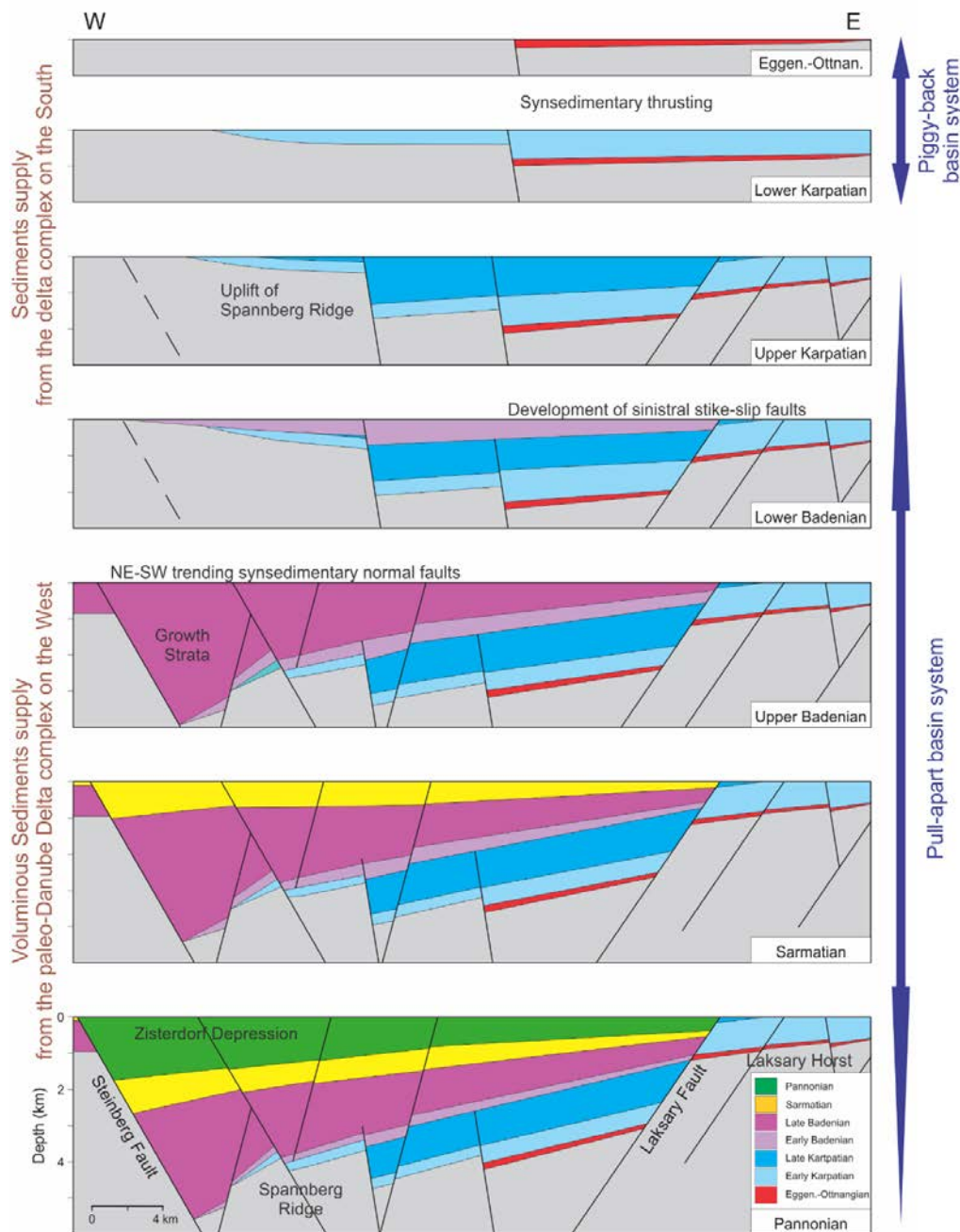


**Figure 4.10.** Schematic profile model for depositional and subsidence evolution of the central Vienna Basin from the Early to Late Miocene.

According to Weissenbäk (1996), towards the end of the Karpatian, subsidence slowed down with the cessation of fault movements. A short-lived inversion period took place in the central Vienna Basin, producing noticeable tectonic uplift of the Matzen/Spannberg ridges. Although, in the early Badenian, the subsidence increased again, the subsidence was not accompanied by synsedimentary fault activity. Hölzel et al. (2008b) explained the different subsidence pattern mainly with a paleoenvironmental effect caused by the Spannberg ridge. The ridge largely restricted sedimentation to the southern part during the early Badenian. Lee and Wagreich (submitted) (Chapter 3) suggested that the regional difference of the Badenian tectonic subsidence might be influenced by a Badenian paleostress change, considering a change of the major tensional regime shifting from transtension to E-W directed extension toward the late Middle Miocene.

The NE-SW trending normal faults, especially the Steinberg fault in the central Vienna Basin, seem to govern the basin development from the late Badenian to the Pannonian (c. 14.2 – 7.8 Ma) in the Vienna Basin. These faults induced subsidence in the Zisterdorf depression and the Moravian-Central depression, while the sinistral strike-slip faults along the southeastern border zone played a minor role. According to Decker (1996), for many normal faults in the Vienna Basin, growth strata show that faulting occurred synsedimentary during the time. The late Badenian - Pannonian stages are characterized by E-W extensional rift-type basement subsidence reaching up to 5.6 km. The extensional subsidence is also reported in the Styrian Basin, the Danube Basin and the western parts of the Pannonian Basin system for the Sarmatian - Pannonian (e.g. Fodor, 1995; Huisman et al., 2001; Kováč et al., 1999; Sachsenhofer et al., 1997; Vass et al., 1990).

The deposition of the late Badenian – Pannonian is strongly related to a large paleo-Danube delta complex on the western flank and smaller deltas in the SW and the NE corners of the Vienna Basin. The paleo-Danube delta system provided sediments eroded from the Molasse foreland basin region, and continued carrying sediments until the Pannonian (Sauer et al., 1992; Seifert, 1992).

## **CHAPTER 5**

## **FINAL CONCLUSIONS**



This thesis investigated the comprehensive basin setting and tectonostratigraphic subsidence evolution of the Vienna Basin, central Europe. This study primarily targeted the northern and central parts of the basin, and collected a large number of well, seismic, and geophysical data. To analyze and model the data, this thesis project started developing a MATLAB-based program (BasinVis 1.0) to visualize extensively the stratigraphic and structural settings and subsidence evolution. The results were compared with previous studies, arranged mainly in the southern and central parts (Austrian part), and discussed intensively in this thesis.

***BasinVis 1.0: A useful program to analyze and visualize sedimentary basin setting and subsidence evolution***

BasinVis 1.0 consists of five main processing steps; 1) setup (study area and stratigraphic units), 2) loading stratigraphic profile or well data, 3) stratigraphic setting visualization, 4) subsidence parameter input and 5) subsidence analysis and visualization. To aid users in the analysis of specific regions, this study provides the 'Cross-section Plot' and 'Dip-slip Fault Backstripping' functions. The graphical user interface guides users through all process stages, and provides tools to analyze and export the results. The structure of the program allows researchers with programming experience to edit and extend the functionalities of the software if needed. All 2D and 3D visualizations are created by using MATLAB plotting functions, which enables users to fine-tune the results using the full range of available plot options in MATLAB.

BasinVis 1.0, the MATLAB-based program, was designed to analyze and visualize stratigraphic setting and subsidence evolution of a sedimentary basin. BasinVis 1.0 performs the goal, and provides geologists with an easy-to-learn and user-friendly program for sedimentary basin analysis. The resulted maps and models are highly useful to understand overall geologic trends and characteristics of each geologic stage. However the interpretation introduces uncertainty into detailed model visualizations. Besides lack of data, the main problem of resulting surface is the smoothing out the sharp features at fault structures and the paleo-environmental features (e.g. delta, valley), because the gradually changing interpolation results fail to capture sudden local changes in sediment thickness. This problem can be mitigated by increasing the number of stratigraphic profiles. However, this study found that using data at important locations was more effective.

To advance BasinVis 1.0, a subsequent study will evaluate the software on example data from various sedimentary basins. This will help to verify and extend usability, efficiency, and potential of the program. This study plans to improve the program by including geostatistic-based interpolation methods and improved modeling interfaces. Furthermore, this study plans to include additional analysis functionalities such as fault displacements.

### ***Polyphase tectonic subsidence history of the Vienna Basin***

Due to the special position of the Vienna Basin, the subsidence history was influenced by the regional tectonics, uplift/exhumation and subsidence of surrounding units – the Eastern Alps, the Western Carpathians and the Pannonian Basin system. This study analyzed a more detailed regional subsidence history of the northern and central parts of the basin to quantify the tectonic evolution. Compared to previous studies conducted on this topic in the southern part, this study covers an extensive region of the basin. Also this study provides a more accurate analysis through the high density of considered boreholes, the geophysical evaluation for more realistic porosity-depth relations and the mapping by employing a 3D interpolation technique.

This study arranged the tectonic subsidence history of the Vienna Basin to five subsidence phases; 1) E-W trending piggy-back subsidence (Eggenburgian-Ottnangian; Early Miocene), 2) NE-SW transtensional subsidence (Late Karpatian; late Early Miocene), 3) NW-SE to E-W transitioning extensional subsidence (Badenian; Middle Miocene), 4) E-W extensional subsidence (Sarmatian-Pannonian; late Middle - Late Miocene) and 5) NE-SW transtensional subsidence (Quaternary).

After shallow and E-W trending subsidence (the piggy-back basin system; c. 20.4 – 16.9 Ma), data show abruptly increasing subsidence during the late Early Miocene (the late Karpatian; c. 16.9 – 16.3 Ma), which initiated the Vienna pull-apart basin system. From the Middle Miocene onwards, the subsidence was decreasing overall, however the tectonic subsidence curves show regionally different patterns. This study found that the tectonic subsidence nearly stops in the northern part, whereas the central part is characterized by a gradually decreasing pattern. There were two suggestions to explain the regionally different subsidence decrease patterns observed in the Vienna Basin. One analyzed uncorrected subsidence curves neglecting compaction of sediments, and failed to explain tectonically why subsidence happened locally in different times. The other proposed a post-rift (thermal) subsidence for the central part, however there is no major thermal anomaly

arguing for backing up the lithospheric extension and the heat flow is uniformly low in the basin

In details of the Badenian (c. 16.3 – 12.8) subsidence rates, the high rate of the early/middle Badenian (the Upper Lagenid Zone) observed in the southern part is missing in the rest of the Vienna Basin. In the northern and central parts, the late Badenian subsidence rate is higher than the early Badenian one. The Middle Miocene evolution was characterized by a combination of strike-slip (transtension) and extensional faulting. The differential subsidence displaying a time-transgressive trend from south to north can be related to a change of the major tensional regime shifting from transtension to E-W directed extension toward the Late Middle Miocene.

From the late Middle Miocene to the Late Miocene (the Sarmatian – Pannonian; c. 12.8 – 7.8 Ma), the tectonic subsidence occurred dominantly along the regional active normal faults (e.g. Steinberg fault), and corresponds to the E-W trending extension. Similar extension is also reported in neighboring basins – the Pannonian basin system, the Styrian Basin and the Danube Basin. However, the Late Miocene subsidence calculated in this study may be biased due to the fact of missing parts of the youngest sedimentary column. In addition, this study found that in some of the well data Quaternary deposits have not been separated from Pannonian sediments.

After the Late Miocene – Pliocene compression and basin inversion, the Vienna Basin is reactivated at a releasing bend along the sinistral strike-slip fault system (Vienna Basin Transfer Fault), and resulted in small Quaternary basins filled mainly by fluvial sediments.

***Basin evolution of the Vienna Basin – Insights from 3D modeling of the depositional setting and subsidence evolution.***

This study analyzed and modeled a study area of 40 x 60 km in the northern and central Vienna Basin, using BasinVis 1.0 for the depositional setting and the subsidence evolution. The results were compared with previous studies to understand the comprehensive basin evolution. The models provided insights into the integrated and extensive basin evolution of the Vienna Basin. The results demonstrate that the basin evolution in the Vienna Basin is closely coupled with changes of the basin structural setting, the regional stress field and the palaeogeographic setting and sediment supply from rising hinterlands.

The deposition and subsidence during the Eggenburgian – Ottnangian (c. 20.4 – 17.5 Ma) were shallow and slowly subsiding in the E-W trending small depressions of the northern and central parts. The early Karpatian basin setting (c. 17.5 – 16.9 Ma) was deeper and NE-SW trending. The depocenter migration in the Early Miocene can be related to an apparent counterclockwise rotation of the Alpine thrust front between the Eggenburgian and the Karpatian. The Early Miocene depressions were filled with sediments supplied from the deltaic system entering from the south.

For the late Karpatian (c. 16.9 – 16.3 Ma), the area of sedimentation and subsidence widened and deepened, developed by synsedimentary sinistral strike-slip faults. After abruptly decreasing deposition and subsidence of the early Badenian (c. 16.3 – 14.2 Ma), the NE-SW trending normal faults accompanying the growth strata, especially the Steinberg fault in the central Vienna Basin, controlled the basin development from the late Badenian to the Pannonian (the Middle – Late Miocene; c. 14.2 – 7.8 Ma). It is characterized by E-W extensional rift-type basement subsidence, and similar extension is reported in neighboring basins. The immense sediments deposited during these stages were provided from a large paleo-Danube delta complex on the western flank and smaller deltas in the SW and the NE corners of the Vienna Basin.

To improve the polyphase basin evolution model of the Vienna Basin, this study will integrate more geological and geophysical data for deep structure and surrounding tectonic units (e.g. Molasse Foreland Basin, Eastern Alps, Western Carpathians and Pannonian Basin System). And the more detailed and quantitative paleogeographic and paleoenvironmental studies will help the comprehensive basin evolution of the Vienna Basin.

## REFERENCES



- Albrecht, J., 2007. Spatial Statistics, in: Key Concepts and Techniques in GIS. Sage Publications Ltd., London, p. 120.
- Allen, P.A., Allen, J.R., 2013. Basin Analysis: Principles and Application to Petroleum Play Assessment, 3rd ed. Wiley-Blackwell, Oxford, p. 642.
- Amidror, I., 2002. Scattered data interpolation methods for electronic imaging systems: a survey. *Journal of Electronic Imaging* 11, 157-176.
- Arzmüller, G., Buchta, S., Ralbovský, E., Wessely, G., 2006. The Vienna Basin, in: Golonka, J., Picha, F.J. (Eds.), AAPG Memoir 84: The Carpathians and Their Foreland: Geology and Hydrocarbon Resources. AAPG, pp. 191-204. doi:10.1306/0-89-181365-9
- Báldi, T., 1980. The early history of Paratethys. *Földtani Közlöny: Bulletin of the Hungarian Geological Society* 110, 456-472.
- Baráth, I., Kováč, M., Hudáčková, N., Hlavatý, I., 2003. The Karpatian in the Vienna Basin, in: Kováč, M., Rögl, F. (Eds.), The Karpatian - a Lower Miocene Stage of the Central Paratethys. Masaryk Univ Press, Brno, pp. 101-106.
- Beidinger, A., 2013. Paleogene and Neogene tectonic evolution of the Alpine-Carpathian fold-thrust belt at the Alpine-Carpathian transition. Ph.D Thesis, University of Vienna, Vienna, Austria. <http://ubdata.univie.ac.at/AC11087532>
- Beidinger, A., Decker, K., 2014. Quantifying Early Miocene in-sequence and out-of-sequence thrusting at the Alpine-Carpathian junction, *Tectonics* 33, 222-252. doi:10.1002/2012TC003250.
- Beidinger, A., Decker, K., Roch, K.H., 2011. The Lassees segment of the Vienna Basin fault system as a potential source of the earthquake of Carnuntum in the fourth century A.D. *International Journal of Earth Sciences* 100, 1315-1329. doi:10.1007/s00531-010-0546-x
- Beidinger, A., Decker, K., 2011. 3D geometry and kinematics of the Lassees flower structure: Implications for segmentation and seismotectonics of the Vienna Basin strike-slip fault, Austria. *Tectonophysics* 499, 22-40.
- Bobach, T., Umlauf, G., 2006. Natural neighbor interpolation and order of continuity. *GI Lecture Notes in Informatics: Visualization of Large and Unstructured Data Sets* 69-86.
- Bond, G.C., Kominz, M.A., 1984. Construction of tectonic subsidence curves for the early Paleozoic miogeocline, southern Canadian Rocky Mountains: implications for

- subsidence mechanisms, age of breakup, and crustal thinning (Canada). *Geological Society of America Bulletin* 95, 155-173.
- Brix, F., Schultz, O., 1993. Veröffentlichungen aus dem Naturhistorischen Museum in Wien, N.F. 19: Erdöl und Erdgas in Österreich. Naturhistorisches Museum, Vienna and F. Berger, Horn.
- Čekan, V., Kocák, A., Tomek, Č., Wessely, G., Zych, D., 1990. Czechoslovak–Austrian cooperation in geophysical structural exploration in the Vienna basin, in: Minaříková, D., Lobitzer, H. (Eds.), *Thirty Years of Geological Cooperation between Austria and Czechoslovakia*. Geological Survey, Prague, pp. 23-31.
- Chen, L., Zhang, Z., Song, H., Li, F., Franke, D., 2013. Numerical modeling of extensional sedimentary basin formation with MATLAB: Application to the northern margin of the South China Sea. *Computers & Geosciences* 51, 153-165. doi:10.1016/j.cageo.2012.07.014
- Cloetingh, S., Ziegler, P.A., 2007. 6 . 11 Tectonic Models for the Evolution of Sedimentary Basins, in: Schubert, G. (Eds.), *Treatise on Geophysics*. Elsevier Science Publishers B. V., Amsterdam, The Netherlands, The Netherlands, pp. 485-611. doi:10.1016/B978-044452748-6.00109-7
- Csontos, L., Nagymarosy, A., Horváth, F., Kováč, M., 1992. Tertiary evolution of the Intra-Carpathian area: a model. *Tectonophysics* 208, 221-241.
- Decker, K., 1996. Miocene tectonics at the Alpine–Carpathian junction and the evolution of the Vienna Basin. *Mitteilungen der Gesellschaft der Geologie- und Bergbaustudenten* 41, 44-55.
- Decker, K., Peresson, H., 1996. Tertiary kinematics in the Alpine-Carpathian-Pannonian system: links between thrusting, transform faulting und crustal extension, in: *EAGE Spec Pub 5: Oil and Gas in Alpidic Thrustbelts and Basins of Central and Eastern Europe*. EAGE, pp. 69-77.
- Decker, K., Peresson, H., Hinsch, R., 2005. Active tectonics and Quaternary basin formation along the Vienna Basin Transform fault. *Quaternary Science Reviews* 24, 307-322.
- Dövényi, P., Horváth, F., 1988. A review of temperature, thermal conductivity, and heat flow data for the Pannonian Basin, in: Royden, L., Horváth, F. (Eds.), *AAPG Memoir 45: The Pannonian Basin: A Study in Basin Evolution*. AAPG, pp. 195-233.
- Fodor, L., 1995. From transpression to transtension: Oligocene-Miocene structural evolution of the Vienna basin and the East Alpine-Western Carpathian junction. *Tectonophysics* 242, 151-182.

- Friedinger, P.J.J., 1988. BASTA—subsidence and paleotemperature modeling of rift basins. *Computers & Geosciences* 14, 505-528. doi:10.1016/0098-3004(88)90032-5
- Fuchs, R., Hamilton, W., 2006. New depositional architecture for an old giant: The Matzen field, Austria, in: Golonka, J., Picha, F.J. (Eds.), *AAPG Memoir 84: The Carpathians and Their Foreland: Geology and Hydrocarbon Resources*. AAPG, pp. 191-204. doi:10.1306/0-89-181365-9
- Gardner, G.H.F., Gardner, L.W., Gregory, A.R., 1974. Formation velocity and density – The diagnostic basics for stratigraphic traps. *Geophysics* 39(6), 770-780.
- Grenerczy, G., Kenyeres, A., Fejes, I., 2000. Present crustal movement and strain distribution in Central Europe inferred from GPS measurements. *Journal of Geophysical Research* 105(B9), 21,835-21,846.
- Hamilton, W., Wagner, L., Wessely, G., 2000. Oil and gas in Austria. *Austrian Journal of Earth Sciences* 92, 235-262.
- Haq, B.U., Hardenbol, J., Vail, P.R., 1987. Chronology of fluctuating sea levels since the Triassic. *Science* 235, 1156-1167.
- Harzhauser, M., Piller, W.E., 2004: Integrated Stratigraphy of the Sarmatian (Upper Middle Miocene) in the western Central Paratethys. *Stratigraphy* 1, 65-86.
- Hinsch, R., Decker, K., Peresson, H., 2005a. 3-D seismic interpretation and structural modeling in the Vienna Basin: implications for Miocene to recent kinematics. *Austrian Journal of Earth Sciences* 97, 38-50.
- Hinsch, R., Decker, K., Wagreeich, M., 2005b. 3-D mapping of segmented active faults in the southern Vienna Basin. *Quaternary Science Reviews* 24, 321-336.
- Hlavaty, V., 1996. The Slovakian part of the Vienna basin - Exploration results, in: Wessely, G., Liebl, W. (Eds.), *EAGE Spec Pub 5: Oil and Gas in Alpidic Thrustbelts and Basins of Central and Eastern Europe*. pp. 41-42.
- Hohenegger, J., Ćorić, S., Wagreeich, M., 2014. Timing of the Middle Miocene Badenian Stage of the Central Paratethys. *Geologica Carpathica* 65, 55-66.
- Hölzel, M., 2009. Quantification of tectonic movement in the Vienna Basin. Ph.D Thesis, University of Vienna, Vienna, Austria.
- Hölzel, M., Decker, K., Zámolyi, A., Strauss, P., Wagreeich, M., 2010. Lower Miocene structural evolution of the central Vienna Basin (Austria). *Marine and Petroleum Geology* 27, 666–681.

- Hölzel, M., Faber, R., Wagneich, M., 2008a. DeCompactionTool: Software for subsidence analysis including statistical error quantification. *Computers & Geosciences* 34, 1454-1460.
- Hölzel, M., Faber, R., Wagneich, M., 2008b. Regional subsidence analysis in the Vienna Basin. *Austrian Journal of Earth Sciences* 101, 88-98.
- Horváth, F., 1993. Towards a mechanical model for the formation of the Pannonian basin. *Tectonophysics* 226, 333-357.
- Huisman, R.S., Podladchikov, Y.Y., Cloetingh, S., 2001. Dynamic modeling of the transition from passive to active rifting, application to the Pannonian basin. *Tectonics* 20, 1021-1039.
- Iske, A., 2004. *Multiresolution Methods in Scattered Data Modelling*. Springer Berlin Heidelberg, p. 188. doi:10.1007/978-3-642-18754-4
- Jin, J., 1994. BSAS: A basic program for two-dimensional subsidence analysis in sedimentary basins. *Computers & Geosciences* 20, 1329-1345.
- Jiříček, R., Seifert, P., 1990. Paleogeography of the Neogene in the Vienna basin and the adjacent part of the foredeep, in: Minaříková, D., Lobitzer, H. (Eds.), *Thirty Years of Geological Cooperation between Austria and Czechoslovakia*. Geological Survey, Prague, pp. 89-105.
- Jiříček, R., Tomek, Č., 1981. Sedimentary and structural evolution of the Vienna Basin. *Earth Evolution Sciences* 3-4, 195-204.
- Kováč, M., Baráth, I., Harzhauser, M., Hlavatý, I., Hudáčková, N., 2004. Miocene depositional systems and sequence stratigraphy of the Vienna Basin. *CFS Courier Forschungsinstitut Senckenberg* 187-212.
- Kováč, M., Holcová, K., Nagymarosy, A., 1999. Paleogeography, paleobathymetry and relative sea-level changes in the Danube Basin and adjacent areas. *Geologica Carpathica* 50, 325-338.
- Kröll, A., Wessely, G., 1993. *Wiener Becken und angrenzende Gebiete - Strukturkarte-Basis der tertiären Beckenfüllung*.
- Kullmann, E., 1966. The role of neotectonic movements in the development of ground water reservoirs in the north-eastern part of the Vienna Basin. *IAHS Redbook* 120, 392-400.

- Lai, M.-J., 2008. Multivariate Splines for Data Fitting and Approximation, in: Neamtu, M., Schumaker, L.L. (Eds.), *Approximation Theory XII: San Antonio 2007*. Nashboro Press, Brentwood, TN, pp. 210-228.
- Lanari, P., Vidal, O., De Andrade, V., Dubacq, B., Lewin, E., Grosch, E.G., Schwartz, S., 2014. XMapTools: A MATLAB®-based program for electron microprobe X-ray image processing and geothermobarometry. *Computers & Geosciences* 62, 227-240.
- Lankreijer, A., Kováč, M., Cloetingh, S., Pitoňák, P., Hlôška, M., Biermann, C., 1995. Quantitative subsidence analysis and forward modelling of the Vienna and Danube basins: thin-skinned versus thick-skinned extension. *Tectonophysics* 252, 433-451. doi:10.1016/0040-1951(95)00099-2
- Lee, E.Y., 2010. Subsidence history of the Gunsan Basin (Cretaceous-Cenozoic) in the Yellow Sea, offshore Korea. *Austrian Journal of Earth Sciences* 103, 111-120.
- Lee, E.Y., Novotny, J., Wagreeich, M., submitted. BasinVis 1.0: A MATLAB®-based program for sedimentary basin subsidence analysis and visualization. Submitted to *Computers & Geosciences*.
- Lee, E.Y., Wagreeich, M., submitted. Polyphase tectonic subsidence evolution of the Vienna Basin inferred from quantitative subsidence analysis. Submitted to *International Journal of Earth Sciences*.
- Lee, E.Y., Wagreeich, M., submitted. 3D modeling of depositional setting and subsidence evolution in the northern and central Vienna Basin. Submitted to *Austrian Journal of Earth Sciences*.
- Lee, E.Y., Zámolyi, A., Beidinger, A., Decker, K., Strauss, P., 2011. Stratigraphy and subsidence history of the Závod region in the Slovak part of the central Vienna Basin, in: 73rd EAGE Conference & Exhibition, Extended Abstract P253.
- Mann, P., Hempton, M.R., Bradley, D.C., Burke, K., 1983. Development of pull-apart basins. *The Journal of Geology* 91, 529-554.
- Marion, D.P., 1990. Acoustic, mechanical, and transport properties of sediments and granular materials. Ph.D Thesis, Stanford University, CA, USA.
- Miall, A.D., 1999. Principles of sedimentary basin analysis, 3rd ed. Springer-Verlag Berlin, Germany, p. 616.
- Mitas, L., Mitasova, H., 1999. Spatial interpolation, in: Longley, P., Goodchild, M.F., Maguire, D.J., Rhind, D.W. (Eds.), *Geographical Information Systems: Principles, Techniques, Management and Applications*. Wiley, pp. 481-492.

- Monnet, C., Bouchet, S., Thiry-Bastien, P., 2003. ISOPAQ, a MATLAB program for stratigraphic and isopach mapping: Example application to the French Bajocian (Jurassic) sediments. *Computers & Geosciences* 29, 1101-1110.
- Ori, G.G., Friend, P.F., 1984. Sedimentary basins formed and carried piggyback on active thrust sheets. *Geology* 12, 475-478.
- Peresson, H., Decker, K., 1997a. Far-field effects of Late Miocene subduction in the Eastern Carpatians: E-W compression and inversion of structures in the Alpine–Carpathian-Pannonian region. *Tectonics* 16, 38-56.
- Peresson, H., Decker, K., 1997b. The Tertiary dynamics of the northern Eastern Alps (Austria): changing palaeostresses in a collisional plate boundary. *Tectonophysics* 272, 125-157.
- Picha, F.J., 1996. Exploring for hydrocarbons under thrust belts - a challenging new frontier in the Carpathians and elsewhere. *American Association of Petroleum Geologists Bulletin* 80, 1547-1564.
- Piller, W.E., Harzhauser, M., Mandic, O., 2007. Miocene Central Paratethys stratigraphy – current status and future directions. *Stratigraphy* 4, 151-168.
- Plašienka, D., Grecula, P., Putiš, M., Kováč, M., Hovorka, D., 1997. Evolution and structure of the Western Carpathians: an overview. In: Grecula, P., Hovorka, D., Putiš, M. (Eds.), *Geological evolution of the Western Carpathians*. Mineralia Slovaca – Monograph, 1-24.
- Ratschbacher, L., Merle, O., Davy, P., Cobbold, P., 1991a. Lateral extrusion in the eastern Alps, part I: boundary conditions and experiments scaled for gravity. *Tectonics* 10(2), 245-256.
- Ratschbacher, L., Frisch, W., Linzer, H.-G., 1991b. Lateral extrusion in the eastern Alps, part II: structural analysis. *Tectonics* 10(2), 257-271.
- Reinecker, J., Lenhardt, W.A., 1999. Present-day stress field and deformation in eastern Austria. *International Journal of Earth Sciences* 88, 532-550. doi:10.1007/s005310050283
- Ricard, L.P., Chanu, J.B., 2013. GeoTemp 1.0: A MATLAB-based program for the processing, interpretation and modelling of geological formation temperature measurements. *Computers & Geosciences* 57, 197-207.
- Royden, L.H., 1985. The Vienna Basin: a thin-skinned pull-apart Basin. In: Biddle, K.T., Christie-Blick, N. (Eds.), *Strike-slip deformation, basin formation and sedimentation*.

- Society for Sedimentary Geology, Special Publication 37, pp. 319-338.  
doi:10.2110/pec.85.37.0319
- Royden, L.H., Horváth, F., Rumpler, J., 1983a. Evolution of the Pannonian Basin System: 1. Tectonics. *Tectonics* 2, 63-90.
- Royden, L.H., Horváth, F., Nagymarosy, A., Stegena, L., 1983. Evolution of the Pannonian Basin System: 2. Subsidence and thermal history. *Tectonics* 2, 91-137.
- Royden, L.H., 1988. Late Cenozoic tectonics of the Pannonian basin system. In: Royden, L.H., Horváth, F. (Eds.), *The Pannonian Basin. A study in Basin evolution*. AAPG Memoir 45, 27-48.
- Sachsenhofer, R.F., 2001. Syn- and post-collisional heat flow in the Cenozoic Eastern Alps. *International Journal of Earth Sciences* 90, 579-592.
- Sachsenhofer, R.F., Lankreijer, A., Cloetingh, S., Ebner, F., 1997. Subsidence analysis and quantitative basin modelling in the Styrian Basin (Pannonian Basin System, Austria). *Tectonophysics* 272, 175-196.
- Salcher, B.C., 2008. Sedimentology and modelling of the Mitterndorf Basin. Ph.D Thesis, University of Vienna, Vienna, Austria. <http://ubdata.univie.ac.at/AC05039496>
- Salcher, B.C., Meurers, B., Smit, J., Decker, K., Hölzel, M., Wagreich, M., 2012. Strike-slip tectonics and Quaternary basin formation along the Vienna Basin fault system inferred from Bouguer gravity derivatives. *Tectonics* 31. doi:10.1029/2011TC002979
- Sauer, R., Seifert, P., Wessely, G., 1992. Part I: Outline of Sedimentation, Tectonic Framework and Hydrocarbon Occurrence in Eastern Lower Austria. *Austrian Journal of Earth Sciences* 85, 5-96.
- Schwanghart, W., Kuhn, N.J., 2010. TopoToolbox: A set of Matlab functions for topographic analysis. *Environmental Modelling and Software* 25, 770-781.
- Sclater, J.G., Christie, P.A.F., 1980. Continental stretching: An explanation of the Post-Mid-Cretaceous subsidence of the central North Sea Basin. *Journal of Geophysical Research* 85, 3711-3739.
- Sclater, J.G., Royden, L., Horvath, F., Burchfiel, B.C., Semken, S., Stegena, L., 1980. The formation of the intra-Carpathian basins as determined from subsidence data. *Earth and Planetary Science Letters* 51, 139-162.
- Seifert, P., 1992. Palinspastic reconstruction of the easternmost Alps between Upper Eocene and Miocene. *Geologica Carpathica* 43, 327-331.

- Seifert, P., 1996. Sedimentary-tectonic development and Austrian hydrocarbon potential of the Vienna Basin, in: Wessely, G., Liebl, W. (Eds.), EAGE Spec Pub 5: Oil and Gas in Alpidic Thrustbelts and Basins of Central and Eastern Europe. EAGE, pp. 331-341.
- Sibson, R.H., 1981. A brief description of natural neighbor interpolation, in: Barnett, V. (Eds.), *Interpreting Multivariate Data*. Wiley, Chichester, pp. 21-36.
- Springer, J., 1993. Decompaction and backstripping with regard to erosion, salt movement, and interlayered bedding. *Computers & Geosciences* 19(8), 1115-1125.
- Stam, B., Gradstein, F.M., Lloyd, P., Gillis, D., 1987. Algorithms for porosity and subsidence history. *Computers & Geosciences*, 13(4), 317-349.
- Steckler, M.S., Watts, A.B., 1978. Subsidence of the Atlantic-type continental margin off New York. *Earth and Planetary Science Letters* 41, 1-13.
- Steininger, F.F., Rögl, F., Hochuli, P., Müller, C., 1988. Lignite deposition and marine cycles, The Austrian Tertiary lignite deposits - A case study. *Sitzungsberichte der Österreichischen Akademie der Wissenschaften, Mathem.-naturw. Kl.* 197, 309-322.
- Steininger, F.F., Wessely, G., 1999. From the Tethyan Ocean to the Paratethys Sea: Oligocene to Neogene Stratigraphy, Paleogeography and Palaeobiogeography of the circum-Mediterranean region and the Oligocene to Neogene Basin evolution in Austria. *Mitteilungen der Österreichischen Geologischen Gesellschaft* 92, 95-116.
- Strauss, P., Harzhauser, M., Hinsch, R., Wagneich, M., 2006. Sequence stratigraphy in a classic pull-apart basin (Neogene, Vienna Basin) - A 3D seismic based integrated approach. *Geologica Carpathica* 57, 185-197.
- Trauth, M.H., Sillmann, E., 2013. *MATLAB® and Design Recipes for Earth Sciences*. Springer-Verlag Berlin Heidelberg, 292 pp.
- ten Veen, J.H., Kleinspehn, K.L., 2000. Quantifying the timing and sense of fault dip slip: New application of biostratigraphy and geohistory analysis. *Geology* 28, 471-474.
- ten Veen, J.H., Postma, G., 1999. Rollback controlled vertical movements of outer-arc basins of the Hellenic subduction zone (Crete, Greece). *Basin Research* 11, 243-266.
- Van Hinte, J.E., 1978. Geohistory Analysis - Application of Micropaleontology in exploration geology. *The American Association of Petroleum Geologists Bulletin* 62, 201-222.

- Vass, D., Pereszlenyi, M., Kováč, M., Král, M., 1990. Outline of Danube basin geology. *Földtani Közlöny: Bulletin of the Hungarian Geological Society* 120, 193-214.
- Wagreich, M., Schmid, H.P., 2002. Backstripping dip-slip fault histories: Apparent slip rates for the Miocene of the Vienna Basin. *Terra Nova* 14, 163-168. doi:10.1046/j.1365-3121.2002.00404.x
- Watson, D.F., 1992. *Contouring: A Guide to the Analysis and Display of Spatial Data*. Pergamon Press, Exeter, p. 321.
- Watson, D.F., Philip, G.M., 1984. Triangle based interpolation. *Journal of the International Association for Mathematical Geology* 16, 779-795. doi:10.1007/BF01036704
- Weissenböck, M., 1996. Lower to Middle Miocene sedimentation model of the central Vienna Basin, in: Wessely, G., Liebl, W. (Eds.), *EAGE Spec Pub 5: Oil and Gas in Alpidic Thrustbelts and Basins of Central and Eastern Europe*. EAGE, pp. 355-363.
- Wessely, G., 1988. Structure and development of the Vienna basin in Austria, in: Royden, L.H., Horváth, F. (Eds.), *AAPG Memoir 45: The Pannonian Basin: A Study in Basin Evolution*. AAPG, pp. 333-346.
- Wessely, G., 1990. Geological results of deep exploration in the Vienna basin. *Geologische Rundschau* 79, 2, 513-520.
- Wessely, G., Kröll, A., Jiříček, R., Nemec, F., 1993. *Wiener Becken und angrenzende Gebiete-Geologische Einheiten des präneogenen Beckenuntergrundes*.
- Whaba, G., 1990. *Spline Models for Observational Data*, CBMS-NSF Regional Conference Series in Applied Mathematics 59. SIAM, Philadelphia, Pennsylvania, p. 180.
- Witten, A., 2004. A MATLAB-based three-dimensional viewer. *Computers & Geosciences* 30, 693-703.
- Witten, A., 2002. Geophysica: MATLAB-based software for the simulation, display and processing of near-surface geophysical data. *Computers & Geosciences* 28, 751-762.
- Xie, X., Heller, P.L., 2009. Plate tectonics and basin subsidence history. *Bulletin of the Geological Society of America* 121, 55-64.
- Yang, T., 1985. *Finite Element Structural Analysis*. Prentice-Hall, Englewood Cliffs, New York, p. 543.



## APPENDIX

#### APPENDIX A. INPUT WELL DATA

- LOCATIONS OF WELLS STUDIED IN THIS THESIS
- INPUT WELL DATA FROM THE SLOVAK AND CZECH PARTS
- WELLS DATA FROM THE AUSTRIAN PART
- WELL DATA OF THE SYNTHETIC WELLS

#### APPENDIX B. DIP-SLIP FAULT BACKSTRIPPING

- PRINCIPLE OF THE DIP-SLIP FAULT BACKSTRIPPING
- VERTICAL FAULT DISPLACEMENT HISTORY IN THE STUDY AREA

## APPENDIX A. INPUT WELL DATA

- LOCATIONS OF WELLS STUDIED IN THIS THESIS

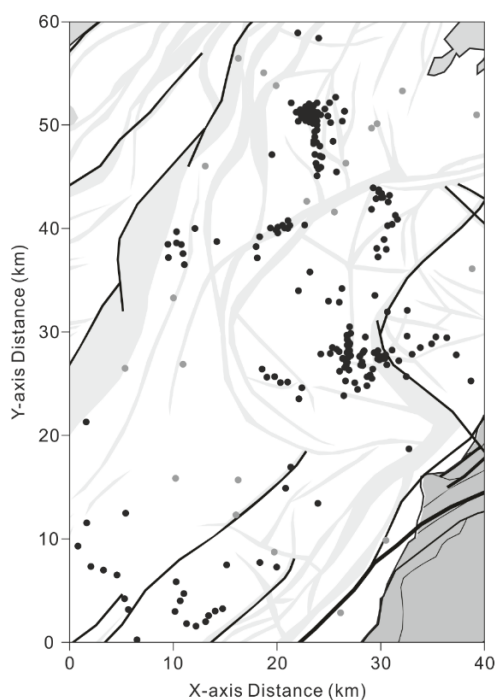


**Figure A.1.** Locations of wells in the study area (see Figure 3.1 for location of the study area). The black spots are locations of wells acquired from the Dionyz Štur Institute and Hölzel (2009), and the grey spots are of synthetic wells.

<i>BJ</i> (Borský Jur)	<i>Lu</i> (Lužice)
<i>Cu</i> (Cunín)	<i>Ma</i> (Malacky)
<i>Du</i> (Dúbrava)	<i>RGL</i> (R)
<i>Gb</i> (Gbely)	<i>Ro</i> (Rohožník)
<i>Kk</i> (Kuklov)	<i>Sa</i> (Šaštín)
<i>Kt</i> (Kúty)	<i>Sm</i> (Smolinské)
<i>Lb</i> (Láb)	<i>St</i> (Studienka)
<i>LNV</i> (Lakšárska Nová Ves)	<i>Vy</i> (Vysoká)
<i>Ln</i> (Lanžhot)	<i>Zv</i> (Závod)

**Table A.1.** Abbreviation and full names of each well block

- INPUT WELL DATA OF THE SLOVAK AND CZECH PARTS

PNB : Pre-Neogene Basement

EO : Eggenburgian – Ottongian, LKA : Lower Karpatian, KA : Karpatian

LBA : Lower Badenian, BA : Badenian, SA : Sarmatian

The top depth of the Pannonian is assumed as 0 km

\*Location of each well is relative in the study area.

Well Name	Location*		Top depth (m) of						
	x	y	PNB	EO	LKA	KA	LBA	BA	SA
BJ 4	30.8	32.1				1130	1030	630	330
BJ 5	32.7	32.3				1120	1030	710	415
BJ 6	29.6	33.7				930	810	420	170
BJ 7	26.1	33.1				1500	1280	700	300
BJ 8	22.2	34.2	3600	3500		2250	1850	950	450
BJ 16	25.1	33.2	3080		2248	1630	1305	735	311
Cu 2	26.4	50.6	983			875		590	4.1
Cu 4	22.8	51.6	980	720		475		390	80
Cu 5	25.3	50.4	830	700		610		460	130
Cu 6	24.0	52.3	855	630		420		375	50
Cu 7	21.5	52.3	995	680		475		375	40
Cu 8	26.6	51.5		700		635		530	250
Cu 9	23.5	51.1	885	845		425		360	75
Cu 10	24.0	50.6	920	670		450		370	0
Cu 11	23.8	49.6	1090	980		395		270	60
Cu 12	23.2	51.0	939	660		430		360	0
Cu 13	23.2	51.4	917	669		437		340	0
Cu 14	23.6	50.4	950	740		430		340	0
Cu 15	23.6	50.8	905	660		440		345	0
Cu 16	22.8	51.2	925	670		440		355	0
Cu 17	24.0	49.7	960	740		435		335	80
Cu 18	23.9	51.0	897	700		430		345	0
Cu 19	22.5	50.9	858	690		465		366	30
Cu 20	23.2	50.5	934	710		445		353	43
Cu 21	22.9	50.6	940	690		460		355	40
Cu 22	23.6	51.6	880	655		425		360	45
Cu 23	22.2	50.6	955	700		495		392	68
Cu 25	24.0	50.2	937	727		432		330	32
Cu 27	22.0	51.4	950	690		450		360	50

Cu 28	23.2	51.8	900	665		450		345	45
Cu 29	24.0	51.4	890	660		440		340	45
Cu 30	22.9	52.0	894	660		445		350	50
Cu 31	22.4	51.7	924	665		450		350	55
Cu 32	22.4	51.3	940	685		410		360	10
Cu 33	23.6	52.1	879	630		440		350	50
Cu 34	23.2	52.2	900	645		455		350	55
Cu 35	25.0	51.1	800	700		560		480	100
Cu 36	24.7	51.7	760	600		330			130
Cu 37	25.2	52.4	800	560		410		300	130
Cu 38	25.8	52.9	860	640		420			220
Cu 39	24.3	51.2	785	620		400		320	40
Du 1	15.3	7.7				1975	1640	980	630
Gb 1	24.3	47.2				500	370	300	0
Gb 3	24.3	48.2				440	390	295	50
Gb 4	23.9	46.5				497	397	317	30
Gb 5	23.8	49.6				404		337	60
Gb 6	23.6	48.6				390		310	50
Gb 7	24.5	47.1				465	375	288	0
Gb 8	24.0	46.2				470	375	296	0
Gb 9	24.0	48.5				405		331	35
Gb 11	24.1	45.9				520	370	295	0
Gb 12	24.3	46.1	1340	1280		500	370	290	0
Gb 13	24.0	45.3	1380			560	390	320	0
Gb 18	23.8	47.4				480	370	294	20
Gb 25	23.6	48.4	1178	1080		400		331	23
Gb 29	24.2	46.7				494.5	382	300.5	0
Gb 36	24.6	47.0				363		292	0
Gb 37	24.6	47.0				366		293	0
Gb 39	23.6	48.2				403		333	30
Gb 114	25.0	45.7						227	67
Gb 119	25.1	46.0				318		225	51
Gb 121	25.9	48.6						221	63
Gb 137	25.5	48.6	1053	940		750		475	68
Kk 3	26.4	34.4	2702		1867	1210	1110	517	170
Kk 4	23.3	36.0	3130						
Kt 15	19.6	47.3				810	670	561	130
Kt 17	20.0	40.1	2220			2120		1350	700
Kt 18	20.6	40.5	2670			2400	2220	1360	720
Kt 21	18.1	38.4				3025	2250	1454	802
Kt 22	20.2	40.3	2400			1880	1750	1380	700

Kt 23	22.8	40.5	2750			2200	1960	1420	730
Kt 24	20.2	39.8					2000	1390	727
Kt 25	18.4	39.4	3250			2300	2100	1450	750
Kt 26	18.2	37.4				3300	2360	1560	780
Kt 33	21.2	40.2			2790	2520	2027	1448	705
Kt 36	19.5	40.2	2025			1740	1515	1360	710
Kt 39	21.2	41.0						1359	698
La 40	20.1	7.5	2300			1763		1075	960
La 90	18.5	7.9	2050			1550	1500	870	560
LNV 1	32.7	29.8	1190	1120	0				
LNV 2	35.0	29.1	1200	1150	0				
LNV 3	37.4	28.0	1100	1050	0				
LNV 4	36.5	29.6	1100	1050	0				
LNV 5	38.8	25.5	800	700	0				
LNV 6	33.1	28.0	1280	1250	0				
LNV 7	33.9	28.7	1562	1412	0				
Ln 2	9.6	37.4				2330		970	500
Ln 3	9.6	38.7				2308	1590	960	485
Ln 4	10.9	38.6				2216		958	454
Ln 8	11.2	36.7				2570	1850	1850	960
Ln 18	10.4	38.8				2267	1638	969	475
Ln 20	12.2	40.2				2102	1548	954	443
Ln 21	11.1	37.8						1640	977
Ln 23	10.4	39.9				2237	1611	980	481
Ln 24	14.3	38.9						1080	715
Lu 103	22.1	59.1	1552	1005				960	453
Lu 120	24.1	58.6	1435	828				792	361
Ma 20	21.0	15.1	3300	3250		2100	1840	1050	630
Ma 22	24.1	13.6	2850	2800		1600	1480	980	640
Ma 64	21.4	17.1				1600		1067	629
R 1	35.4	29.7	1243	1172	10	0			
Ro 1	32.8	18.9	3050	3000		2260	1960	1360	860
Sa 9	29.7	38.3	1450			450	380	150	0
Sa 10	30.4	39.1	1700	1650		470		290	0
Sa 11	30.6	38.2	1980	1750		380		180	0
Sa 12	29.9	37.4	2150	1900		470		330	0
Sm 5	31.0	43.4		985		755		536	211
Sm 6	29.9	43.7		1080		756		570	285
Sm 7	29.7	43.1	1290	1200		830		635	280
Sm 8	29.2	42.1	1500			980		750	315
Sm 9	29.4	44.1		1070		835		650	325

Sm 10	30.8	42.8		1125		720		520	250
Sm 11	30.2	43.6		1045		752		560	267
Sm 12	30.3	43.2		1077		732		545	257
Sm 13	30.1	43.2		1115		765		555	265
Sm 14	30.8	40.5	1500	1250		720		570	280
Sm 15	30.2	43.4		1059		765		546	264
Sm 16	29.9	43.9		1075		798		545	235
Sm 17	31.7	41.1	1265	1080		485		330	220
Sm 18	31.2	40.6	1335	1260		600		350	245
Sm 19	31.5	41.5	1295	1250		695		540	270
St 1	29.3	25.7					1270	725	465
St 2	26.7	25.5				1815	1436	710	500
St 3	31.2	28.4	1740	1610		1360	1117	810	600
St 4	32.6	25.9				1420		975	775
St 5	30.7	27.0	2333			1650	1315	827	543
St 6	27.9	24.6					1385	750	550
St 8	30.6	28.0						820	610
St 11	29.0	26.0				1305		770	550
St 14	30.5	27.6					1216	810	585
St 15	28.8	25.0					1345	780	450
St 31	29.4	26.6				1593	1257	798	525
St 32	30.2	27.6					1208	805	590
St 33	30.3	27.8					1210	715	561
St 34	29.7	28.1					1233	750	460
St 35	29.8	27.6					1220	739	542
St 36	27.6	25.3				1590	1351	835	532
St 37	31.9	27.4	1675	1588		1280	1250	900	650
St 38	30.3	27.4					1210	755	575
St 39	28.8	25.9	3290	3160		1670	1310	827	525
St 40	29.9	27.9					1221	757	525
St 41	29.8	28.4					1246	775	460
St 42	30.3	27.6					1218	875	585
St 43	29.5	28.2					1232	735	440
St 44	28.5	28.4					1261	700	405
St 45	30.0	27.5					1207	845	565
St 83	26.6	24.0	3087	3011	2140	1803	1386	900	500
Vy 4	13.5	2.8	3050			1975	1530	1125	763
Vy 11	14.9	3.5						1050	690
Vy 13	11.1	4.9						1005	660
Vy 14	10.3	3.2						1010	661
Vy 15	10.8	4.2						1020	666

Vy 17	12.3	1.8						1020	720
Vy 18	14.2	3.2						960	675
Vy 19	10.4	6.1						1060	680
Vy 20	13.2	2.2						995	794
Vy 23	11.1	2.1	2630			1970	1490	960	640
Zv 3	25.3	28.1				1610		820	330
Zv 6	26.9	28.2				1520	1323	780	415
Zv 9	27.2	29.1				1485	1313	760	395
Zv 10	28.2	27.0				1600	1400	694	400
Zv 13	27.1	26.5					1305	790	425
Zv 17	27.0	28.5					1330	770	400
Zv 18	25.9	28.5						675	310
Zv 20	27.1	28.4					1300	790	420
Zv 21	28.4	27.0				1590	1380	700	390
Zv 26	26.9	29.5				1500	1305	760	400
Zv 28	28.6	29.7				1350	1150	710	320
Zv 29	26.9	27.3					1320	800	420
Zv 30	26.9	27.3					1335	800	420
Zv 33	27.2	30.1					1305	730	390
Zv 36	26.2	26.4					1340	790	460
Zv 37	27.1	30.7					1290	730	370
Zv 38	27.1	28.9					1300	760	405
Zv 39	27.0	29.2					1297	760	395
Zv 40	26.1	28.3						680	315
Zv 42	26.9	29.8					1300	740	380
Zv 43	28.1	27.8							390
Zv 44	26.9	29.9					1300	730	370
Zv 45	26.5	27.7					1340	700	450
Zv 46	26.5	27.6					1350	780	450
Zv 47	28.4	28.2					1170	550	300
Zv 57	28.1	27.9	2950	2900		1530	1345	760	400
Zv 61	26.9	28.9					1303	780	425
Zv 62	27.0	28.9					1320	800	435
Zv 63	27.2	27.9					1306	790	440
Zv 64	26.8	26.9					1326	800	473
Zv 65	26.7	26.8					1344	810	470
Zv 67	26.8	27.3					1318	820	460
Zv 68	25.5	28.7	3170	3040		1630	1370	700	330
Zv 69	27.0	27.7					1320	800	420
Zv 70	28.3	27.3							418
Zv 71	24.3	28.1				1580	1380	730	350

Zv 72	19.9	25.9	4150		3750	2350	1650	850	480
Zv 76	21.1	25.4	4078		3660	2440		1122	652
Zv 89	19.1	25.8	4359		3875	2855	2210	1403	802
Zv 90	20.4	25.3	4125		3630	2562	1915	1270	708
Zv 92	22.5	24.8	4205		3105	2020	1654	1090	574
Zv 94	18.7	26.6	4195		3875	2876	2210	1425	815
Zv 97	22.2	23.7				2128	1745	1123	613

- WELLS DATA FROM THE AUSTRIAN PART (from Hölzel, 2009)

Well Name	Location*		Top depth (m) of						
	x	y	PNB	EO	LKA	KA	LBA	BA	SA
EbT 1	5.5	12.7					2218	1334	875
PrTS 1	2.2	7.5					1672	970	675
SpT 1	1.8	11.7					1812	1228	792
SpT 3	0.9	9.5					1812	1142	831
TaS 1	5.4	4.4					1870	1081	715
TaT 1	4.7	6.7					1842	1001	703
TaW 2	3.4	7.2					1850	1043	687
Zist 4	2.6	22.0					3575	1818	700
ZwT 1	5.8	3.4					1850	1091	739

- WELL DATA OF THE SYNTHETIC WELLS

Well Name	Location*		Top depth (m) of						
	x	y	PNB	EO	LKA	KA	LBA	BA	SA
G 1	32.2	53.5	1128	991	860	792	792		
G2-1	29.8	50.3	1680	1404	1264	991	991		
G 2-2	29.2	49.9	1471	1264	1059	726	726		
G 2-3	26.7	46.5	1263	1128	860	600	600		
G 3	25.7	41.8	2426	2052	1862	1404	1404		
G 4	23.0	42.8	1680	991	792	600			
G 5	13.2	46.2	3799	3300	2426	1404	1128	860	
Ga	16.4	15.9	4444	4444		2292		1082	705
Husky	18.8	55.2	2600	2600	2600	2600	2600	1500	700
La	19.9	8.9	2300	2300	2300	1587	1587	986	633
Lu 1	32.8	59.1	200	100	100	100	100	100	0
Mor 1	16.4	56.6	3800	3800	3800	3300	3300	1540	726
Ow	6.6	0.5	3133	3133	3133	2208	1625	1076	730
Podivin	15.2	60.0	600	600	600	600	600	400	200

Ri	11.1	27.1	4231	4231	3975	3975	3700	1859	1258
Stein 1	5.5	26.7	5900	5900	5900	5800	5550	2000	1000
Stein 2	10.1	33.5	4000	4000	3800	3300	3300		
Such1	10.3	16.1	5046	4300	3692	3045			
Such3	16.2	12.5	4045	3921	3545	2610			
Sur 1	39.4	51.2	100		0	0	0	0	0
Sur 2	38.9	36.3	140		0	0	0	0	0
Sur 3	30.6	10.1	600	600	600	200	0	0	0
Sur 4	26.2	3.1	800	800	800	300	0	0	0
Tynec	20.0	54.0	2300	2000	2000	1500	1500	1000	500

## APPENDIX B. DIP-SLIP FAULT BACKSTRIPPING

### • PRINCIPLE OF THE DIP-SLIP FAULT BACKSTRIPPING

This study indicated the major fault activities during the Middle – Late Miocene in the study area. To analyze vertical fault displacement through time, this study used the dip-slip fault backstripping introduced by ten Veen and Postma (1999), ten Veen and Kleinspehn (2000) and Wagreich and Schmid (2002).

The method uses basement subsidence curves without sea-level corrections for two stratigraphic profiles from the footwall and hanging wall blocks of synsedimentary faults (Fig. B.1a). Segments of convergence or divergence record times of dip-slip activity (Wagreich and Schmid, 2002).

The difference in vertical position of two basement subsidence points at a given time  $i$  is expressed as  $\Delta S$ . The dip-slip values are calculated by subtracting  $\Delta S_{i-1}$  from  $\Delta S_i$  and divided by the duration of the stratigraphic interval (Fig. B.1b; see also Hölzel, 2009). The results are presented in step plots of the slip rate vs. time (Fig. B.1c). The values indicate the sense of dip-slip for relative block movement and, in zero values, fault inactivity or pure strike-slip motion (Wagreich and Schmid, 2002).

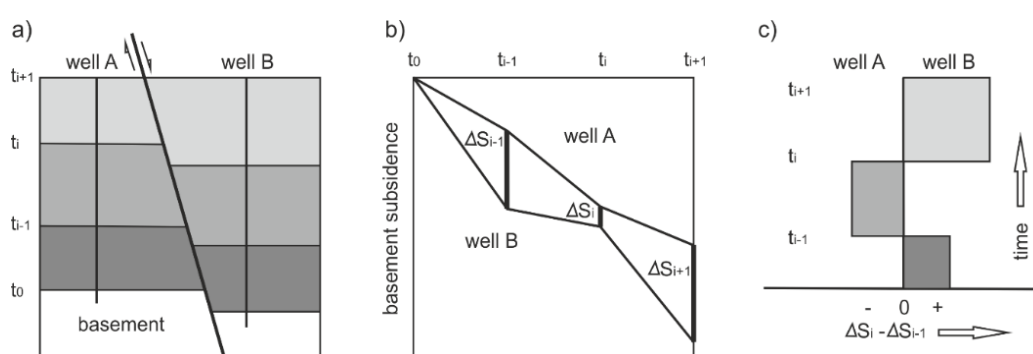


**Figure B.1.** The dip-slip fault backstripping procedure (revised from Wagreich and Schmid, 2002). a) Two wells A and B on the footwall and the hanging wall of a synsedimentary normal fault, b) Basement subsidence curves of the two wells, and their difference ( $\Delta S$ ), c) Step plot of the apparent dip-slip rates ( $\Delta S_i - \Delta S_{i-1}$ ) vs. stratigraphic time along the fault.

### • VERTICAL FAULT DISPLACEMENT HISTORY IN THE STUDY AREA

The dip-slip fault backstripping is analyzed for the Lab fault, the Moravsky Jan fault, the Laksary fault in the central part, the Hodonin-Gbely fault in the northern part, and the Lanzhot-Hrusky fault in the northern basement high (Fig. B.2). Two faults (A and E) are NE-SW striking, and two faults (B and C) of NW-SE striking, one fault (D) of NS striking. The early Miocene phase was excluded from the dip-slip backstripping, because the Lower Miocene tectonic history differs strongly from the later.

Faults in the central part show a similar displacement pattern. After the dip-slip rate ranging up to 200 m/Ma of the Lower Badenian, the rates are significantly high during the Upper Badenian. And then the dip-slip rates decrease until the Pannonian. Although the dip-slip rate of the Lower Badenian is missing, the dip-slip trend of the Hodonin-Gbely fault is similar with the central part from the Upper Badenian to Pannonian. The dip-slip rate of the Lanzhot-Hrusky fault in the northern basement high is indicated only during the Sarmatian – Pannonian. In general, the vertical displacement rates of the NW-SE striking faults are higher than rates of the NE-SW and NS striking faults. It is more evident in the Sarmatian and Pannonian time.

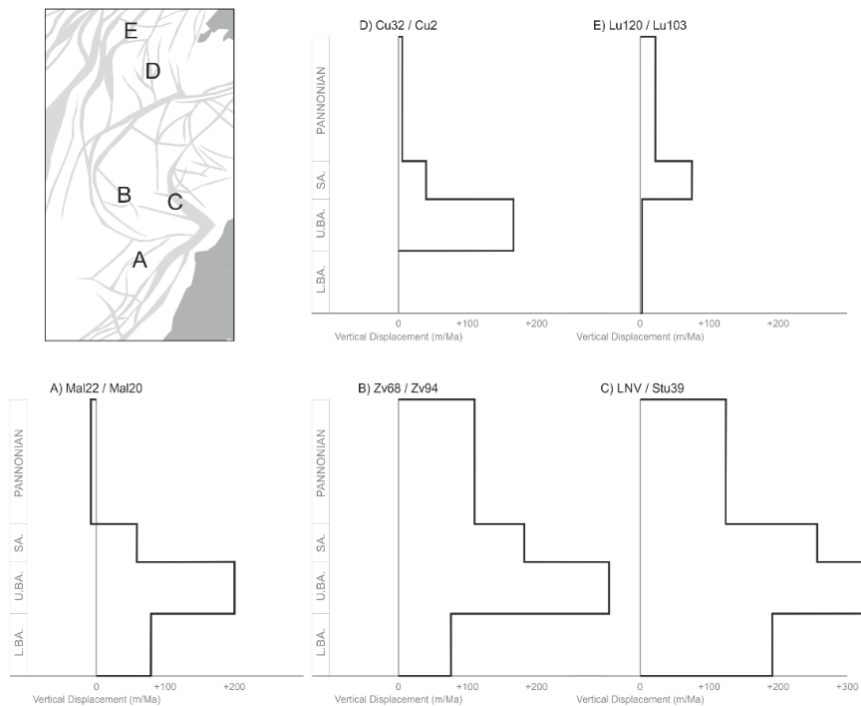


**Figure B.2.** Vertical displacement rates of the faults (A – E) in the study area. A: Lab fault, B: Moravsky Jan fault, C: Laksary fault, D: Hodonin-Gbely fault and E: Lanzhot-Hrusky fault.

## ***CURRICULUM VITAE AND LIST OF PUBLICATIONS***

### ***PERSONAL DATA***

Name Eun Young Lee  
Address UZAll 2A351 Althanstrasse 14, 1090 Vienna Austria  
E-mail eun.lee@univie.ac.at  
Office Tel. +43-1-4277-9805762 Fax. +43-1-4277-9543  
Nationality Republic of Korea  
Language Korean (Native), English (Professional), German

### ***RESEARCH INTERESTS***

- Quantitative and Integrated Basin Analysis
- Interplay of Sedimentation and Tectonics
- Interpretation and Analysis of 2D/3D Seismic, Well, Logging and Geophysical data
- Modeling of Stratigraphic, Structural, Tectonic and Subsidence Evolution

### ***EDUCATION***

2015 **Dr.rer.nat.** UNIVERSITY OF VIENNA (Universität Wien), Vienna, Austria  
Department of Geodynamics and Sedimentology  
Advisors: Prof. Dr. Michael Wagreich, Dr. Kurt Decker  
2010 **M.S.**, KOREA UNIVERSITY OF SCIENCE AND TECHNOLOGY, Daejeon, Korea  
Department of Petroleum Resources Technology  
2007 **B.Sc.**, KOREA UNIVERSITY, Seoul, Korea  
Department of Earth and Environmental Sciences

### ***RESEARCH & PROFESSIONAL EXPERIENCES***

2015 - **SEDIMENTOLOGIST** IODP-USIO Expedition 356 Indonesian Throughflow  
4/2011-10/2015 **GRADUATE RESEARCH** University of Vienna  
Integrated basin analysis of the Vienna Basin, central Europe  
12/2013-7/2014 **CONFERENCE ORGANIZER** EKC2014  
EU-Korea Conference on Science and Technology, Vienna, Austria

- 9/2009-5/2011     **GEOLOGIST** University of Vienna & OMV  
Karpatian Tectonics Slovakia (funded by OMV E&P)
- 3/2007-8/2010     **GRADUATE RESEARCH** Korea University of Science and Technology  
Tectonic evolution of the Gunsan Basin in offshore Korea (funded by KIGAM)
- 3/2007-2/2009     **RESEARCH ASSISTANT** Korea Institute of Geoscience & Mineral resources  
Petroleum geology of petroliferous basins and international cooperation with  
oil/gas-producing countries

### **AWARDS & HONORS**

- 1/2015     **SCHOLARSHIP** Korean Scientists and Engineers Association in Austria
- 8/2014     **TRAVEL GRANT** International Sedimentological Congress, IAS
- 7/2014     **POSTER AWARD** EU-Korea Conference on Science and Technology, Austria
- 1/2014     **TRAVEL AWARD** Korea Institute of Ocean Science & Technology
- 12/2013     **TRAVEL GRANT** for AGU, University of Vienna
- 7-8/2009     **SCHOLARSHIP** Deutschen Akademischen Austauschdienstes (DAAD), Germany
- 5-6/2009     **SCHOLARSHIP** for overseas research, Korea University of Science and Technology
- 3/2007     **2 full-year SCHOLARSHIP** for M.S. research, Korea Institute of Geoscience and  
Mineral resources
- 9/2006     **1<sup>st</sup> PRIZE** in Student Research&Presentation Contest, Korea Basic Science Institute
- 9/2006     **SCHOLARSHIP** for High graded students, Korea University
- 7/2000     **SILVER MEDAL** in Earth Science, Science Contest, Gyeonggi Provincial Office of  
Education, Korea

### **WORKING AND TEACHING EXPERIENCES**

- 4/2015     **CONFERENCE ASSISTANT** EGU General Assembly 2015, Vienna, Austria
- 3/2010-7/2012     **KOREAN LANGUAGE TEACHER** Koreanische Schule Wien, Vienna, Austria
- Winter 2012     **PETROPHYSICS INTERN** HOTWELL G.m.b.H., Burgenland, Austria
- 4/2012     **CONFERENCE ASSISTANT** EGU General Assembly 2012, Vienna, Austria
- 5/2010     **CONFERENCE ASSISTANT** EGU General Assembly 2010, Vienna, Austria
- W2008     **TEACHING ASSISTANT** 02083-01: Sequence Stratigraphy, UST, Korea
- Summer 2008     **GEOSCIENCE INTERN** Korea National Oil Company (KNOC), Ansan, Korea
- S/W2006     **SCIENCE TEACHER** Hansaem Academy, Seoul, Korea
- Summer 2006     **GEOSCIENCE INTERN** Korea Basic Science Institute, Daejeon, Korea
- 9/2005-6/2006     **LAB. ASSISTANT** Geochemistry lab., Korea University, Seoul, Korea

**SHORT COURSES**

5-6/2015	Oil & Gas: from exploration to distribution, IFP school, France
2/2012	Junior Petrophysicist Training, HOTWELL, Klingenberg, Austria
2/2010	Balanced Profile, Geologischen Vereinigung, Berlin, Germany
5/2008	OSL analysis, Korea Basin Science Institute, Daejeon, Korea
8/2007	Technology for Overseas Petroleum Development, Korea Petroleum Association, Daejeon, Korea
6/2006	ICP-AES analysis, Korea Basin Science Institute, Seoul, Korea
7-9/2005	Environmental Policy & Assessment, Korea Environment Institute, Korea
5/2005	XRD analysis, Korea Basin Science Institute, Seoul, Korea

**ACADEMIC ACTIVITIES**

10/2014 -	<b>COORDINATOR</b> Korean Energy & Environment Expert in Europe
9/2009 -	<b>MEMBER</b> Korean Scientists and Engineers Association in Austria (KOSEAA)
8/2012-5/2013	<b>VISITING STUDENT</b> Center of Active Visualization in the Earth Sciences, UC DAVIS, CA, USA
7-8/2009	<b>EXCHANGE STUDENT</b> Steinmann-Institute, University of Bonn, Germany
5-6/2009	<b>VISITING STUDENT</b> Structural Processes Group, University of Vienna, Austria
9/2007-3/2009	<b>FOUNDER&amp;PRESIDENT</b> Women Scientist&Engineer Club, UST, Korea
7/2007	<b>FIELD RESEARCH</b> Gobi desert, KSEEG, Mongolia

**COMPUTING PROFICIENCY**

Seismic Interpretation	GeoFrame Charisma (Schlumberger), GeoGraphix (Landmark)
Visualization	Illustrator & Photoshop (Adobe), CorelDRAW (Corel)
Office	Word, Excel, PowerPoint

**CERTIFICATES**

Computer	Level 2, Word Processor, Korea Chamber of Commerce & Industry Level 3, Ability of Utilizing Computer, Korea Chamber of Commerce & Industry
English	TOEIC score 975, Test of English for International Communication, ETS FCE, Cambridge English Language Assessment
German	ösd B1, Austrian-German Language Diploma
Chinese	Level 4, Korea Hanja (Chinese Letter) Qualification Test Association
Korean	Korean Language Instructor, Digital Seoul Culture Arts University

### **SCIENTIFIC ARTICLES**

- **Lee, E.Y.**, Wagneich, M., submitted. 3D modeling of depositional setting and subsidence evolution in the northern and central Vienna Basin. Submitted to Austrian Journal of Earth Sciences.
- **Lee, E.Y.**, Novotny, J., Wagneich, M., submitted. BasinVis 1.0, a MATLAB®-based program for sedimentary basin subsidence analysis and visualization. Submitted to Computers & Geosciences.
- **Lee, E.Y.**, Wagneich, M., submitted. Polyphase tectonic subsidence evolution of the Vienna Basin inferred from quantitative subsidence analysis. Submitted to International Journal of Earth Sciences.
- **Lee, E.Y.**, 2010. Subsidence History of the Gunsan Basin (Cretaceous-Cenozoic) in the Yellow Sea, offshore Korea. Austrian Journal of Earth Sciences, 103/1, 111–120.
- **Lee, E.Y.**, 2010. Subsidence History of the Central Sub-basin in the Northern South Yellow Sea Basin, offshore Korea. Proceeding paper of 6<sup>th</sup> International Symposium on Geophysics.
- Ko, J.H., **Lhee, E.Y.**, 2007. Petroleum Geology of the Timan-Pechora Basin in Russia. Journal of the Korean Society for Geosystem Engineering, 44/4, 342–356.

### **INDUSTRY REPORTS**

- **Lee, E.Y.**, Lee, S.W., 2015. Industry and Strategy Overview of the Austrian Integrated Energy Company OMV. Korea Evaluation Institute of Industrial Technology.
- Decker, K., Beidinger, A., **Lee, E.Y.**, Zamolyi, A., 2011. Tectonics of the Slovak part of the Vienna Basin and the adjacent Western Carpathians during the Lower Miocene. OMV-Karpatian Tectonics Slovakia Final Report.
- Decker, K., Beidinger, A., Hoprich, M., **Lee, E.Y.**, Zamolyi, A., 2010. Tectonics of the Slovak part of the Vienna Basin and the adjacent Western Carpathians during the Lower Miocene. OMV-Karpatian Tectonics Slovakia Mid-term Report.

### **PRESENTATIONS AND INVITED TALKS**

- **Lee, E.Y.**, Novotny, J., Wagneich, M., 2015. A MATLAB®-based program for visualization of stratigraphic setting and subsidence evolution of sedimentary basins: example application to the Vienna Basin. EGU General Assembly, Vienna, Austria, 12-17 April, 2015.
- **Lee, E.Y.**, Novotny, J., Decker, K., Wagneich, M., 2014. Basin Evolution of the Vienna Basin –Insights from 3D subsidence modeling of the central and northern parts. 19<sup>th</sup> International Sedimentological Congress, Geneva, Switzerland, 18-22 August 2014.
- **Lee, E.Y.**, Novotny, J., Decker, K., Wagneich, M., 2014. A MATLAB program for subsidence analysis and 3D modelling: Application to a case study of Miocene sediments of the Vienna

Basin. 19<sup>th</sup> International Sedimentological Congress, Geneva, Switzerland, 18-22 August 2014.

- **Lee, E.Y.**, Novotny, J., Decker, K., Wagreich, M., 2014. Quantitative subsidence analysis and 3D modelling of the central and northern parts of the Vienna Basin, central Europe. EU-Korea Conference on Science and Technology, Vienna, Austria, 22-25 July 2014.
- Novotny, J., **Lee, E.Y.**, Decker, K., Wagreich, M., 2014. 3D Modelling with MATLAB for stratigraphic and subsidence mapping of sedimentary basins: Example application to the Vienna Basin. EU-Korea Conference on Science and Technology, Vienna, Austria, 22-25 July 2014.
- **Lee, E.Y.**, 2014. Overview of Petroleum Geology and Exploration in Austria. EU-Korea Conference on Science and Technology, Vienna, Austria, 22-25 July 2014.
- **Lee, E.Y.**, Novotny, J., Wagreich, M., 2013. Regional subsidence history and 3D visualization with MATLAB of the Vienna Basin, central Europe. AGU Fall Meeting, San Francisco, California, 9-13 December 2013.
- **Lee, E.Y.**, Wagreich, M., Decker, K., 2012. Miocene sediments distribution in the central and northern parts of the Vienna Basin, central Europe. AGU Fall Meeting, San Francisco, California, 3-7 December 2012.
- **Lee, E.Y.**, Zámolyi, A., Beidinger, A., Decker K., Strauss, P., 2011. Stratigraphy and subsidence history of the Závod region in the Slovak part of the central Vienna Basin. 73<sup>rd</sup> EAGE Conference & Exhibition incorporating SPE EUROPEC, Vienna, Austria, 23–26 May 2011. (extended abstract)
- Beidinger, A., Decker K., Zámolyi, A., **Lee, E.Y.**, 2011. Deciphering polyphase deformation in the Zilina segment of the Pieniny Klippen belt (Steny ridge, NW Slovakia). 9<sup>th</sup> CETeG, Lísk, Czech Republic, 13-17 April 2011.
- Beidinger, A., Decker K., Zámolyi, A., **Lee, E.Y.**, 2011. Paleogene to Neogene kinematics of the Outer West Carpathian fold-and-thrust belt and Miocene strike-slip faulting at the front of the Magura superunit (Slovakia and Czech Republic). 9<sup>th</sup> CETeG, Lísk, Czech Republic, 13-17 April 2011.
- **Lee, E.Y.**, 2011. Quantification of extension ( $\beta$ ) and Miocene uplift of the Gunsan Basin in the Yellow Sea, offshore Korea. EGU General Assembly, Vienna, Austria, 3-8 April 2011.
- **Lee, E.Y.**, Ryu I.C., 2011. Backstripping analysis of the Kachi-1 well in the Gunsan Basin in Yellow Sea, offshore Korea. EGU General Assembly, Vienna, Austria, 3-8 April 2011.
- **Lee, E.Y.**, 2010. Subsidence history of the Gunsan Basin in the Yellow Sea. Geophysical modeling of the lithosphere in the Yellow Sea area, NE Asia – an application of GRACE-GOCE gravity data German-Korean Workshop, Kiel, Germany, 10–12 August 2010.
- **Lee, E.Y.**, 2010. Subsidence History of the Northern South Yellow Sea Basin, offshore Korea. EGU General Assembly, Vienna, Austria, 2-7 May 2010.

- Zámolyi, A., **Lee, E.Y.**, Beidinger, A., Hoprich, M., Strauss, P., Decker, K., 2010. Miocene deformation of the central Vienna Basin (Austria-Slovakia). EGU General Assembly, Vienna, Austria, 2-7 May 2010.
- Beidinger, A., Decker, K., Zámolyi, A., **Lee, E.Y.**, Hoprich, M., Strauss, P., 2010. Oligocene to Miocene kinematics of the Outer West Carpathians and the Vienna Basin area. EGU General Assembly, Vienna, Austria, 2-7 May 2010.
- **Lee, E.Y.**, 2009. Subsidence History of the Central Sub-basin in the Northern South Yellow Sea Basin, offshore Korea. 6<sup>th</sup> International Symposium on Geophysics, Tanta, Egypt, 11-12 November 2009.
- Ko, J.H., **Lhee, E.Y.**, 2008. Tertiary tectonics of the Yellow Sea: Formation and evolution of the Gunsan Basin, Korea. 33<sup>rd</sup> International Geological Congress, Oslo, Norway, 6–14 August 2008.
- Ko, J.H., **Lhee, E.Y.**, 2007. Petroleum Geology of the Timan-Pechora Basin in Russia. Geological Society of Korea annual Conference, Chuncheon, Korea, 25-26 October 2007.

## **REFERENCES**

**Ao.Univ.Prof.Dr. Michael Wagreich** (Doctoral Advisor)

Department of Geodynamics and Sedimentology, University of Vienna, Austria

michael.wagreich@univie.ac.at

**Dr. Kurt Decker** (Doctoral Advisor)

Department of Geodynamics and Sedimentology, University of Vienna, Austria

kurt.decker@univie.ac.at